Aus dem Zentrum für Kardiologie
der Universitätsmedizin der Johannes Gutenberg-Universität Mainz

The role of plasma cell-free DNA as predictor of clinical outcome in heart failure – Results from the MyoVasc study

Die Rolle zellfreier DNA in der Vorhersage des klinischen Outcomes bei Herzinsuffizienz – Ergebnisse der MyoVasc Studie

Inauguraldissertation
zur Erlangung des Doktorgrades der
Medizin
der Universitätsmedizin
der Johannes Gutenberg-Universität Mainz

Vorgelegt von

Tim Jeremy Hankeln
aus Wiesbaden

Mainz, 2025

Wissenschaftlicher Vorstand:	Univ.-Prof. Dr. Hansjörg Schild
1. Gutachter:	Univ.-Prof. Dr. Philipp Wild
2. Gutachter:	Univ.-Prof. Dr. Dr. Perikles Simon

Tag der Promotion: 15.07.2025

For my family.

Deutschsprachige Zusammenfassung

Herzinsuffizienz (HI) ist mit einer Prävalenz von 1 bis 2 % in der erwachsenen Bevölkerung eine der Haupttodesursachen in den Industrieländern. Mit zunehmender Alterung der Bevölkerung wird auch die Bedeutung der HI in den kommenden Jahren zunehmen. Dies geht mit einem starken Anstieg der Gesundheitskosten einher und stellt eine erhebliche Belastung für die Gesellschaft dar. Die Identifizierung von HI-Risikopatienten zu einem früheren Zeitpunkt, möglicherweise sogar noch vor Auftreten von Symptomen, ist von entscheidender Bedeutung, um rechtzeitig Maßnahmen wie Lebensstiländerungen oder eine medikamentöse Therapie einleiten zu können. In der Präventivmedizin spielt die Identifizierung geeigneter Biomarker eine Schlüsselrolle, da sie eine objektive und frühzeitige Krankheitserkennung ermöglichen.

Zellfreie DNA (cfDNA) ist ein weit verbreiteter diagnostischer Biomarker in klinischen Bereichen wie der Onkologie oder der Transplantationsmedizin. In der klinischen Kardiologie spielt die cfDNA-Analytik jedoch bislang noch keine große Rolle. Nur eine Handvoll eher kleinerer Studien hat bisher das Potenzial der cfDNA-Diagnostik bei HI-Patienten untersucht. Diese Arbeiten deuten jedoch darauf hin, dass cfDNA ein unabhängiger Risikofaktor für Herz-Kreislauf-Erkrankungen und die Gesamtmortalität sein könnte. Ziel der vorliegenden Arbeit war es daher, das Potenzial von cfDNA in der HI-Diagnostik in einer größeren Studienkohorte zu untersuchen und ihre Vorhersagekraft mit dem derzeit am häufigsten verwendeten Biomarker, NT-proBNP, zu vergleichen.

Um dies zu erreichen, musste eine zuverlässige, reproduzierbare und schnelle Hochdurchsatzmethode zur Quantifizierung von cfDNA implementiert werden. Der bestehende manuelle, zeit- und arbeitsaufwändige qPCR-Assay wurde durch die Erprobung und Etablierung eines INTEGRA-Pipettierroboters automatisiert und dessen Arbeitsablauf auf die speziellen Bedürfnisse hochviskoser Plasmaproben hin abgestimmt. Der Assay wurde so angepasst, dass er zuverlässig die gleichen Testergebnisse liefert wie der bereits publizierte qPCR-Assay von Neuberger et al. (182). Auf diese Weise wurde eine konsistente Messung der Studienproben sichergestellt. Die cfDNA-Konzentration wurde in 3109 EDTA-Plasmaproben der prospektiven MyoVasc-Studie (NCT04064450) analysiert. Zur Quantifizierung der cfDNA und zur Berechnung des cfDNA-Integritätsindex wurden zwei qPCR-Assays mit unterschiedlichen Amplikonlängen (cfDNA90 bp/ cfDNA222 bp) verwendet, die beide auf ein repetitives LINE1-Element abzielen. Um die Assoziationen von cfDNA mit der Verschlechterung von HI zu untersuchen, wurden “Competing risk models“ angewandt. Cox-Proportional-Hazard-Regressionsanalysen wurden verwendet, um die Endpunkte Herztod und Gesamtmortalität zu bewerten. Zusätzlich wurden C-Statistiken für jedes Modell berechnet und verglichen. Die Teilnehmer wurden als 0 (gesund) oder als HI-Stadien A (Risiko für HI) bis D (fortgeschrittene HI) gemäß der aktuellen universellen Definition der

Herzinsuffizienz eingestuft. Die Analysen wurden für Alter, Geschlecht, kardiovaskuläre Risikofaktoren (CVRF) und Medikamente (Modelle 1-3) sowie zusätzlich für NT-proBNP (Modell 4) adjustiert. Die Ergebnisse wurden als kumulative Inzidenzdiagramme für die cfDNA-Assays 90bp und 222bp sowie für den Integritätsindex, der den Fragmentierungsgrad der cfDNA beschreibt, dargestellt.

Die Kohorte umfasste 3109 Studienteilnehmer mit einem Alter zwischen 34 und 85 Jahren bei einem Frauen-Anteil von 35,7 %. Personen im Stadium 0/A (n=534) zeigten mit 10,99 (8,70/13,93) ng/ml (Median (Q1/Q3)) die niedrigsten cfDNA90bp-Konzentrationen. Probanden im Stadium B (prä-HI) (n=923) oder im Stadium C/D (n=1652) wiesen erhöhte cfDNA90bp-Konzentrationen von 13,37 (10,35/18,11) bzw. 17,11 (12,56/22,80) ng/ml auf. Cox-Proportional-Hazard-Regressionsanalysen zeigten, dass die cfDNA90bp-Konzentration ein relevanter prognostischer Marker für die Gesamtmortalität ist, sofern eine Adjustierung für Alter, Geschlecht, CVRF und Medikation vorgenommen wurde (HR = 1,312 [1,205-1,430], $p < 0,0001$). Nach zusätzlicher Adjustierung für den etablierten Marker NT-proBNP waren die Effektschätzungen geringer, aber immer noch statistisch signifikant (HR = 1,173 [1,073-1,282], $p = 0,00046$). Für die Endpunkte „Verschlechterung der HF“ und „Herztod“ waren die Effektschätzer nach Adjustierung für NT-proBNP hingegen nicht mehr statistisch signifikant. Ein C-Index-Vergleich zeigte ebenfalls einen statistisch signifikanten Zusatznutzen der cfDNA zusammen mit der Bestimmung von NT-proBNP bei Betrachtung der Gesamtmortalität (C = 0,807 vs. C = 0,805; $p = 0,050$). Diagramme für kumulative Inzidenzen von NT-proBNP- und cfDNA-Werten (dichotomisiert) zeigten die höchsten Inzidenzraten hingegen sogar für alle drei Endpunkte bei Patienten mit gleichzeitiger Erhöhung beider Biomarker. Die Inzidenzen waren signifikant höher als bei Patienten mit einer reinen Erhöhung von NT-pro BNP.

Die Ergebnisse deuten darauf hin, dass cfDNA ein Risikofaktor ist, der unabhängig von NT-proBNP zur Vorhersage der Gesamtmortalität in der Studienkohorte beiträgt. cfDNA besitzt offenbar auch einen zusätzlichen Nutzen zu NT-proBNP für die Vorhersage einer Verschlechterung der HI und des Herztodes.

Table of contents

I. List of abbreviations

%	Percent
°C	Degree Celsius
AF	Atrial fibrillation
APACHE	Acute Physiology and Chronic Health Evaluation
BNP	B-type natriuretic peptide
bp	Base pairs
C. revasc.	Coronary revascularization
CAD	Coronary artery disease
CAD	Caspase-activated DNase
cf-mtDNA	Mitochondrial cell free DNA
cf-nDNA	Nuclear cell free DNA
cfDNA	Cell free DNA
CHF	Chronic heart failure
CI	Confidence interval
CK	Creatine kinase
CKD	Chronic kidney disease
CLD	Chronic liver disease
conc.	Concentration
COPD	Chronic obstructive pulmonary disorder
Cq	Cycle of quantification
Cq_Diff	Difference between two Cq values
CRP	C-reactive protein

CSF	Cerebrospinal fluid
ctDNA	Circulating tumour DNA
CV	Coefficient of variation
CVD	Cardiovascular disease
CVRFs	Cardiovascular risk factors
DAMP	Damage-associated molecular pattern
ddcfDNA	Donor-derived cfDNA
ddPCR	Digital droplet PCR
DNA	Deoxyribonucleic acid
dNTPs	Deoxynucleotide triphosphates
dsDNA	Double-stranded DNA
DT_E	Deceleration time
E/A	Ratio for estimating blood flow via mitral valve
E/E'	Ratio for estimating left ventricular end-diastolic pressure
ECG	Electrocardiography
EDTA	Ethylenediaminetetraacetate
EF	Ejection fraction
EV	Extracellular vesicle
FDA	Food and Drug Administration
Fig.	Figure
FITC	Fluorescein-5-Isothiocyanate
g	Gram
g	G / Gravitational constant
GCS	Glasgow Coma Scale

GDMT	Guideline-directed management and therapy
GE	Genome equivalents
h	Hour
H_2O	Water
HF	Heart failure
HFmrEF	Heart failure with mildly reduced ejection fraction
HFpEF	Heart failure with preserved ejection fraction
HFrEF	Heart failure with reduced ejection fraction
HR	Hazard ratio
hs-cTn	High-sensitivity troponin-T
ICD	Implantable cardioverter-defibrillator
ICU	Intensive care unit
ISR	Incurred sample reanalysis
kDa	Kilo-Dalton
l	Litre
L1PA2	Long interspersed nuclear element 1 family 2
LINE1	Long interspersed nuclear element 1
LOD	Limit of detection
LVEF	Left ventricular ejection fraction
M	Molar mass
Mean/M.	Mean value
mg	Milligram
MI	Myocardial infarction
min	Minutes

miRNA	Micro RNA
MKP	Multichannel pipette (“Mehrkanalpipette”)
MM	MasterMix
mm	Millimetre
MODS	Multi Organ Dysfunction Syndrome
MRD	Minimal residual disease
mrEF	Mildly reduced ejection fraction
mRNA	Messenger RNA
mRS	Modified Rankin scale
NAFLD	Non-alcoholic fatty liver disease
NETs	Neutrophil extracellular traps
ng	Nanogram
NGS	Next-generation sequencing
NIHSS	National Institutes of Health Stroke Scale
NIPD	Non-invasive prenatal diagnostics
nm	Nanometre
NSCLC	Non-small cell lung cancer
NT-proBNP	N-terminal natriuretic peptide type B
NTC	Non-template control
NYHA	New York Heart Association
OR	Odds ratio
PAD	Peripheral artery disease
PCR	Polymerase chain reaction
pEF	Preserved ejection fraction

pg	Picogram
pH	Potentia hydrogenii / Hydrogen potential
PM	PrimerMix
PMM	PrimerMasterMix
POST	Lat. after
PRÄ	Lat. before
qPCR	Quantitative Polymerase chain reaction
rEF	Reduced ejection fraction
RefSamples	Reference samples
RFU	Relative fluorescence unit
RNA	Ribonucleic acid
rpm	Rounds per minute
RT	Room temperature
rt	Real-time
SBP	Systolic blood pressure
SD	Standard deviation
sec	Second
SLE	Systemic lupus erythematosus
SOFA	Sequential Organ Failure Assessment
SOPs	Standard operating procedures
ssDNA	Single-stranded DNA
Tab.	Table
TBI	Traumatic brain injury
TIA	Transient ischaemic attack

TLR9	Toll-like receptor 9
tRNA	Transfer RNA
U	Unit
UA	Uric acid
UV	Ultra-violet
VAFs	Variant allele fractions
VTE	Venous thromboembolism

II. List of figures

Appendix

III. List of tables

1 Introduction

In developed countries, **heart failure** (HF) represents a major cause of mortality with a prevalence of 1-2% of the adult population (1). With ageing of the population, the impact of HF is suspected to increase in future. Health care costs for treatment of HF also underlie a constant rise and pose a significant burden for society (2). Therefore, it will be important to identify HF risk in patients earlier, possibly even before the onset of clinical symptoms, to immediately start interventions like lifestyle changes or medication.

Cell-free DNA (cfDNA) is released from cell nuclei into blood and other body fluids, in particular after diverse kinds of stress-induced cell damage (3). Elevated levels of cfDNA could thus be associated with disease conditions like cancer, sepsis, stroke, trauma, autoimmune diseases and cardiological diseases (4). Consequently, cfDNA bears the promise to serve as a valuable biomarker and in fact is already being applied in the framework of 'liquid biopsies' for detecting and monitoring cancer entities (5). In the field of cardiology, however, the research on cfDNA and its potential application as a diagnostic tool is still in its infancy. Only a limited number of studies, often using rather small cohorts, have addressed cfDNA in different cardiological diseases like myocardial infarction, hypertension, and HF (6-8). It is thus currently unclear, if cfDNA quantification offers an improved sensitivity and earlier detection of cardiological conditions like HF, rather than the use of established biomarkers like the protein NT-proBNP.

The prospective **MyoVasc** study (NCT04064450), comprising n=2700 probands with heart failure and n=500 control subjects, offers a unique opportunity to investigate cfDNA as a potential biomarker in a much larger cohort than used in previous studies. MyoVasc has collected biosamples in a systematic way, in addition to obtaining comprehensive data from echocardiography, carotid sonography, ankle-brachial index, body plethysmography, capacity exercise testing, blood pressure measurements, ECGs, health surveys and blood tests over a period of 6 years for each of the 3200 subjects enrolled. The MyoVasc samples will thus facilitate searching for correlations between cfDNA levels and HF pathologies, which might ultimately improve disease outcome prediction in HF patients.

The overarching objective of the present work is thus to explore the potential use of **cfDNA as a predictive diagnostic tool for HF**. *Total* cfDNA levels will be measured in the baseline plasma samples of the MyoVasc probands, as such *total* cfDNA quantification will be more applicable for actual clinical diagnostics due to its relative ease of use. So far, however, a lack of standardization for quantitative cfDNA measurements complicates the comparison between

different study results and clinical laboratories. Most studies (e.g., (9, 10)) still use extraction of DNA prior to the measurement, which reduces DNA yield and increases variability dramatically. Furthermore, the different quantification methods used cannot be compared in terms of sensitivity/specificity and limits of detection (LOD). Therefore, a technical goal of this thesis is to establish a **reliable, standardized method for cfDNA quantification in a high number of study samples**. At the same time, the procedure should be easy to perform, time-efficient and resistant to inter-operator influences.

For cfDNA quantification, an already established direct qPCR protocol shall be applied, which detects multicopy transposons from a human LINE sequence family (11). This approach has superb sensitivity and low LOD, and it promises to be cost-effective for a large number of samples. Two different qPCR assays with amplicon lengths of 90 and 222 base pairs (bp), respectively, will be compared to obtain additional information on cfDNA length by calculating the integrity index. Instead of manually pipetting each sample in triplicates, the plan is to **establish a robotic system** based on the INTEGRA Assist Plus, which will help reduce manual labour, time needed per sample, and which will be less prone to inter-operator variabilities.

The results of *total* cfDNA quantification will be statistically analyzed in the context of the already existing data of the MyoVasc study in an explorative way. Associations between cfDNA levels and all kinds of clinical parameters, especially NT-proBNP levels, will be addressed. Cox proportional hazard regression models and survival analyses should help defining the relevance of cfDNA levels in the prediction of disease progression while looking at three different outcomes, i. e. worsening of HF, cardiac death and all-cause death.

2 Literature discussion

2.1 Definition and history of cfDNA

Cell-free DNA (cfDNA) is a type of DNA that is not anymore contained within intact cells, but rather circulates freely in the bloodstream and other body fluids such as urine (12), saliva (13), bronchial lavage fluid (14), cerebrospinal fluid (CSF) (15), amniotic fluid (16), seminal fluid (17) and even stool (18). cfDNA is released by cells as they undergo normal processes of life, as well as during cellular stress conditions including inflammation, injury, tumorigenesis, and cell death. Under these pathological conditions, the amount of cfDNA can be increased substantially up to 12-fold (19). cfDNA circulates in a fragmented form, with fragment sizes mostly ranging from around 50 to 200 base pairs (bp). The average molecule of cfDNA is ~166 bp long and mostly double-stranded (20). While cfDNA is mainly of nuclear origin (and thus sometimes also called cf-nDNA, also mitochondrial DNA can occur freely in body fluids and is termed cf-mtDNA (21). For a complete overview on the nomenclature of cfDNA components, see Bronkhorst et al. (22).

Historically, extracellular nucleic acids (RNA and DNA) were first described in human blood plasma by Mandel and Metais in 1948 (23). In 1966, Tan et al. (24) discovered an increased concentration of cfDNA in patients with active systemic lupus erythematosus (SLE) and considered this as a potential trigger for the formation of SLE-typical antibodies against double-stranded DNA. Leon et al. (25) in 1977 detected an increase in cfDNA concentration in over half of their cancer patients, showing that cfDNA concentration was significantly higher in patients with metastatic cancer compared to non-metastatic cancer. In this study it was even possible to highlight the effect of radiation therapy in patients by measuring a decrease of cfDNA concentration. With the advent of molecular analytical methods, Stroun et al. (26) in 1989 gave first evidence that cfDNA molecules isolated from the plasma of cancer patients in fact originated from cancer cells. Five years later, Vasioukhin et al. (27) proved this by showing tumour-specific mutations in the N-RAS oncogene within plasma cfDNA from patients suffering from myelodysplastic syndrome or acute myelogenous leukaemia. The possibility to extract and analyse the circulating tumour DNA (ctDNA) from patients' blood paved the way for the non-invasive diagnostical tool of liquid biopsy. The emergence of new technologies for DNA analysis like polymerase chain reaction (PCR) and – in recent years – next-generation sequencing (NGS) enabled more sensitive and accurate detection of cfDNA, thus leading to the rapid expansion of this field of research.

One of the first clinical applications of cfDNA was in prenatal testing of foetal genetic disorders. In 1997, Lo et al. (28) discovered foetal cfDNA to be present in maternal blood samples. This opened up the possibility of non-invasive prenatal diagnostics (NIPD) of genetic disorders with simple sample collection from the mother's bloodstream. NIPD was a major technological breakthrough since it eliminated the need for risky invasive procedures such as amniocentesis or chorionic villus sampling. In the subsequent years, studies showed that -like nuclear DNA - cfDNA is methylated and exploited its use as an epigenetic biomarker. For example, Esteller et al. (29) in 1999 first detected aberrant promoter hypermethylation of tumour suppressor genes in the cfDNA of non-small cell lung cancer patients, and Wong et al. (30) reported aberrant p16 methylation in cfDNA from liver cancer patients.

The past 25 years have seen an ever-increasing use of cfDNA as a diagnostic marker in many medical conditions. Particularly in the field of oncology, cfDNA has been shown to be a potent biomarker for diagnosis, treatment monitoring and detection of tumour recurrence (5). Of note, cfDNA originating from tumours carries cancer-associated genetic mutations, which can be diagnosed via DNA-sequencing. In transplantation medicine, the analysis of donor-derived cfDNA (ddcfDNA), which carries diagnostic donor-specific genetic variants, can detect early signs of organ rejection, allowing for prompt intervention to prevent organ loss (31). In intensive care units (ICU), cfDNA levels can be a powerful marker for the prediction of mortality in septic patients (32). Quantitative cfDNA analysis in stroke patients also showed a high predictive value in mortality as well as correlations with short-term neurological outcome, results of therapeutic intervention and size of ischaemic areas (33). In trauma patients, increased concentrations of cfDNA correlated with the severity of trauma and predicted the mortality (19). During myocardial infarction, cfDNA concentrations significantly increased within the first two hours after onset of chest pain. After percutaneous coronary intervention, concentration levels sank to baseline values within two days, in contrast to the commonly used troponin, which remained elevated (6). Moreover, increased cfDNA levels have been shown to correlate with several cardiometabolic risk factors and with higher blood pressure (7). McCarthy et al. (34) demonstrated the activation of the immune system leading to an increased arterial blood pressure by the binding of cf-mtDNA to Toll-like receptor 9 (TLR9) in spontaneously hypertensive rats.

In addition to its clinical applications, cfDNA is currently also investigated and applied as a tool in non-medical research fields such as forensics (35) and environmental monitoring (4, 36).

2.2 Size distribution and cellular origins of cfDNA

cfDNA can not only occur freely in plasma in the form of nucleosomal DNA (20), but also be transported inside extracellular vesicles (e.g., exosomes, apoptotic bodies) (37) or in complexes with other proteins like immunoglobulins (38), albumin (39) and lipoproteins (40). cfDNA is also found bound to cell surfaces of erythrocytes and leukocytes (41-43).

cfDNA of nuclear (cf-nDNA) or mitochondrial (cf-mtDNA) origin can have different length distributions. While cf-nDNA fragments tend to have an average length of 166 bp, which approximates the size of nucleosomal DNA, cf-mtDNA seems to have shorter fragments with a peak between 125 - 150 bp (44), possibly because mtDNA is free of nucleosomes. The size distribution of ctDNA was not clear for a long time. While some groups reported an increased integrity of ctDNA with a higher proportion of longer fragments (45-47), others detected higher ctDNA levels when using shorter PCR amplicons, indicating a shift towards shorter ctDNA fragments in tumour patients (48, 49). Mouliere et al. (49) claimed the majority of fragments being < 100 bp. By applying massively parallel sequencing, Jiang et al. (44) could demonstrate that the size profile shifted to shorter fragments with increasing fractional concentrations of ctDNA. Of note, in patients with lower ctDNA concentrations, they observed an apparently longer size distribution, suggesting the presence of an additional cfDNA component potentially originating from non-neoplastic tissues surrounding the tumour (44). A high level of fragmentation resulting in shorter fragments is equal to a low integrity of the cfDNA (50). The ratio of short to long fragments is described as the cfDNA integrity index (51). It remains to be demonstrated whether this integrity index of cfDNA may have diagnostic value and clinical importance in future.

The cellular origin of cfDNA can vary depending on the specific biological context. There are four different mechanisms contributing to the release of DNA into the extracellular space: apoptosis, necrosis, active DNA release and exogenous sources (52).

• **Apoptosis**, also known as programmed cell death, can be triggered by many different physiological and pathological factors. The main characteristic of apoptosis is cell shrinkage and degradation within its intact plasma membrane. The DNA released during this process is degraded first into larger (50-300 kb) and then into shorter (180-200 bp) fragments. The shorter fragments correspond to the size of nucleosome units and are characteristic for degradation via the caspase-activated DNase (CAD) (53). Consequently, there also exist multiples of

nucleosomal units with up to 1000 bp in cfDNA, which can be observed in a typical ladder pattern in gel electrophoresis.

• **Necrosis**, in contrast, is premature cell death due to injury caused by external triggers like infection, toxins, hypoxemia or other aggressive environmental conditions such as heat, radiation or UV light. In difference to apoptosis, the cells begin to swell, the plasma membrane disintegrates and the cell content is released in an unorganized way (54). As necrosis happens faster than apoptosis, but degradation of the necrotic cells is slower, the cfDNA fragments released during necrosis tend to be much longer than apoptotic DNA fragments with lengths of > 10.000 bp (50, 55-57).

Due to the predominant size profile of cfDNA investigated in healthy and diseased patients of 166 bp, it is concluded that the bulk of cfDNA originates from apoptosis rather than from necrosis (53, 57-59). Other groups however observed larger cfDNA fragments in the blood of cancer patients, suggesting that these originate from necrosis (46, 47, 60-62). One other point that speaks against necrosis as the major cfDNA release mechanism is that cfDNA levels decrease drastically after radiation therapy, which induces necrosis. Clearly, the opposite should happen, if necrosis were to be the main source of cfDNA (25, 63). On the other hand, one could argue that this effect occurs due to inhibition of the cfDNA release pathways of healthy cells by radiation (62).

• An **active release of cfDNA** was first described by Stroun et al. (64) and Rogers et al. (65). *In vitro* experiments with human osteosarcoma cells by Bronkhorst et al. (66) confirmed that the main source of cfDNA after 24h of incubation was the active release of DNA, rather than apoptosis or necrosis. Wang et al. (67) showed a positive correlation between cfDNA levels and the number of cells being in the actively synthesizing G1 phase. Aucamp et al. (68) studied eight different cell lines and found a correlation between their active release levels and the cells' growth rates as well as their cancer status. The authors hypothesised that these active cfDNA release mechanisms could be used for communication between cells.

Rogers et al. (65) discovered active release of cfDNA from stimulated lymphocytes. Other groups confirmed the origin of cfDNA from lymphoid and myeloid hematopoietic cells (20, 69-71). These data suggest that the majority of cfDNA originates from hematopoietic cells and is released by active secretion.

According to current knowledge (52), NETs (neutrophil extracellular traps), extracellular vesicles and erythroblast enucleation are mechanistically involved in active cfDNA release:

(i) NETs are shed by neutrophils in an active process called NETosis (72). They represent web-like structures of extracellular DNA, histones, antimicrobial enzymes, and proteins (73, 74). NETs serve as a defence against exogenous threats such as bacteria, viruses, fungi and parasites (75). Recent studies have also promoted a potential role of NETs in the emergence of non-infectious diseases such as systemic lupus erythematosus (76), atherosclerosis (77, 78), endothelial cell damage (79), vasculitis (80), trauma (81), thrombosis (82), cancer (83), sepsis (84, 85) and in the inflammatory response (86, 87). High levels of NETs – and their associated cfDNA – have also been observed after intense physical exercise (43, 88). The contribution of NETosis to the origin of cfDNA is an area of active research, and further studies are needed to fully understand the role of NET-derived cfDNA in various disease conditions.

NETosis can be divided in two forms: suicidal and vital NETosis. While suicidal NETosis leads to membrane lysis and cell death, vital NETosis is performed by blebbing of the nucleus and exocytosis of DNA-filled vesicles through the intact plasma membrane, leaving the neutrophils alive and able to keep their phagocytic functions (89-91). Suicidal NETosis can take up to hours, while vital NETosis can happen within minutes (89). NETosis does only occur in neutrophils, but similar processes have been described in eosinophils, basophils, monocytes, macrophages, B cells and mast cells (87). It is then commonly referred to as “Etosis”.

(ii) Extracellular vesicles (EVs) are small particles surrounded by a lipid bilayer and are shed by almost all types of cells (92). Those vesicles can originate from the endosomal part of the cell membrane and are then called exosomes. If they originate from the outer surface of a cell, they are called microvesicles. In the literature, the differentiation is not always taken into account and extracellular vesicles and exosomes are often used synonymously. Exosomes contain proteins and lipids specific for their cell of origin (93). They also incorporate different types of RNA such as mRNA, miRNA and tRNA (94) as well as cfDNA of genomic or mitochondrial origin (93, 95). Although cfDNA can be found both on the surface and in the lumen of exosomes (93), Neuberger et al. (96) could show that most of the associated DNA is found on the surface of extracellular vesicles. As studies suggest, exosomes – and thus their associated cfDNA – play a fundamental, but yet not fully understood role in cell-to-cell communication, transfer of macromolecules between cells and in maintaining cellular homeostasis (97-99). In terms of contribution to *total* cfDNA levels, EVs yet only play a minor role (96).

(iii) Erythroblast enucleation is yet another source of actively released cfDNA (52). While the erythroblasts mature to fully functioning erythrocytes, they need to get rid of their nuclei to

optimise for their function in oxygen transport. Enucleation involves processes such as apoptosis, DNase II digestion in macrophages and autophagy of nuclei, all which represent a natural source of cfDNA (100).

• Last but not least, cfDNA can not only originate from the organism itself, but also from **exogenous sources** like the host microbiome (101), bacterial or viral infections (102, 103), parasites (104) or even ingested food (105). Foetal cfDNA in maternal blood (106) and donor-derived cfDNA in organ transplant recipients (107) also represent an exogenous source of cfDNA.

In conclusion, the cellular origins of cfDNA are highly diverse and biologically complex, requiring further research. The understanding of the cellular origin and the underlying release mechanisms involved is crucial for the application of cfDNA as a biomarker.

2.3 Clearance and kinetics of cfDNA

Levels of cfDNA depend both on the release and on the degradation and clearance of DNA. If these processes are disturbed, this leads to a shift in homeostasis and altered, most often increased cfDNA concentrations. Multiple studies found that low cfDNA concentrations in healthy subjects correlate with high levels of DNase in blood, while the opposite is true in diseased patients (108-111). As Velders et al. (111) further reported, rising cfDNA levels during exercise in healthy subjects triggered an increase of endogenous DNase activity to maintain homeostasis.

Instead of extracellular degradation via DNase, cfDNA is also internalised and digested intracellularly. The recycled mononucleotides get transported into the nucleus and are ready to be reused (39).

The remaining cell-free DNA is eliminated through the organs. While the liver plays the biggest role in absorbing and metabolising cfDNA (112, 113), a smaller amount is excreted via the kidneys (114). While ssDNA is preferentially metabolised in the liver, dsDNA is excreted via the kidneys. This is one cause leading to a longer retention of dsDNA in the bloodstream (115).

By studying foetal cfDNA in maternal blood, Lo et al. (116) measured a mean half-life of circulating foetal DNA of 16,3 min. Diehl et al. (117) estimated the half-life of ctDNA as 114 min by analysing patients' plasma at multiple timepoints after complete tumour resection.

2.4 Significance of cfDNA as a biomarker

2.4.1 Applications in oncology

In general, cfDNA can be studied as a biomarker either with quantitative or qualitative analytics. In oncological research, both approaches are applied to analyse ctDNA for its quantity, its cellular origin, and eventual tumour-specific genetic mutations, which provide valuable information for diagnosis, treatment monitoring and detection of tumour recurrence (5).

As *total* cfDNA levels were neither sensitive, nor specific enough to determine overall tumour burden, nowadays only its ctDNA fraction is routinely tested. ctDNA makes up part of the cfDNA at variant allele fractions (VAFs) mostly ranging from <0.1% to 10% (118), though it can be much higher, e.g., in some metastatic patients (119, 120). Higher VAFs correlate with increased tumour burden and worsening of prognosis. Recent studies also demonstrated the use of ctDNA quantification to detect minimal residual disease (MRD) (121, 122) as well as for primary blood-based cancer screening test (123, 124). These studies also showed limitations of ctDNA analysis, as some cancer types released less DNA than others for unknown reasons. Despite all these studies showing promising results in quantitative analytics of ctDNA, real clinical utility in terms of improving patients' outcomes could not be shown yet in studies (118). That is the reason why until now only qualitative ctDNA analyses mostly involving the sequence analysis of characteristic mutations in known tumour-suppressor or oncogenes are used for clinical decision making. With the advent of next generation sequencing (NGS), ctDNA is now being investigated for several such mutations in many candidate genes, thereby opening the possibility for targeted therapy (118). Using NGS during anti-cancer therapy, one can also identify emerging resistance mutations, which predict poor response to respective drugs. Until now however, sequencing of ctDNA is less sensitive than the equivalent analytics of tissue DNA. To reach comparable results, multiple time-consuming NGS runs with more plasma volume, extensive bioinformatics and overall higher costs are needed. However, with the improvement of NGS technologies and decreasing costs, it could soon be possible to reach equal sensitivity (118). An advantage of liquid biopsies over serial tissue biopsies is the capability of better capturing the genomic complexity of the whole tumour including metastatic sites (125).

To determine the tissue origin of ctDNA, methylation analyses can be performed. Via bisulphite treatment followed by NGS, one can distinguish methylated from unmethylated genomic regions and thereby draw conclusions about the origin of the ctDNA (124). Another way of identifying the tissue of origin is by analysing the ctDNA's fragmentation pattern (126).

2.4.2 Applications in transplantation medicine

In transplantation medicine, injury or rejection of the graft pose the biggest problem. Therefore, monitoring the recipients' immune reaction and regular assessments of organ function need to follow the initial transplantation. The currently used diagnostics primarily involve biopsies in addition to organ specific blood markers and duplex sonography. While these currently used blood markers often do not indicate organ rejection until late in the process, biopsies have a significant complication rate of, e.g., 1% in kidney recipients (127).

As Lo et al. first described in 1998 (31), cfDNA derived from the donor's organ can be detected in the recipient's blood. This so-called donor-derived cell-free DNA (ddcfDNA) therefore opens possibilities to monitor graft health via liquid biopsy, allowing for prompt intervention to prevent organ loss (128). Citing the latest review by Oellerich et al. (127) on this topic, the analysis of ddcfDNA represents a promising tool in management of transplanted patients and is already used for routine testing in the US.

Either the absolute level of ddcfDNA or the fraction of ddcfDNA in relation to the *total* cfDNA can be determined. For the most comprehensive diagnostic information in clinical practice, a combination of both values should be used, as fractional ddcfDNA is easily influenced by variations in *total* cfDNA. The overall downside of ddcfDNA is its missing specificity concerning rejection, as elevated levels can be also observed due to other causes of graft injury. To prove clinical utility, controlled studies are currently running to compare clinical outcomes in patients monitored with ddcfDNA and without monitoring (127).

2.4.3 Applications in intensive care during sepsis, stroke, and trauma

In intensive care, cfDNA can be used to assess several acute diseases like sepsis, trauma, and stroke. By analysing blood samples for cfDNA taken on admission to the ICU, Rhodes et al. (32) could detect higher levels of cfDNA in ICU patients compared to healthy controls. As the levels were also significantly higher in patients, who developed sepsis or died subsequently, cfDNA may be a useful early prognostic marker of mortality and sepsis in intensive care patients (32). In septic patients, a correlation with maximum lactate value and Sequential Organ Failure Assessment (SOFA) score was shown (129). Dwivedi et al. (130) demonstrated a better prognostic utility for cfDNA than MODS (Multi Organ Dysfunction Syndrome) or APACHE (Acute Physiology and Chronic Health Evaluation) II scores in septic patients. The predictive power of cfDNA could potentially be even stronger by combining it with protein C and MODS scores (130).

Rainer et al. (33) recruited patients presenting with stroke-like symptoms to the emergency department for cfDNA analysis. cfDNA levels were significantly increased (fivefold) in patients who died compared to those who survived at discharge or even 6 months later and correlated with the Glasgow Coma Scale (GCS), cerebral haemorrhage volume, post-stroke modified Rankin Score and quality of life loss (33). Vajpeyee et al. (131) studied the outcome of stroke patients undergoing therapeutic intervention. cfDNA levels correlated with severity of stroke at the time of admission assessed with The National Institutes of Health Stroke Scale (NIHSS). The values also predicted poor outcome at three months measured by modified Rankin scale (mRS) score and correlated with the outcome in patients after therapeutic intervention (131). Therefore, quantitative cfDNA analysis in stroke patients shows high predictive value in mortality and morbidity.

Trauma patients studied by Lo et al. (19) also showed significantly increased cfDNA levels correlating with the severity of trauma. cfDNA levels were around 12-fold higher in patients who subsequently developed severe complications including death compared to those who did not. In these trauma patients, cfDNA also served as a prognostic biomarker for mortality and morbidity. In patients suffering from traumatic brain injury (TBI), Shaked et al. (132) demonstrated cfDNA as a sensitive biomarker for the severity of injury and reported prognostic significance regarding interventions and neurological sequelae.

2.4.4 Applications in autoimmune diseases

The first clinical study on cfDNA was performed in patients suffering from systemic lupus erythematosus (SLE) by Tan et al. in 1966 (24) and showed significantly elevated cfDNA levels compared to healthy individuals. These results were confirmed in several subsequent studies (133-136). Others, however, could not confirm a positive correlation between cfDNA concentration and disease severity (137, 138). Inconsistent results were also found for the dynamics of cfDNA levels due to therapeutic interventions (135, 138).

For rheumatoid arthritis, which primarily affects and destroys patients' joints, studies could also demonstrate a significant increase in cfDNA plasma concentrations (139-141). In synovial fluid even higher cfDNA levels could be detected (139, 141). These studies suggest a strong correlation between disease activity, response to therapy and cfDNA levels (140, 141).

2.4.5 Applications in perinatal medicine

Lo et al. (28) first proved the presence of foetal cfDNA in maternal blood. Following this discovery, analyses for foetal sex determination and risk assessment of pre-eclampsia were successfully performed (142, 143). A meta-analysis of 60 studies as well as a prospective study with 3322 participants could show a sensitivity and specificity of >99 % for sex determination via the presence/absence of Y- and X-chromosomal DNA sequences (144, 145). The same sensitivity and specificity could be reached in determination of the foetal rhesus factor (146).

The possibilities of non-invasive prenatal diagnostics (NIPD) of genetic disorders such as numerical and structural chromosomal aberrations have also been investigated and showed promising results (145, 147, 148). The screening for foetal trisomy 21 showed with >99 % a slightly better sensitivity and specificity than for trisomy 18 and 13, which only reached a sensitivity of 97,7% and 90,6%, respectively. Due to the low prevalence of common sex chromosome aneuploidies, the analyses showed limited positive predictive value despite their relatively high sensitivity and specificity (144, 145). Structural chromosomal aberrations in genetic diseases like achondroplasia and β-thalassaemia could be detected effectively via NIPD in small studies, but further investigations are needed to proof clinical utility (147, 148).

2.4.6 Applications in sports medicine

Physiological stress like exercise also leads to the release of cfDNA in the human body and results in up to 20-fold (149) increased cfDNA levels compared to baseline values at rest. This has already been shown in sports disciplines like endurance running (150) and cycling (151), interval training (152), strength training (153) and rowing (111).

While the origin of exercise-induced cfDNA release is still controversially discussed, studies could narrow down the main cellular sources. Beiter et al. (154) could show that immune-activated neutrophils releasing NETs contribute a large part to *total* cfDNA concentration during exercise. By studying sex-mismatched hematopoietic stem cell transplantation patients, Tug et al. (70) suggested cells of the hematopoietic lineage to be the main source of cfDNA during exercise. With targeted CpG site methylation analysis, Neuberger et al. (149) showed that granulocytes are the major source of cfDNA during exercise. A single bout of high-intensity exercise triggers a concomitant rise in DNase I activity, which efficiently counterbalances the increase in cfDNA in healthy individuals. This leads to a decrease of cfDNA levels close to baseline values within 30 min after completion of exercise (111, 154). While these rapid kinetics primarily apply to high intensive anaerobic exercise, long-lasting aerobic sports and

repetitive, intensive training stimuli rather lead to longer times of increased cfDNA levels. Apoptotic and necrotic processes based on local damage and inflammation of muscles seem to play a major role in these slower dynamics (43). Infiltrating lymphocytes and neutrophils degrade injured muscle cells through inflammatory immune response. This immunological response is terminated by apoptosis of leukocytes which also leads to post-exercise lymphocytopenia (155) and could contribute to the long-term elevated cfDNA levels (150, 156). In a twelve-week resistance training program, Fatouros et al. (153) could measure increased cfDNA concentrations up to 96 h after training, accompanied by other elevated biomarkers like C-reactive protein (CRP), creatine kinase (CK), and uric acid (UA), indicating muscle damage and inflammation. They suggested cfDNA to be a marker for monitoring and quantification of overtraining in athletes (153). By analysing fragment lengths of cfDNA during and after exercise, Tug et al. (151) could show a shift towards shorter fragments during exercise and to longer fragments afterwards, which fits the theory of different release mechanisms of cfDNA. In summary, not only the duration but also the exertion of the exercise, the duration of breaks in interval training and the associated types of metabolism (aerobic/anaerobic) have an influence on the dynamics of cfDNA (43, 157, 158).

All these results offer potential advantages of cfDNA over lactate as a biomarker in performance diagnostics. Lactate does not increase linearly during endurance exercise (159), does not correlate with the total distance covered in one football season (157) and is not influenced by the exercise intensity in weightlifting (158). The only drawback of cfDNA could be the difficulty to distinguish trained and un-trained probands, as it is possible with lactate (154). Overall, cfDNA therefore seems to have big potential for monitoring training load in athletes and prevent overtraining (160), but further, larger studies are needed to confirm this.

2.4.7 Applications in cardiology

In the field of cardiology, prompt diagnosis and treatment are of utmost importance, and novel, fast and easy detectable biomarkers are therefore highly relevant. Damage to the heart or the circulatory system should in principle lead to a release of cfDNA. In this respect, cfDNA has previously been studied in different cardiological diseases including myocardial infarction (6, 161), hypertension (7, 34) and heart failure (8, 162-164).

In their pioneer study, Chang et al. (161) detected more than 10-fold higher cfDNA concentrations in sera of patients (n=55) diagnosed with **myocardial infarction** (MI). While increased creatine kinase (CK) levels in blood were associated with elevated cfDNA levels, there were no correlations between cfDNA concentrations and the concentrations of CK,

troponin I and C-reactive protein (CRP). In a later pioneer study using epigenetic marks, Zemmour et al. (6) were the first to perform methylation-based quantitative analysis of *cardiac-specific* cfDNA in n=57 patients with MI. Unlike *total* cfDNA, *cardiac* cfDNA levels correlated well with CK and high-sensitivity troponin-T (hs-cTn). *Cardiac* cfDNA showed similar specificity as cardiac troponin and even greater specificity than the general muscle markers CK or myoglobin. In sensitivity, *cardiac* cfDNA was slightly inferior to troponin. Regarding its kinetics, *cardiac* cfDNA levels significantly increased 0-2 h after onset of chest pain, thus enabling early detection of patients with MI. Percutaneous coronary intervention led to a drastic increase in *cardiac* cfDNA and troponin levels as an indicator of successful reperfusion. *Cardiac* cfDNA levels returned to baseline after 1-2 days, while troponin levels remained elevated. The authors proposed *cardiac* cfDNA as a specific biomarker for myocardial cell damage, complementing currently used markers like CK and troponin.

In a large cross-sectional health examination survey with 1337 participants in Finland, Jylhävä et al. (7) showed a correlation of increased *total* cfDNA levels with several **cardiometabolic risk factors** like high blood pressure, unfavourable lipid metabolism profile and systemic inflammation in both sexes. Higher cfDNA levels were also associated with low-grade inflammation markers like Interleukin-6 and Interleukin-8. Furthermore, elevated cfDNA levels indicated a decrease in arterial elasticity in women not using hormonal replacement therapy and could therefore be an indicator of arterial stiffness (7). The Finnish group also identified cfDNA levels to be an independent predictor of all-cause mortality in patients with or without already existing cardiovascular diseases (CVDs) (165). Pointing in the same direction, McCarthy et al. (34) reported that in spontaneously hypertensive rats cf-mtDNA binding to Toll-like receptor 9 (TLR9) led to an activation of the immune system, resulting in higher arterial blood pressure.

Polina et al. (166) proposed *total* cfDNA as a potential marker for the development of post-MI **heart failure** (HF), as cfDNA could potentially trigger the activation of inflammatory cells leading to cardiac remodelling and HF after MI. However, it remained elusive how cfDNA correlated with MI-induced complications like HF mechanistically. As a possible molecular explanation, Dutta et al. (164) reported that cfDNA was released from the myocardium as a damage-associated molecular pattern (DAMP), signalling danger due to persisting stress in cardiomyocytes. DAMPs typically induce inflammatory signalling by activation of fibroblasts, macrophages, and other immune cells, which leads to interstitial tissue fibrosis and

cardiomyocyte cell death. This in turn would result in HF due to loss of contractility and reduced cardiac function.

Also investigating cfDNA in the context of HF, Yokokawa et al. (162) found significantly elevated levels of *cardiomyocyte-specific* cfDNA in heart failure patients (n=32) compared with control subjects (n=28), while *total* cfDNA levels did not differ between the groups. Another study (n=39 subjects) even showed a decrease of *total* cfDNA plasma levels in heart failure patients after administration of the calcium sensitizer levosimendan, accompanied by an increase in myocardial performance (8, 167). Salzano et al. (163), however, measured six-fold higher *total* cfDNA levels in HF patients (n=71) than in healthy subjects (n=64) and showed significant correlations of cfDNA levels with the New York Heart Association (NYHA) classes and with blood markers like albumin, calcium, creatine phosphokinase and beta-2 globulin. cfDNA levels also added to patient risk stratification when combined with B-type natriuretic peptide (BNP), with cfDNA being the weighing factor. The authors therefore suggested cfDNA quantification as an additional method to monitor and stratify the risk of outcome in HF patients.

As reviewed by Devaux (8), the currently used biomarker for heart failure detection, N-terminal pro B-type natriuretic peptide (NT-proBNP), failed to accurately predict left ventricular remodelling after myocardial infarction, which can lead to heart failure in 20% of the cases. He also noted that NT-proBNP plasma levels can be elevated due to non-cardiovascular causes. Here, cfDNA could hypothetically improve the predictive value for these patients. Devaux suggested that it could also be interesting to investigate the differences in circulating profiles of cfDNA according to the aetiology of heart failure (8).

In conclusion, there is still a rather limited number of studies which investigated cfDNA in the context of cardiology. Moreover, most studies comprised comparatively low numbers of subjects and were not designed to gather long-term data. In particular, it is still unclear, if the successful application of cfDNA as a biomarker in cardiology will require the rather tedious and expensive analysis of *cardiac* cfDNA via detection of epigenetic marks, or if the much more straightforward analysis of *total* cfDNA from blood plasma suffices.

Figure 1 gives an overview of the currently used clinical applications and potential use of cfDNA in the human body (4).

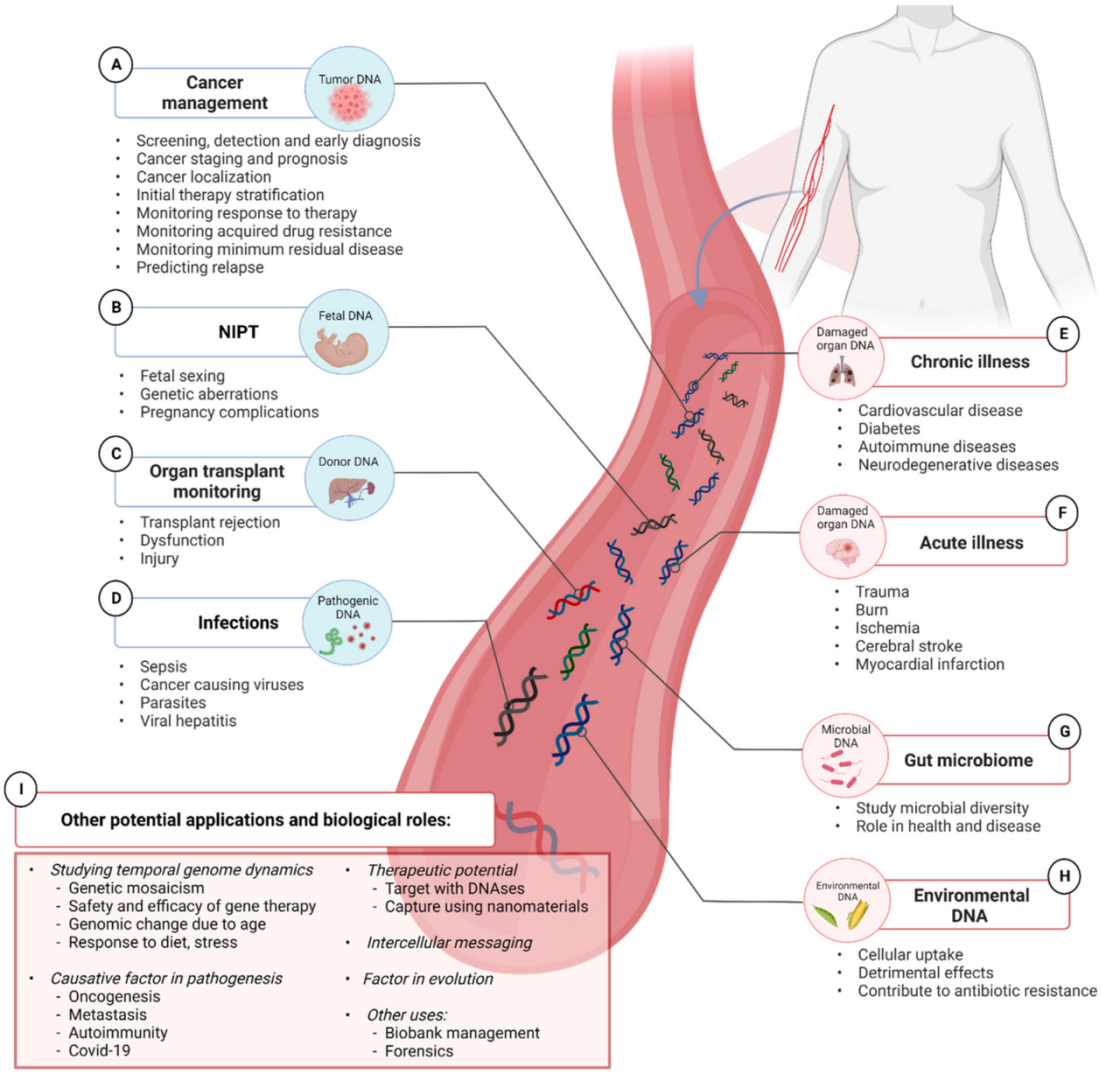

Figure 1 - Clinical applications and potential roles of cfDNA in human biology, extracted from Bronkhorst et al. (4)

2.5 Pre-analytical considerations and methods for the quantification of cfDNA

In conclusion of chapter 2.4, cfDNA is a promising field of basic research with a wide range of potential clinical applications in various medical fields, including cardiology. While significant progress has been made in cfDNA analytics, several challenges still exist, including the need for more sensitive and specific methods of cfDNA detection and analysis. In particular, the standardization of protocols for cfDNA extraction and analysis has to be improved, and

protocols have to be adapted for analysing high numbers of samples to account for large study cohorts.

Accurate measurements of cfDNA concentration and its fragmentation size distribution are of course key to provide valuable information, whenever cfDNA is intended to be applied as a biomarker. For a standardised analysis, however, also pre-analytical steps like sample collection and processing are essential. Until today, there are no universal standard operating procedures (SOPs) for sample processing established, but respective literature-based guidelines were recently published (9).

In general, while planning a cohort-based comparative study, biological and behavioural factors such as male sex, older age, menopause, smoking, increased body mass index, exercise and fasting need to be taken into consideration, since they knowingly have an increasing effect on cfDNA levels (152, 168). While one study did not find a correlation with chronological age consistently across all samples (169), another even reported lower cfDNA levels in older patients (170). The latter study also showed higher cfDNA levels in female sex (170), representing a relatively inconsistent study situation regarding these factors.

In the initial step of blood collection, large-lumen needles should be used to avoid cell damage and thereby sample adulteration through genomic DNA (9). Blood collection tubes made out of polyallomer have lower DNA binding properties than polypropylene tubes and should therefore be favoured (171). Ethylenediaminetetraacetate (EDTA) prevents blood clotting and cell lysis and is preferred over heparin and citrate, which could inhibit the later performed qPCR (172). Meddeb et al. (9) advised to further process the samples as soon as possible as cell lysis and potential changes in DNA concentrations cannot be excluded. Cooling down to 4 °C is suggested to prevent potential nuclease activity. Plasma is preferred over serum due to changes in DNA concentration during the clotting process and several other disadvantages (9). EDTA blood collection tubes should be centrifuged twice, first at a lower speed around 1000 g to remove the blood cells and then at around 16000 g to get rid of remaining cell organelles and debris (173). While Meddeb et al. (9) and Bronkhorst et al. (10) proposed DNA extraction from plasma to reduce potential degradation/fragmentation due to storage and use, Breitbach et al. (11) developed an easier-to-perform direct quantification PCR assay from unpurified plasma, thereby reducing DNA losses during extraction and reaching higher DNA yield. Sample storage in aliquots of small volume (< 2 ml) at -80 °C was recommended to reduce damage due to repeated freeze-thaw cycles (9).

Several different methods exist for the quantification of cfDNA, each having advantages and disadvantages regarding sensitivity, specificity, cost-effectiveness, and ease of use:

Detection of cfDNA by spectrophotometry and fluorometry both work without any amplification step but need cfDNA extraction prior to analysis for reliable results. In fluorometric detection (174), fluorescent dyes like PicoGreen® binding specifically to DNA improve sensitivity and specificity over spectrophotometry by reducing the contaminating effect of proteins, RNA, and other organic molecules. In some devices like the NanoDrop 3300, both methods can be performed as emissions can be measured at different wave lengths (260 nm in spectrophotometry, 530 nm for detection of PicoGreen in fluorometry) (175). However, both methods do not provide information on the size distribution of cfDNA fragments. Despite occasionally showing significant correlation with β-globin qPCR in clinical use (176), fluorometric cfDNA quantification with PicoGreen® showed variances of up to 60 % compared to qPCR analyses (177).

Next-generation sequencing (NGS) is a recently emerged, very powerful analytical method, which can be used for quantifying and analysing cfDNA, but has its main application in the qualitative analyses of DNA sequences, thereby facilitating the detection of mutations and methylation patterns in cfDNA (118, 178). NGS provides information on the concentration and size distribution of cfDNA fragments by analysing the read depth of the sequencing data and the size distribution of the reads. However, NGS is still relatively expensive compared to other analytical methods and needs extra bioinformatic skills. It is therefore rarely used if the main task is only the quantification and size distribution analysis of cfDNA.

Quantitative polymerase chain reaction (qPCR) is currently the gold standard and mostly used method for accurate quantification of cfDNA (177). It involves amplification of a defined PCR target sequence and the real-time detection of the amplificates via double-stranded DNA-binding dyes (e.g., SYBR Green) or via dye-labelled oligonucleotide probes, which bind to the amplicon DNA. Initially, qPCR was used with extracted cfDNA from plasma or serum and mostly targeted nuclear single copy genes like β-globin (e.g., Chiu et al. 2002 (148)). Umetani et al. (46) were the first who established a direct quantification method of cfDNA without preceding DNA extraction from serum. To improve sensitivity, the authors simply treated the sera with buffer and proteinase K after centrifugation to remove proteins and then PCR-targeted the highly repetitive ALU sequences in the human genome. These repetitive ALU sequences have already been targeted by other groups before (62). Breitbach et al. (11) subsequently developed a direct PCR quantification assay targeting another class of human

genome repeats, the long interspersed nuclear element 1 (LINE1) family 2 (L1PA2). With double-centrifuged plasma and a special polymerase for the amplification of difficult templates they avoided the addition of chemicals like buffer and proteinase K to the plasma samples. Generally, the PCR targeting of highly repetitive sequences like LINE1 and ALU substantially increased the assays' sensitivity and facilitated a lower limit of detection (LOD). Breitbach et al. (11) could also show that – even without the need for DNA extraction – an up to 3-fold higher cfDNA concentration could be measured. This result highlights the relatively low yield of many DNA extraction kits. Furthermore, extraction-free qPCR protocols reduced the unavoidable variability in measurements, which was observed between laboratories due to different extraction methods (179). Until now, there have not yet been systematic experiments comparing the relative efficiencies of ALU and LINE1 targeting primers. Multiplex PCRs can nowadays combine different targets in one PCR run and thereby enable distinguishing between ctDNA and cfDNA or foetal and maternal cfDNA concentrations in one assay (44, 180). Multiplex PCRs also allow for detection of several sequence-specific mutations in ctDNA (181).

The more recently introduced digital droplet PCR (ddPCR) is based on the same principles as qPCR, but by running the amplification process in small droplets of femtoliters either containing one or none of the PCR target sequences, it increases the contrast between targets and unspecific amplificates and thereby achieves higher sensitivity. ddPCR is considered optimal for detection of low-frequency target sequences like low levels of ctDNA (117). Ease of use, no need for reference samples and lower inter-operator variability are other often mentioned advantages. As a drawback, ddPCR currently cannot process as many samples per run as qPCR and is therefore not well suitable for high throughput applications. qPCR on the other hand also has a broader dynamic range and is more economical for large screening studies (182).

3 Material and methods

3.1 Material

3.1.1 Chemicals

The chemicals listed in *Table 1* were used to perform the qPCR assays.

Table 1 - Chemicals

Chemicals	Manufacturer/Supplier/Distributor
DNA Away	Carl Roth GmbH + Co. KG, Karlsruhe
dNTP's	Bioline GmbH, Luckenwalde
Ethanol	Carl Roth GmbH + Co. KG, Karlsruhe
Fluorescein isothiocyanate (FITC)	Sigma-Aldrich Chemie GmbH, Taufkirchen
Hifi Buffer (Art.-Nr. BIO-21098)	Bioline GmbH, Luckenwalde
PicoGreen®	Invitrogen., Life Technologies GmbH, Darmstadt
Surface disinfectant Schülke mikrozid®	Schülke & Mayr GmbH, Norderstedt
SYBR® Green I (10,000x)	Invitrogen, Life Technologies GmbH, Darmstadt
VELOCITY DNA Polymerase (Art.-Nr. BIO-21098)	Bioline GmbH, Luckenwalde
Water ultra-pure (H2O)	Gibco®, Life Technologies GmbH, Darmstadt

3.1.2 Primer

The following primers (*Table 2*) were specifically designed to target the hominoid-specific long interspersed nuclear element 1 (LINE1) family 2 (L1PA2). They were used in the qPCR assays to detect cfDNA levels in the plasma samples.

Table 2 - Primer

Primer	Direction	Sequence (5'-3')	Length (bp)
L1PA2 for	sense	TGCCGCAATAAACATACGTG	20

L1PA2 rev 90bp	antisense	GACCCAGCCATCCCATTAC	19
L1PA2 rev 222bp	antisense	AACAACAGGTGCTGGAGAGG	20

3.1.3 Consumables

The consumables in *Table 3* were used to establish the automated pipetting method and to perform the final measurements in the study samples.

Table 3 - Consumables

Consumables	**Manufacturer/Supplier/Distributor**
Adhesive foil qPCR 384 well plate, Ampiseal	Greiner Bio-One GmbH, Frickenhausen
Falcon Tubes 15 ml (Art.-Nr. 188 261)	Greiner Bio-One GmbH, Frickenhausen
Falcon Tubes 50 ml (Art.-Nr. 227 261)	Greiner Bio-One GmbH, Frickenhausen
Glassware (bottles, measuring cups)	Carl Roth GmbH + Co. KG, Karlsruhe
MICRONIC Manual Push Cap Decapper (Art.-Nr. MP54001)	MICRONIC, Lelystad, Netherlands
MICRONIC Push Caps TPE pink (Art.-Nr. MP53069)	MICRONIC, Lelystad, Netherlands
MICRONIC Tube Rack 96-2-DM (Art.-Nr. MP51225)	MICRONIC, Lelystad, Netherlands
MICRONIC Tubes 0,75ml Push Caps 2D Data-Matrix U-bottom (Art.-Nr. MP52304)	MICRONIC, Lelystad, Netherlands
Nitrile disposable gloves (Art.-Nr. 112-2373)	VWR International GmbH, Darmstadt
Pipette tips 10 µl, Filter (Art.-Nr. 70.3010.255)	SARSTEDT AG & Co. KG, Nümbrecht
Pipette tips 10 µl, Low Retention, Filter (Art.-Nr. 31737)	Axon Labortechnik GmbH, Kaiserslautern
Pipette tips 100 µl, Low Retention, Filter (Art.-Nr. 31739)	Axon Labortechnik GmbH, Kaiserslautern

Pipette tips 100 µl, Filter (Art.-Nr. 70.3030.255)	SARSTEDT AG & Co. KG, Nümbrecht
Pipette tips 1000 µl, Avantgµard, Low Binding, Filter (Art.-Nr. 23217)	Axon Labortechnik GmbH, Kaiserslautern
Pipette tips epT.I.P.S.® 384, 20 µl, PCR clean (Art.-Nr. 0030076001)	Eppendorf AG, Hamburg
Pipette tips GRIPTIPS® 12,5 µl, Long, Low Retention, Sterile, Filter (Art.-Nr. 6505)	INTEGRA Biosciences GmbH, Biebertal
Pipette tips GRIPTIPS® 12,5 µl, Low Retention, Sterile, Filter (Art.-Nr. 6555)	INTEGRA Biosciences GmbH, Biebertal
Pipette tips GRIPTIPS® 125 µl, Low Retention, Sterile, Filter (Art.-Nr. 6565)	INTEGRA Biosciences GmbH, Biebertal
Plastic goods (measuring cups, measuring cylinders)	Carl Roth GmbH + Co. KG, Karlsruhe
qPCR Plates FrameStar® 384 well (Art.-Nr. 34-480LC-0384)	Bio-Budget Technologies GmbH, Krefeld
qPCR Plates my-Budget 96 well (Art.-Nr. 30-SP-1900)	Bio-Budget Technologies GmbH, Krefeld
Reaction Tubes 0,5 ml (Art.-Nr. 667 201)	Greiner Bio-One GmbH, Frickenhausen
Reaction Tubes 1,5 ml (Art.-Nr. 616 201)	Greiner Bio-One GmbH, Frickenhausen
Reaction Tubes 2 ml (Art.-Nr. 623 201)	Greiner Bio-One GmbH, Frickenhausen
Reservoir INTEGRA 10 ml (Art.-Nr. 4373)	INTEGRA Biosciences GmbH, Biebertal
Reservoir INTEGRA 25 ml divided (Art.-Nr. 4353)	INTEGRA Biosciences GmbH, Biebertal
Sapphire PCR Tubes 0,2 ml (Art.-Nr. 683 201)	Greiner Bio-One GmbH, Frickenhausen
Waste bags INTEGRA Assist Plus (Art.-Nr. 4570)	INTEGRA Biosciences GmbH, Biebertal

3.1.4 Devices

Table 4 lists all devices used for establishing the method and measuring the study samples.

Table 4 - Devices

Device	Manufacturer/Supplier/Distributor
Autoclave, Systec VX 150	Systec GmbH Labor-Systemtechnik, Wettenberg
Carrier vessel INTEGRA 10 ml reservoir (Art.-Nr. 4306)	INTEGRA Biosciences GmbH, Biebertal
Centrifuge 5424R	Eppendorf AG, Hamburg
Centrifuge 5810R	Eppendorf AG, Hamburg
Dishwasher, Miele Reinigungs- und Desinfektionsautomat, G 7883	Miele & Cie. KG, Friedberg
Dual Reservoir Adapter INTEGRA (Art.-Nr. 4547)	INTEGRA Biosciences GmbH, Biebertal
Ice maker, Scotsman Flockeneisbereiter, AF-80	MS Laborgeräte GmbH, Wiesloch
Mini table-top centrifuge, Mini Centrifuge	Labnet International, Inc, Edison, NJ, USA
Mini table-top centrifuge, Mini Star	VWR International GmbH, Darmstadt
Mini table-top centrifuge, Rotilabo®-Mini-Zentrifuge	Carl Roth GmbH + Co. KG, Karlsruhe
NanoDrop™ 3300	Thermo Fisher Scientific Inc., Waltham, MA, USA
PCR workbench Herasafe™ KS	Thermo Fisher Scientific Inc., Waltham, MA, USA
Pipette charging cable INTEGRA (Art.-Nr. 4549)	INTEGRA Biosciences GmbH, Biebertal
Pipette Eppendorf Xplorer® plus Move It® 12-channel, 20µl (Art.-Nr. 4861000782)	Eppendorf AG, Hamburg
Pipette Eppendorf Xplorer® plus Move It® 8-channel, 20µl (Art.-Nr. 4861000781)	Eppendorf AG, Hamburg

Pipette INTEGRA Voyager 8-channel, 12,5µl (Art.-Nr. 4721)	INTEGRA Biosciences GmbH, Biebertal
Pipette INTEGRA Voyager 8-channel, 125µl (Art.-Nr. 4722)	INTEGRA Biosciences GmbH, Biebertal
Pipetting robot INTEGRA Assist Plus (Art.-Nr. 4505)	INTEGRA Biosciences GmbH, Biebertal
Thermoblock SmartBlock PCR 384 (Art.-Nr. 5307000000)	Eppendorf AG, Hamburg
Thermoblock SmartBlock PCR 96 (Art.-Nr. 5306000006)	Eppendorf AG, Hamburg
Thermocycler CFX384 Opus™ Real-Time PCR Detection System	Bio-Rad Laboratories GmbH, München
Thermocycler CFX384 Touch™ Real-Time PCR Detection System	Bio-Rad Laboratories GmbH, München
ThermoMixer® C (Art.-Nr. 5382000015)	Eppendorf AG, Hamburg
Vortexer RS-VA 10	Phoenix Instrument GmbH, Garbsen
Vortexer Vortex-Genie® 2	Scientific Industries, Inc., NY, USA
Water bath WiseBath	witeg Labortechnik GmbH, Wertheim

3.1.5 Software

The software listed below (*Table 5*) was applied to plan, execute and evaluate the experiments.

Table 5 - Software

Software	**Developer/Supplier/Distributor**
Bio-Rad CFX Maestro 2.3	Bio-Rad Laboratories GmbH, München
Endnote 20	Thomson Reuters, Philadelphia, PA, USA
Microsoft Excel (2013/2016) Microsoft PowerPoint (2013/2016)	Microsoft Corporation, Redmond, WA, USA

Microsoft Word (2013/2016)	
NanoDrop 3300 2.8.0	Thermo Fisher Scientific Inc., Waltham, MA, USA
R	The R Project for Statistical Computing
VIALAB 3.1.0	INTEGRA Biosciences GmbH, Biebertal

3.2 Methods

3.2.1 Sample collection, processing, and storage

The plasma samples used for analysing the concentration of cfDNA were bio-banked during the baseline examination of each participant included in the MyoVasc study. Venous blood was collected in the study centre using EDTA tubes. The tubes were centrifuged twice at 2500 *g* and 22 °C for 10 min. Afterwards, 200 µl of the generated plasma were transferred into 0,75 ml MICRONIC tubes and frozen at -80 °C. The MICRONIC racks containing all samples were then stored at -80 °C and transported on dry ice to our facilities for measurements of cfDNA concentration.

3.2.2 Real time qPCR of cfDNA in Plasma

3.2.2.1 Calculation of the qPCR reaction mix

The reaction mix used for the INTEGRA Assist Plus pipetting robot was based on the mix previously used for our manual qPCR protocol. It was adapted in a way that allowed us to optimally choose pipetting volumes and reduce potential pipetting errors due to a high viscosity of the liquids. To be able to increase the volume of plasma dilution added to the PCR reaction, we chose a 1:15 dilution instead of 1:10. This also reduced the viscosity of the plasma dilution. For compensation, we reduced the amount of water used for preparation of the MasterMix. All calculations were done based on a final volume of 5 µl per well for each sample, pipetted in duplicates. This resulted in a mix of 1 µl plasma dilution, 3,9 µl MasterMix and 0,1 µl PrimerMix per well with a final primer concentration of 140 nM. The recipes for MasterMix and PrimerMix are displayed in *Table 6*.

Table 6 - MasterMix and PrimerMix recipes as used in the qPCR assay

Volume for 1 ml Mastermix	Chemicals
608,97	H2O
307,69	HiFi buffer (Bioline)
38,46	dNTPs
19,23	SYBR
25,64	Polymerase
1000,00	

	Amount (µl) of 100 µM primer stock
Primer forward (100µM)	14
Primer reverse (100µM)	14
Add H2O	172
Total (140 nM primer mix)	200

Calculating the volume of MasterMix and PrimerMix for a full 384-well qPCR plate, we included a certain amount of surplus volume to safely cover the bottom of the reservoir placed on the INTEGRA Assist Plus. This led to a volume of 1731,6 µl MasterMix and 44,4 µl PrimerMix per PCR run.

Due to an extra step of creating a sub mix in the 222bp PCR assay, we added further 20% surplus volume per well, resulting in a volume of 1950 µl MasterMix and 50 µl PrimerMix for the full qPCR plate.

3.2.2.2 Preparation of reference samples

On each PCR plate we included eight different reference samples (RefSamples) to be measured in each PCR run. All dilutions of RefSamples were prepared in advance to the experiments. Samples were diluted in a 1,5 ml tube with 100 µl of plasma added to 1,4 ml of water (1:15 dilution). They were then distributed into 50 aliquots of 30 µl each and stored at -80 °C.

The first two RefSamples (#1 NTC H_2O; #2 NTC DNA-free plasma) were non-template negative controls. The third and fourth RefSamples (#3 N PRE; #4 N POST) were previously measured PRE- and POST-exercise samples used for interplate calibration. The other RefSamples (#5 Interplate PRE 1; #6 Interplate POST 1; #7 Interplate PRE 2; #8 Interplate POST 2) represented two different PRE- and POST-exercise samples re-measured on each plate for quality control.

3.2.2.3 Sample preparation for qPCR

Before qPCR, the plasma was diluted with water. The MICRONIC racks containing the plasma samples were thawed in the WiseBath water bath for 10 min at 30 °C. Then, the racks were dried, and each corner of the rack was vortexed three times on the Vortex-Genie® 2. In between each vortex cycle, the rack was flipped top down to thoroughly mix the plasma. To finish this step, the rack was shortly centrifuged for 5 sec to remove the plasma from the tube caps.

In the meantime, 96-well plates were prepared for the upcoming dilution step by labelling them with the rack number, date of dilution and by placing them on the INTEGRA Assist Plus pipetting robot (*Figure 2*) (position B and C). To get the calculated 1:15 dilution, we mixed 21 µl of ultra-pure water (position A) with 1,5 µl of plasma.

So, the first step was to distribute the water onto a full plate, except for the 12th column, which was left empty for the already prepared dilutions of reference samples. For this first step of qPCR setup, the Assist Plus program "230102_MV_1" was used in combination with the 125 µl pipette INTEGRA Voyager 8-channel and the corresponding standard GRIPTIPS® filter tips. 21 µl of water were distributed into each well in multi-dispense mode with an added pre- and post-dispense volume of 2 µl.

Figure 2 - INTEGRA Assist Plus pipetting robot

(With kind permission of www.integra-biosciences.com)

In the second step, 1,5 µl plasma from each MICRONIC tube were transferred into its corresponding well in the 96-well dilution plate (position B). The top caps of the tubes were removed using the manual MICRONIC decapper. The whole MICRONIC rack with open tubes was placed on the pipetting robot (position C) and the program "230102_MV_2" was selected together with the use of the 12,5 µl INTEGRA Voyager 8-channel pipette and corresponding long low-retention GRIPTIPS® filter tips. The plasma transfer was performed with a speed of 3. Directly after, the dilution was mixed ten times with a speed of 10 and a mixing volume of 12 µl. Tips were changed after each transfer. Afterwards, the last column of the 96-well plate was manually filled with our already prepared dilutions of eight reference samples.

To finish this step, the 96-well plate, now containing 22,5 µl of plasma dilution in each well, was sealed with a sticking foil and vortexed on the Eppendorf ThermoMixer© C for 4,5 min at 30 °C and 2000 rpm. The resulting dilutions were either directly used for a qPCR run or stored at -20 °C for later use.

3.2.2.4 qPCR protocol

The qPCR MasterMix (MM) was prepared according 2.2.2.1. It was prepared in volumes needed for 5 to 10 qPCR runs and then aliquoted to tubes with the exact volume needed for one qPCR run. These tubes were stored at -20 °C and thawed at room temperature (RT) once, directly before use. The PrimerMix (PM) was also prepared according to 2.2.2.1 and stored in tubes at -20 °C. These tubes could be thawed at RT and frozen several times.

MasterMix and PrimerMix were manually combined to a PrimerMasterMix (PMM) directly before use. Both tubes were vortexed, centrifuged and the needed volume of PrimerMix was pipetted into the MasterMix tube. This tube then was vortexed and centrifuged again. It was kept away from light to prevent degradation of the SYBR dye due to UV light. The PMM was filled into an INTEGRA 25 ml divided reservoir utilizing the dual reservoir adapter, which was placed on the robot (position A) (*Figure 3*).

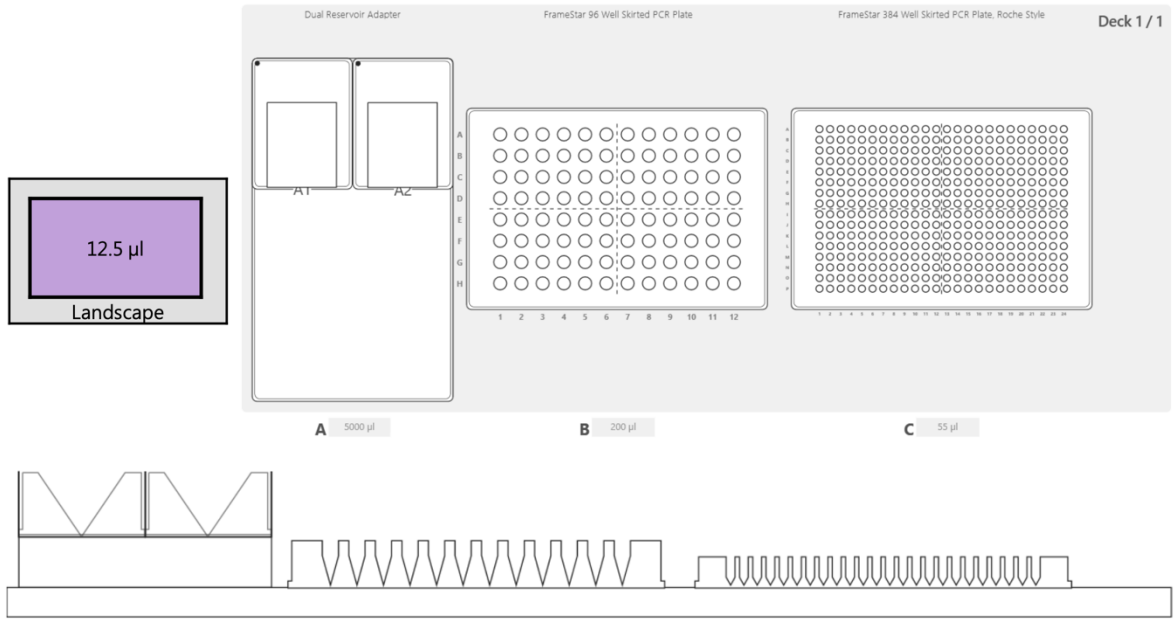

Figure 3 – Pipetting robot setup used for the qPCR protocol

(Purple) pipette tips box, (A) dual adapter reservoir, (B) 96-well plate, (C) 384-well qPCR-plate

From this step on, the protocols for the 90bp and the 222bp PCR assay differed slightly:

3.2.2.4.1 90bp PCR assay protocol

The PMM was distributed directly onto the 384-well qPCR plate (position C) by starting the program “230102_MV_3” using the 12,5 µl pipette INTEGRA Voyager 8-channel with low-retention GRIPTIPS® filter tips. With single-dispense mode, a pipetting speed of 4 and 0,5 µl post-dispense volume, 4 µl of PMM were pipetted into each well. Meanwhile, the foil from the vortexed dilution plate was removed and the plate was placed on the Assist Plus in position B. After distributing the PMM, the robot went on by adding 1 µl of sample dilution to each well with a speed of 3 in single-dispense mode. After each dispense, a mixing step with five cycles, a mixing volume of 2 µl and a speed of 5 was applied and then the tips were discarded. A first 96-well plate containing

plasma dilutions was pipetted in duplicates in the upper half of the qPCR plate. Then, the 96-well sample plate was changed, and another 96 plasma dilutions were added to the lower half. After this step, the qPCR plate was sealed with a foil and vortexed for 1,5 min at 2000 rpm and RT on the ThermoMixer© C to ensure proper mixing of the reaction mix. The dilution plates were sealed too and frozen for later use.

3.2.2.4.2 222bp PCR assay protocol

Since the 222bp assays were measured after the 90bp assays, the dilution plates were frozen in between. To start, the dilutions needed to be thawed for 5 min at 30 °C and 300 rpm on the ThermoMixer© C. Then they were vortexed for 4,5 min at 30 °C and 2000 rpm. Different to the 90bp assay, the PMM was first distributed onto an empty 96 well plate (position C) with 20% surplus volume (9,6 µl per well). Then the plasma dilutions (position B) were added to this plate, also with 20% surplus volume (2,4 µl per well). For these steps the program “230309_MV_3_222” was selected using the 12,5 µl pipette INTEGRA Voyager 8-channel together with low-retention GRIPTIPS® filter tips. Pipetting mode, speed and change of tips were the same as for the 90 bp assay. This way, we created a sub-reaction mix from which the duplicates were pipetted in the next step. This sub-reaction mix was sealed and vortexed for 1,5 min at 2000 rpm and RT, and then placed on position B.

With the empty 384-well qPCR plate on position C, we started program “230309_MV_4_222” on the 12,5 µl pipette INTEGRA Voyager 8-channel, in which the sub reaction mix was pipetted in 5 µl duplicates onto the upper half of the qPCR plate. Low-retention GRIPTIPS® filter tips were used. Multi-dispense mode with two steps of 5 µl, pipetting speed of 3, 0,5 µl post-dispense volume, 1 sec aspiration delay and slow liquid exit were chosen as setting. This step was repeated with the next 96 samples for the lower half. Afterwards the qPCR plate was sealed and vortexed (1,5 min, 22 °C, 2000 rpm). The dilution plates were sealed too and frozen again for later use.

To start the PCR reaction, the sealed qPCR plates were centrifuged (2 min, 21 °C, 1000 rpm) and then placed in the Bio-Rad CFX384 Opus™ cycler. The cycler protocol was set to the following conditions to allow optimal performance of our assay: 95 °C for 2 min, followed by 35 cycles of 95 °C for 10 sec (denaturation) and 64 °C for 10 sec (annealing/extension) including the plate read-out. To accommodate the change from our older, slightly slower Bio-Rad CFX384 Touch™, on which the assay was established, and to keep the same assay performance, the ramp rate of both steps was slowed down to 1,3 °C per second. This way,

the total run time stayed the same with 1:09 h. The run was ended with a melting curve ranging from 65-95 °C with 0,5 °C increments for 5 sec.

3.2.2.5 Calculation of L1PA2 copy numbers per genome

To reach high target detection sensitivity, multi-locus primers targeting the hominoid-specific long interspersed nuclear element 1 (LINE1) family 2 (L1PA2) were used due to its abundance and specificity in the human genome (183, 184). Two different primer pairs of the same genomic region were used to address shorter (90 bp) and longer (222 bp) cfDNA fragments. The primer sequences are listed in 2.1.2. To determine the number of hits per human genome targeted by the L1PA2_90bp and L1PA2_222bp primers, the UCSC Genome Browser *In-Silico PCR* tool (185) was used. The "Max Product Size", which can potentially be amplified during the set elongation time of 10 sec in the cycler program, was set to 600bp. The "Min Perfect Match", which defines the number of bases that match exactly with the corresponding bases of the primers 3' end, was set to 19bp. This way the tool calculated an estimated 3416 hits for L1PA2_90bp and 3237 hits for L1PA2_222bp in the human genome.

3.2.2.6 Calculation of cfDNA concentration in plasma samples

To calculate the cfDNA concentration in ng/ml from the Cq values, the following equation was applied: $ng/ml \triangleq pg/\mu l = \frac{10^{\frac{Cq-intercept}{slope}}}{5\mu l} * \frac{75}{number\ of\ hits} * 3.23pg$

With the slope and the intercept generated by a validated standard curve, the total copy number per 5 µl reaction could be calculated. Divided by 5, we obtained the copy number per µl. Due to a total dilution factor of plasma of 1:75 (plasma dilution 1:15 plus qPCR dilution: 1 µl of plasma dilution per 5 µl reaction), we multiplied this value by 75. This copy number per µl was divided by the number of predicted hits in the human genome (3416 for L1PA2_90bp, 3237 for L1PA2_222bp). The result gave us the number of genome equivalents (GE) per µl of plasma. Considering the expected weight of a haploid genome, we multiplied the GE by 3,23 pg to obtain the concentration of cfDNA in plasma in pg/µl, which equals ng/ml.

3.2.2.7 PCR run interplate calibration

As the Bio-Rad CFX-System calculates the Cq values based on the point at which the samples' fluorescence crosses an auto-calculated fluorescence threshold, the setting of this threshold is decisive for the calculation of the values. However, this auto-calculated threshold can vary with the number of samples and their fluorescence intensity. To compensate for this dependency, we analysed two reference samples (#3 and #4) per plate. These samples were

PRE- and POST-exercise plasma samples from one single, healthy subject, collected by venous blood withdrawal. They were centrifuged twice directly afterwards (10 min, 22 °C, 1.600 rpm and 5 min, 22 °C, 16.000 rpm). Before the present study, these reference samples were measured on a total of 20 plates by three different operators and the means of the auto calculated Cq values were formed. Given this reference mean Cq value, the threshold of each study run was set so that the mean of the reference samples on this plate equalled the pre-defined mean Cq value.

A statistical analysis was performed to determine the sample size at which the median of a sample of measurements approximated the true population value with sufficient accuracy. Accuracy was defined by a tolerance range of ±15% of the nominal value, in accordance with bioanalytical guidelines (186). To investigate the convergence of the median, 30 iterations (referred to as trace in the graph, the legend only displays 17 traces) were performed, with 37 plates selected in random order from existing qPCR data (D POST sample) in each iteration. The median was calculated successively for growing subsets of these plates. For each iteration, the median was stepwise calculated by including an increasing number of plates.

This iterative process was performed for both uncalibrated (*Figure 4*) and calibrated (*Figure 5*) measurements. The results showed that for uncalibrated values, a larger number of plates was required to stabilize the median within the ±15% tolerance range due to higher starting variance. For the calibrated values with already reduced variance, the median approached the nominal value more quickly. It was determined that after a sample size of 20 plates, the median was reliably within the tolerance range in both cases. Therefore, it was decided to calculate the median of “N PRE” and “N POST” from 20 different qPCR runs (calibrated with the before existing reference samples “D PRE and D POST”) and use these as the new reference sample values for this study.

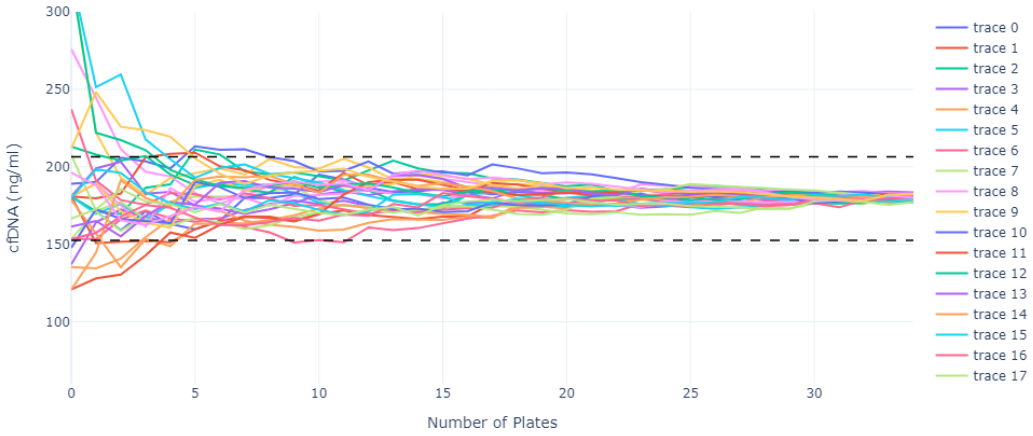

Figure 5 – Statistical analysis with approximation of the true value for repeated measurements of a reference sample (D POST, ***uncalibrated values****)*

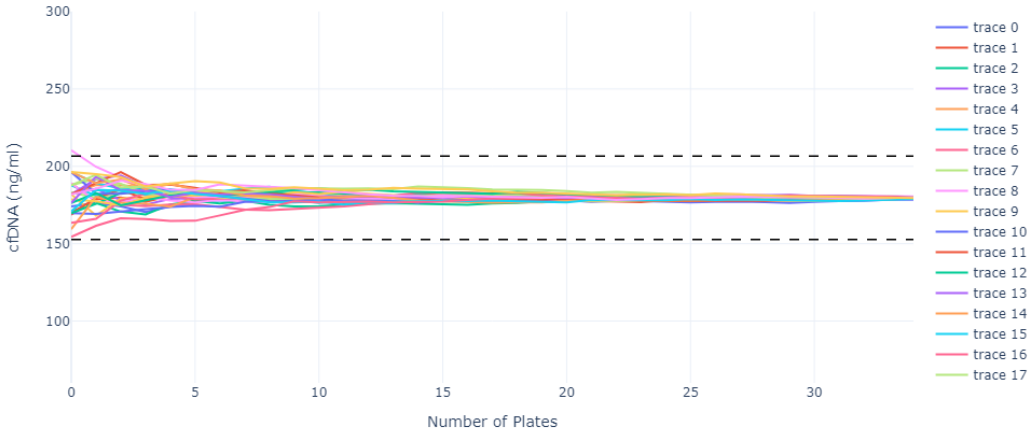

Figure 5 - Statistical analysis with approximation of the true value for repeated measurements of a reference sample (D POST, ***calibrated values****)*

3.2.3 Methods used in the development of qPCR automation

3.2.3.1 Manual qPCR protocol

Before explaining the process of automation, it is necessary to describe the current protocol of the manual qPCR method, as used and tested in our lab for the last 9 years and published by Breitbach et al. (11) and Neuberger et al. (183). The manual technique forms the basis for the automation approach and was initially used to establish it.

The key steps of the manual protocol are the same as for the novel, automated method, consisting of the sample dilution, the production of the reaction mix and the final pipetting of

triplicates onto the qPCR plate. For the dilution step, all plasma samples stored in reaction tubes were thawed at RT, subsequently vortexed by hand approx. three times for three seconds and then shortly centrifuged. The 1:10 dilutions were performed by distributing 18 µl of H_20 to empty reaction tubes and then adding 2 µl of plasma. This mix was vortexed and centrifuged again.

In the next step, the MasterMix and PrimerMix were thawed at RT, vortexed and centrifuged. They were then mixed in the correct ratio in a 1,5 ml reaction tube, vortexed and centrifuged again. The correct volumes were calculated with our Excel sheet according to the number of samples and considering a surplus volume for each distribution step. The PrimerMasterMix created was then spread into 0,2 ml reaction tubes with a volume of 14,3 µl per tube. After this, the plasma dilutions were added to these tubes with a volume of 2,2 µl. In advance, the dilutions were shortly vortexed again by hand. The resulting reaction mix had a total volume of 16,5 µl per tube for each sample, which equals 10 % surplus volume to the later needed 15 µl.

These tubes were then manually vortexed before dispensing the reaction mix with reverse pipetting in triplicates of 5 µl each onto the qPCR plate. The process was finished by sealing the qPCR plate, centrifuging it for 2 min at 1000 rpm and 21 °C, placing it in the Bio-Rad CFX Touch™ and starting the L1PA2 cycler protocol.

3.2.3.2 Electronic multichannel pipette qPCR protocol

Moving towards higher-throughput analysis, the 8- and 12-channel electronic Eppendorf Xplorer® plus Move It® pipette (*Figure 6*) was used. Its width adjustment feature made it usable for the dilution step with 1,5 ml reaction tubes, as well as for the pipetting of triplicates from 0,2 ml tubes into a 384 well qPCR plate. Since the 12-channel pipette is restricted to a width adjustment from a 384- to a 96-well format, it was not working with 1,5 ml reaction tubes placed in suitable racks, as they are essentially in a 48-well format. Therefore, only the 8-channel pipette width adjustable from 384 to 48 wells could be used for this step.

Figure 6 - Eppendorf Xplorer® plus Move It® pipette

(With kind permission of www.eppendorf.com)

PrimerMasterMix (PMM) preparation and distribution into 0,2 ml reaction tubes were done manually, using tube strips containing eight 0,2 ml tubes. Compared to the completely manual method, with the multichannel pipettes the surplus volume was doubled to 20%, producing a volume of 15,6 µl PMM per tube. The increase

of the PMM surplus volume also entailed an increase of volume in added plasma dilution in the next step. After vortexing the tubes with plasma dilution, 2,4 µl each were aspirated with the 8-channel pipette and transferred to the corresponding tube strips containing the PMM. The so-created reaction mixes of 18 µl per tube were then sealed with lid-strips, vortexed and transferred in triplicates to the qPCR plate by using the multi-dispense mode with three steps of 5 µl.

The finishing step was the same as for the manual method (2.2.3.1).

3.2.3.3 Mixing protocols using the Eppendorf ThermoMixer® C

Since the MyoVasc study samples were delivered in a 96 well format, we also planned to prepare the plasma dilutions in 96 well plates. For standardised vortexing and mixing of the sample plates the Eppendorf MixMate® was introduced. A comparison test was conducted to compare different mixing protocols with our manual vortexing for the best homogenisation of plasma in water dilutions.

We thawed plasma samples and shortly vortexed them three times by hand. All dilution steps were made with the multi-channel pipette by distributing water and adding plasma in 0,2 ml tubes. Those tubes then were vortexed either three times manually (standard method) or with four different MixMate® protocols (1650 rpm for 30 s, 1650 rpm for 1,5 min, 2000 rpm for 1,5 min, 2600 rpm for 3 min). The rest of the qPCR protocol was the same for all samples (see 2.2.3.1). To compare with the standard method, the percentage deviation in cfDNA concentration was calculated.

Figure 7 - Eppendorf ThermoMixer® C

(With kind permission of www.eppendorf.com)

To further improve the vortexing process of these dilutions and to be able to faster thaw 96 well dilution plates, we opted to buy the Eppendorf ThermoMixer® C (*Figure 7*) instead with additional heating and cooling function. The vortexing functions stayed the same as with the MixMate®.

From then on, all dilutions were mixed at 30 °C and 2000 rpm for 4,5 min to ensure homogeneity. Frozen dilutions could be thawed for 5 min at 30 °C and 300 rpm and subsequently mixed for 4,5 min at 30 °C and 2000 rpm.

To mix the reaction mix after combination of PrimerMasterMix and plasma dilution, 1,5 min at 22 °C and 2000 rpm were sufficient to provide proper assay function with good fluorescence intensity and repeatable measurement results.

3.2.4 Measurement of the MyoVasc study samples

3.2.4.1 INTEGRA Assist Plus pipetting protocol

The protocol for the INTEGRA Assist Plus was designed with their own VIALAB program. All consumables and devices directly interfering with the robotic system are proprietary for the Assist Plus and manufactured by INTEGRA.

We decided to split our protocol into the three respectively four programs already described in chapter *2.2.2.4 qPCR protocol*. This simplified the lab ware change in between the different programs and ensured safety of the experiments, as the robot automatically stopped after each program and gave the user enough time to prepare the needed materials.

The programs “230102_MV_1” and “230102_MV_2” were used to prepare the plasma sample dilutions, while programs “230102_MV_3” or “230309_MV_3_222” and “230309_MV_4_222” were used to pipette the final reaction mix and fill the qPCR plate in duplicates.

After designing the programs on the PC with the VIALAB program, they were synchronised with the pipette to be used. These INTEGRA Voyager pipettes act as the brain of the robotic system, as they wirelessly pair with the Assist Plus station and give the commands for the movement of the robotic arm. Therefore, one written program can only include one type of pipette, with which it will be synchronized. The pipettes and corresponding tips are color-coded to improve user experience. Only for program “230102_MV_1” a 125 µl Voyager pipette (yellow) was used to enable the water distribution of 21 µl. For all other programs the smaller 12,5 µl pipette (purple) was used.

All detailed program reports are attached in the appendix (Figure A1).

3.2.4.2 Outlier remeasurements

For the quantification of cfDNA all samples were pipetted in duplicates. The mean value of those duplicates was used for calculating the cfDNA concentrations. As indicator of accuracy, the difference in Cq values of both wells in a duplicate was calculated and called “Diff_Cq”. With a Diff_Cq > 0,5 cycles, the measurement was rejected as incorrect and a remeasurement followed as recommended in a nature protocol (187). For the remeasurements the plasma samples were diluted again.

3.2.4.2.1 90 bp assay remeasurements

The samples were measured up to four times. After these measurements no outliers with Diff_Cq > 0,5 were left. After the outlier remeasurements we decided for a different calibration of the raw values. Therefore, also the Diff_Cq values changed slightly, and we were left with 46 samples > 0,5 cycles difference. Because these samples could not be measured again, we chose to accept those higher Diff_Cq's up to 0,76 considering the number of 3109 samples in total.

3.2.4.2.2 222 bp assay remeasurements

The samples were measured up to three times. After these measurements we were left with 35 samples which still had Diff_Cq's > 0,5. We compared all three measurements of each sample and chose the median value to be accepted.

3.2.4.3 Incurred Sample Reanalysis

To verify our measurements, the first and the last four samples of each MICRONIC rack, in total 296 samples, were reanalysed with newly prepared dilutions. This number fulfils FDA's Bioanalytical Method Validation guideline (186), as at least 206 samples should have been reanalysed. The percentage difference of cfDNA concentration between the first and the second measurement is calculated with the following equation: $\frac{Second-First}{Mean} * 100$

As this guideline recommends for ligand binding assays, at least 67% of the samples should be within ± 30% of the mean. However, as newer guidelines specifically for qPCR recommend, at least 67% of the samples should be within ± 45% of the mean value (188).

3.2.4.4 Interplate quality control

To consistently monitor accuracy of the qPCR runs, we analysed four quality control samples with known cfDNA concentrations in each run. Under- or overestimated values for all quality controls have been a sign of under- or overperformance of the assay and led to a direct re-measurement of the whole run.

3.2.5 Analysis of the raw data

The data produced by the Bio-Rad CFX cycler comes in an unreadable *.zpcr* file. By opening this file with the Bio-Rad CFX Maestro software, a new *.pcrd* file is created automatically. Within the CFX Maestro software you can now edit the plate setup to define the sample containing wells. For our purpose of the MyoVasc study, one plate template file (.pltd) (*Figure 8*) for each assay was created, which could then be easily loaded.

	1	2	3	4	5	6	7	8	9	10	11	12	13	14	15	16	17	18	19	20	21	22	23	24
A	U-13 90bp	U-13 90bp	U-14 90bp	U-14 90bp	U-15 90bp	U-15 90bp	U-16 90bp	U-16 90bp	U-17 90bp	U-17 90bp	U-18 90bp	U-18 90bp	U-19 90bp	U-19 90bp	U-20 90bp	U-20 90bp	U-21 90bp	U-21 90bp	U-22 90bp	U-22 90bp	U-23 90bp	U-23 90bp	T-1 90bp H2O	T-1 90bp H2O
B	U-24 90bp	U-24 90bp	U-25 90bp	U-25 90bp	U-26 90bp	U-26 90bp	U-27 90bp	U-27 90bp	U-28 90bp	U-28 90bp	U-29 90bp	U-29 90bp	U-30 90bp	U-30 90bp	U-31 90bp	U-31 90bp	U-32 90bp	U-32 90bp	U-33 90bp	U-33 90bp	U-34 90bp	U-34 90bp	T-2 90bp ee Plasm	T-2 90bp ee Plasm
C	U-35 90bp	U-35 90bp	U-36 90bp	U-36 90bp	U-37 90bp	U-37 90bp	U-38 90bp	U-38 90bp	U-39 90bp	U-39 90bp	U-40 90bp	U-40 90bp	U-41 90bp	U-41 90bp	U-42 90bp	U-42 90bp	U-43 90bp	U-43 90bp	U-44 90bp	U-44 90bp	U-45 90bp	U-45 90bp	U-1 90bp N Pre	U-1 90bp N Pre
D	U-46 90bp	U-46 90bp	U-47 90bp	U-47 90bp	U-48 90bp	U-48 90bp	U-49 90bp	U-49 90bp	U-50 90bp	U-50 90bp	U-51 90bp	U-51 90bp	U-52 90bp	U-52 90bp	U-53 90bp	U-53 90bp	U-54 90bp	U-54 90bp	U-55 90bp	U-55 90bp	U-56 90bp	U-56 90bp	U-3 90bp N Post	U-3 90bp N Post
E	U-57 90bp	U-57 90bp	U-58 90bp	U-58 90bp	U-59 90bp	U-59 90bp	U-60 90bp	U-60 90bp	U-61 90bp	U-61 90bp	U-62 90bp	U-62 90bp	U-63 90bp	U-63 90bp	U-64 90bp	U-64 90bp	U-65 90bp	U-65 90bp	U-66 90bp	U-66 90bp	U-67 90bp	U-67 90bp	U-5 90bp nter Pre	U-5 90bp nter Pre
F	U-68 90bp	U-68 90bp	U-69 90bp	U-69 90bp	U-70 90bp	U-70 90bp	U-71 90bp	U-71 90bp	U-72 90bp	U-72 90bp	U-73 90bp	U-73 90bp	U-74 90bp	U-74 90bp	U-75 90bp	U-75 90bp	U-76 90bp	U-76 90bp	U-77 90bp	U-77 90bp	U-78 90bp	U-78 90bp	U-7 90bp nter Post	U-7 90bp nter Post
G	U-79 90bp	U-79 90bp	U-80 90bp	U-80 90bp	U-81 90bp	U-81 90bp	U-82 90bp	U-82 90bp	U-83 90bp	U-83 90bp	U-84 90bp	U-84 90bp	U-85 90bp	U-85 90bp	U-86 90bp	U-86 90bp	U-87 90bp	U-87 90bp	U-88 90bp	U-88 90bp	U-89 90bp	U-89 90bp	U-9 90bp nter Pre	U-9 90bp nter Pre
H	U-90 90bp	U-90 90bp	U-91 90bp	U-91 90bp	U-92 90bp	U-92 90bp	U-93 90bp	U-93 90bp	U-94 90bp	U-94 90bp	U-95 90bp	U-95 90bp	U-96 90bp	U-96 90bp	U-97 90bp	U-97 90bp	U-98 90bp	U-98 90bp	U-99 90bp	U-99 90bp	U-100 90bp	U-100 90bp	U-11 90bp nter Post	U-11 90bp nter Post
I	U-101 90bp	U-101 90bp	U-102 90bp	U-102 90bp	U-103 90bp	U-103 90bp	U-104 90bp	U-104 90bp	U-105 90bp	U-105 90bp	U-106 90bp	U-106 90bp	U-107 90bp	U-107 90bp	U-108 90bp	U-108 90bp	U-109 90bp	U-109 90bp	U-110 90bp	U-110 90bp	U-111 90bp	U-111 90bp	U-112 90bp	U-112 90bp
J	U-113 90bp	U-113 90bp	U-114 90bp	U-114 90bp	U-115 90bp	U-115 90bp	U-116 90bp	U-116 90bp	U-117 90bp	U-117 90bp	U-118 90bp	U-118 90bp	U-119 90bp	U-119 90bp	U-120 90bp	U-120 90bp	U-121 90bp	U-121 90bp	U-122 90bp	U-122 90bp	U-123 90bp	U-123 90bp	U-124 90bp	U-124 90bp
K	U-125 90bp	U-125 90bp	U-126 90bp	U-126 90bp	U-127 90bp	U-127 90bp	U-128 90bp	U-128 90bp	U-129 90bp	U-129 90bp	U-130 90bp	U-130 90bp	U-131 90bp	U-131 90bp	U-132 90bp	U-132 90bp	U-133 90bp	U-133 90bp	U-134 90bp	U-134 90bp	U-135 90bp	U-135 90bp	U-136 90bp	U-136 90bp
L	U-137 90bp	U-137 90bp	U-138 90bp	U-138 90bp	U-139 90bp	U-139 90bp	U-140 90bp	U-140 90bp	U-141 90bp	U-141 90bp	U-142 90bp	U-142 90bp	U-143 90bp	U-143 90bp	U-144 90bp	U-144 90bp	U-145 90bp	U-145 90bp	U-146 90bp	U-146 90bp	U-147 90bp	U-147 90bp	U-148 90bp	U-148 90bp
M	U-149 90bp	U-149 90bp	U-150 90bp	U-150 90bp	U-151 90bp	U-151 90bp	U-152 90bp	U-152 90bp	U-153 90bp	U-153 90bp	U-154 90bp	U-154 90bp	U-155 90bp	U-155 90bp	U-156 90bp	U-156 90bp	U-157 90bp	U-157 90bp	U-158 90bp	U-158 90bp	U-159 90bp	U-159 90bp	U-160 90bp	U-160 90bp
N	U-161 90bp	U-161 90bp	U-162 90bp	U-162 90bp	U-163 90bp	U-163 90bp	U-164 90bp	U-164 90bp	U-165 90bp	U-165 90bp	U-166 90bp	U-166 90bp	U-167 90bp	U-167 90bp	U-168 90bp	U-168 90bp	U-169 90bp	U-169 90bp	U-170 90bp	U-170 90bp	U-171 90bp	U-171 90bp	U-172 90bp	U-172 90bp
O	U-173 90bp	U-173 90bp	U-174 90bp	U-174 90bp	U-175 90bp	U-175 90bp	U-176 90bp	U-176 90bp	U-177 90bp	U-177 90bp	U-178 90bp	U-178 90bp	U-179 90bp	U-179 90bp	U-180 90bp	U-180 90bp	U-181 90bp	U-181 90bp	U-182 90bp	U-182 90bp	U-183 90bp	U-183 90bp	U-184 90bp	U-184 90bp
P	U-185 90bp	U-185 90bp	U-186 90bp	U-186 90bp	U-187 90bp	U-187 90bp	U-188 90bp	U-188 90bp	U-189 90bp	U-189 90bp	U-190 90bp	U-190 90bp	U-191 90bp	U-191 90bp	U-192 90bp	U-192 90bp	U-193 90bp	U-193 90bp	U-194 90bp	U-194 90bp	U-195 90bp	U-195 90bp	U-196 90bp	U-196 90bp

Figure 8 - Plate template MyoVasc study 90 bp assay (90bp_full.pltd)

This template was used to analyze the qPCRs with the CFX Maestro software.

Under the heading “Quantification data” you could now find the uncalibrated, raw values for each sample. The calibration was performed as mentioned in chapter 2.2.2.6 by setting the fluorescence threshold. The calibrated values were then copied and pasted into our pre-designed Excel analysis sheet. Here, the cfDNA concentration in ng/ml was calculated by applying the equation from chapter 2.2.2.2. The Diff_Cq values were also calculated automatically. To identify the samples, a preformed plate layout list matching the plate number was pasted into the Excel sheet. This method ensured faster sample labelling and avoidance of careless mistakes.

3.2.6 Data management

Having one Excel result file per PCR run, we needed to combine all files to get one result list for all samples. To read out the required data from these Excel files, we used a command written in *R*. The resulting list was then combined in *R* with a list of all samples with matched sample IDs to check for any missing measurements. Two final Excel lists of the separate 90 bp and 222 bp PCR assay measurements, as well as a combined list of both assays with the calculated integrity index were forwarded to the MyoVasc study management via an upload in a data transfer tool.

3.2.7 Disease definitions

HF phenotypes were defined with the following echocardiographic criteria: (i) no cardiac dysfunction: LVEF ≥ 55%, E/A ≥ 0.75, E/E' < 10 and DT_E ≥ 140; (ii) preserved ejection fraction (pEF): LVEF ≥ 50% and one of the following: (E/A < 0.75 and E/E' < 10), (E/A ≥ 0.75 and E/E' ≥ 10 and DT_E ≥ 140 ms) or (E/A > 2 and E/E' ≥ 10 and DT_E < 140 ms); (iii) mildly reduced ejection fraction (mrEF): LVEF of 41-49%; (iiii) reduced ejection fraction (rEF): LVE ≤ 40%. Symptomatic HF was defined in patients with echocardiographic findings according to (ii), (iii) or (iiii) who had at least one of the following: New York Heart Association (NYHA) functional class ≥ II; (bilateral ankle swelling OR rales OR nocturia) AND N-terminal natriuretic peptide type B (NT-proBNP) > 125 pg/mL; NYHA class I AND NT-proBNP > 125 pg/mL AND HF medication. HFpEF was defined as symptomatic HF with pEF, HFmrEF as symptomatic HF with mrEF, and HFrEF as symptomatic HF with rEF.

HF stages were defined as the following: (I) stage 0: no heart failure; (II) stage A: “at risk for HF” due to existing cardiovascular risk factors (CVRFs) or a positive family history, but without any symptoms, structural cardiac changes or elevated biomarkers of HF; (III) stage B: “pre-HF” without any symptoms of HF, but with structural heart disease or abnormal cardiac function or elevated NT-proBNP levels; (IV) stage C: “heart failure” with any symptoms of HF caused by structural or functional cardiac abnormality; (V) stage D: “advanced HF” with severe HF symptoms at rest, recurrent hospitalizations despite guideline-directed management and therapy (GDMT), refractory or intolerant to GDMT, requiring advanced therapies (e.g. transplantation, palliative care).

According to these criteria, the analysis sample included n = 683 subjects with HFpEF, n = 383 with HFmrEF, and n = 329 with HFrEF. The cohort consisted of n = 571 healthy controls (stage 0/A), n = 977 subjects with pre-HF (stage B), and n = 1741 subjects with HF stage C/D.

3.2.8 Statistics

Statistics were performed in the Center for Cardiology at University Medical Center Mainz.

Study outcome was defined as exacerbation of HF, a composite of transition from asymptomatic to symptomatic HF and cardiac death in asymptomatic HF patients, and a composite of hospitalization due to exacerbation of HF and cardiac death in symptomatic HF patients.

Statistical analysis was performed after data quality control, which included a check for completeness and plausibility by the data management unit. Clinical baseline characteristics of the study sample were described by tables for sex, quartiles of cfDNA concentration, and HF stages.

Continuous variables were described by mean values ± standard deviation (SD) or with median + interquartile range (Q1, Q3) for values with |skewness| > 1. Categorical variables were described by absolute and relative frequencies. *P*-values for continuous variables were estimated by a double-sided, unpaired T-test or by the Mann-Whitney-U-test for values with |skewness| > 1. *P*-values for trends were estimated via Jonckheere-Terpstra test for continuous variables. For dichotomous variables the Chi-square (x^2) test was applied.

Associations of cfDNA levels, separately for the 90bp and 222bp assays, and the integrity index were assessed using multivariable linear regression models adjusted for age and sex (model 1), age, sex, and cardiovascular risk factors (CVRFs) (model 2) or age, sex, CVRFs, and medication (model 3). Beta estimates for NT-proBNP, LVEF (%) and E/E' ratio were given per 1 standard deviation (SD) of the trait.

Logistic regression analyses regarding cfDNA concentration and integrity index were performed for the categorical variables of HF stage C/D vs 0/A. Odds ratios (OR) and 95% confidence intervals (CI) were calculated. The models were adjusted as in linear regression analysis (model 1-3).

Survival analyses for cfDNA levels were performed with competing risk models for worsening of HF, and cox proportional hazard regression models for cardiac death and all-cause death. Various stages of HF were considered. C statistics were calculated and compared for each of the cox regression models. Hazard ratios (HR) and 95 % confidence intervals (CI) were calculated. Analyses were adjusted for age, sex, CVRFs and medication (model 1-3) and additionally for NT-proBNP (model 4). Outcome data for worsening of HF were presented as cumulative incidence plots for quartiles of cfDNA 90bp and 222bp levels and of the integrity

index, with Grey's test for differences between curves. For cardiac death and all-cause death, cumulative incidence plots were created, with Logrank test for differences between curves.

A forest plot was used to show the association between cfDNA concentrations and worsening HF and all-cause death.

A *p*-value < 0.05 was considered as statistically significant. In the context of this exploratory study, the p-value should be seen as a continuous measure of the strength of evidence for an association. The smaller the p-value, the more likely a relevant association is. All statistical analyses were performed with the R software package, version 3.6.0 (http://www.r-project.org).

4 Results

4.1 Development of an automated qPCR method for cfDNA quantification

4.1.1 Establishment of a faster workflow using an electronic multichannel pipette

Until the present study, the working group never had performed cfDNA quantifications with such a high sample count as in the MyoVasc study, and the qPCRs were usually run with only half of a 384-well plate filled. Preparing to analyze the high sample numbers required by the MyoVasc study, I simplified and standardized our previous manual method first by application of an 8- and 12-channel electronic Eppendorf Xplorer® plus Move It® pipette.

This made it possible to process 8 or 12 samples in parallel and to speed up the analytical process substantially. The width adjustment feature facilitated use of the pipette with 1,5 ml reaction tubes, as well as with 0,2 ml tubes and a 384-well plate. Unluckily, the 12-channel pipette was restricted to a maximum of 96 wells. Therefore, it did not work with 1,5 ml reaction tubes placed in suitable racks, as they are essentially in a 48-well format. Only the 8-channel pipette could thus be used for this step.

The preparation of the PrimerMasterMix and the subsequent distribution into 0,2 ml reaction tubes was still done by hand. Here, the use of a multi-channel pipette would have required a reservoir to aspirate the liquid, which would have needed too much surplus volume compared to the number of samples measured on one plate at this time. Instead of individual tubes, we utilized tube strips containing eight 0,2 ml tubes with one lid strip. This substantially reduced the time spent on opening tubes. As a drawback compared to the manual method, the surplus volume had to be doubled to 20%. This was due to a more difficult, simultaneous handling of all eight channels in individual tubes. The increase of the PMM surplus volume also entailed an increase of volume in added plasma dilution in the next step, which however was not limiting.

To establish the multi-channel pipette, we conducted a series of experiments to compare its accuracy with our manual pipetting method. Therefore, we used the multi-channel pipetting protocol as described in the methods section (2.2.3.2) and pipetted another row of the same samples with our manual method. This way, we kept every step the same except for the pipetting of triplicates in the last step. After qPCR, the coefficient of variation in cfDNA concentration between both methods were calculated.

Table 7 - Coefficient of variation (CV) in cfDNA concentration between manual pipetting and the use of an electronic multichannel pipette.

The red fields indicate standard deviation outliers (SD > 0,4) in pipetted duplicates.

Date	Name	Procedure	Samples	CfDNA (ng/ml)	SD Cq	log_cfDNA	SD (MKPvsManual; same operator; same day; raw data)	CV (MKPvsManual; same operator; same day; raw data)
31.Aug	TH	MKP	RL7 Pre	9,58	0,21	0,98	0,07	0,72%
31.Aug	TH	MKP	RL7 Post	98,58	0,44	1,99	3,22	3,37%
31.Aug	TH	MKP	RL8 Pre	26,18	0,24	1,42	0,22	0,83%
31.Aug	TH	MKP	RL8 Post	76,45	0,21	1,88	2,26	2,87%
31.Aug	TH	MKP	RL10 Pre	11,92	0,21	1,08	1,02	7,86%
31.Aug	TH	MKP	RL10 Post	245,75	0,22	2,39	15,53	6,75%
31.Aug	TH	MKP	RL13 Pre	16,36	0,49	1,21	0,33	2,01%
31.Aug	TH	MKP	RL13 Post	149,60	0,17	2,17	3,07	2,01%
31.Aug	TH	Manuell	RL7 Pre	9,72	0,24	0,99		
31.Aug	TH	Manuell	RL7 Post	92,14	0,39	1,96		
31.Aug	TH	Manuell	RL8 Pre	26,62	0,45	1,43		
31.Aug	TH	Manuell	RL8 Post	80,97	0,23	1,91		
31.Aug	TH	Manuell	RL10 Pre	13,96	0,29	1,14		
31.Aug	TH	Manuell	RL10 Post	214,68	0,45	2,33		
31.Aug	TH	Manuell	RL13 Pre	17,03	0,02	1,23		
31.Aug	TH	Manuell	RL13 Post	155,74	0,31	2,19		

The results showed no relevant differences between both pipetting methods (comp. *Table 7* "CV" values). With the multichannel pipette method ("MKP"), neither the standard deviation between the triplicates (SD Cq), nor the percentage difference in cfDNA concentration (CV) differed relevantly from the manual pipetting method ("Manuell").

In conclusion the electronic multi-channel pipette emerged as an equally accurate, labour- and time-saving alternative to the manual pipetting protocol. However, handling of the 8-channel pipette required substantial training and could be easily influenced by individual manual skills. Calculation of the reachable throughput of this method (max. 2-3 plates per day) revealed that an even higher degree of automation would be necessary to reproducibly process over 3000 samples from the MyoVasc study.

4.1.2 Optimisation of mixing protocols using the Eppendorf ThermoMixer® C

To further standardise and simplify the qPCR protocol we also looked at our manual vortexing methods and initially tested the MixMate® from Eppendorf.

To test the mixing capability of plasma dilutions in a 96 well format, we performed a trial run with our standard manual vortexing method and four different mixing protocols on the MixMate®. The results are shown in *Figure 9* as percent difference from the standard method (dashed line) on the y-axis. On the x-axis in graph A, the four mixing protocols are displayed each as one bar. For graph B, the total number of revolutions of each mixing protocol was calculated by multiplying the duration (min) with the speed (revolutions per minute/rpm). The total number of revolutions are displayed on the x-axis as $\log_{10}$(revolutions).

The curve shows a clear regression with increasing number of revolutions, reaching a plateau between the third (1,5 min, 2000 rpm) and fourth (3 min, 2600 rpm) mixing protocol with an acceptable difference of less than ± 20 % compared to our manual vortexing method.

As the later chosen Eppendorf ThermoMixer® C could only do 2000 rpm with a 96 well format plate, we decided to mix the dilutions for 4,5 min at this speed of 2000 rpm.

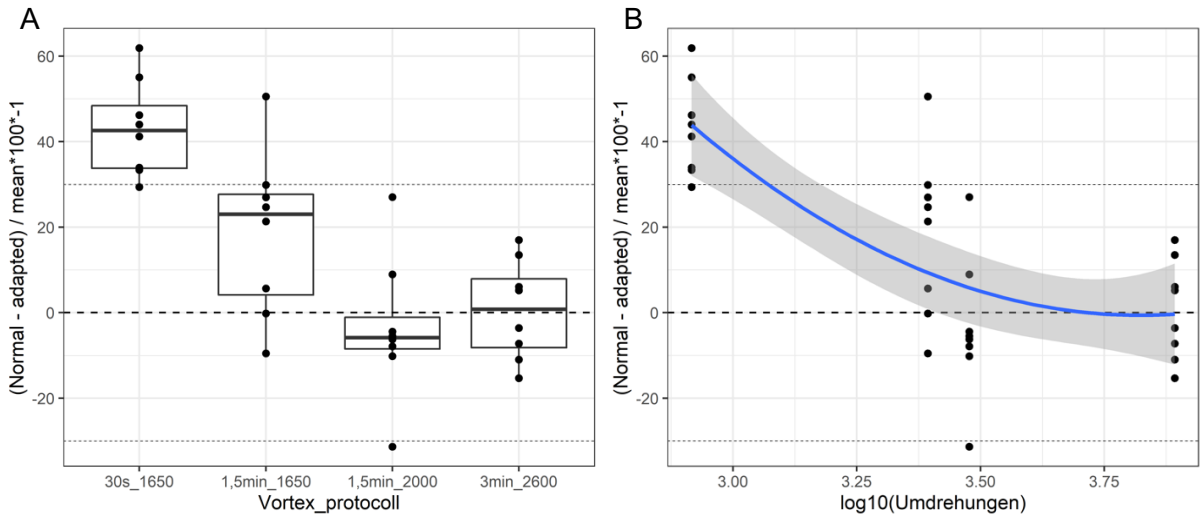

Figure 9 - CfDNA concentration differences depending on four different mixing protocols

(A) Results for four different mixing protocols (time_rpm) presented as box plots. (B) Results for four different mixing protocols, each converted into one value of log_{10}(revolutions), presented with a regression line.

4.1.3 Establishment of the INTEGRA Assist Plus pipetting robot

For the establishment of a qPCR protocol using the INTEGRA Assist Plus pipetting robot, we tried to mirror our manual pipetting techniques in the settings of the robot.

After setting and testing of the first program, minor adjustments were performed run by run to finally match the accuracy and reproducibility of our manual pipetting protocol. We also reduced the running costs by setting the minimal possible volumes and reducing the consumption of plastic ware like tips, reservoirs, and plates.

The main challenge in the establishment of an automated qPCR method lay in the number of available settings for the pipetting process on the robot. Besides the right choice of labware and the setting of the pipetting hight, pipetting modes such as single- or multi-dispense,

pipetting speed, and source or target mixing played were critical parameters, which had to be optimised stepwise.

For the non-proprietary labware we stayed with the 384-well FrameStar® qPCR plates which had already been used successfully for years. For the additionally needed 96-well plates, we chose skirted ones from Bio-Budget, which fitted snug on the robot's deck. The remaining labware like tips and reservoirs were selected from INTEGRA. For the highest precision we chose the sterile, low-retention GRIPTIPS® filter-tips.

In the pipetting protocol, no mixing was needed for the first step (water distribution). A pre- and post-dispense volume of 2 µl was added, which increased precision. In the multi-dispense mode, the pipetting was faster than in single-dispense mode. INTEGRA's 125 µl standard GRIPTIPS® were used, as a special low-retention coating was not needed for the pipetting of water.

In the second pipetting step – plasma dilution – we chose INTEGRA's 12,5 µl long low-retention GRIPTIPS® to better reach lower liquid levels in the MICRONIC tubes. The plasma had to be transferred into the water with a low speed (adjusted to 3) due to the plasma's high viscosity. The dilution was then mixed ten times with a high speed (adjusted to 10) and a volume of 12 µl to rinse the tip and completely submerge the plasma in the water. The tips were changed after each transfer to avoid contamination. The success was proven by negative non-template controls.

Slightly different pipetting protocols turned out to be advantageous for the different 90 and 222 bp assays.

In the third pipetting step of the 90 bp assay, the PrimerMasterMix was initially distributed onto the 384 qPCR well plate. We achieved consistent conditions for every well over the whole plate using single-dispense mode and a 0,5 µl post-dispense volume. A lower pipetting speed of 4 took the higher viscosity of buffer in the PMM into account. After discarding the tips, the dilution was transferred into each well of the qPCR plate using single-dispense mode and a speed of 3. We found that single dispense-mode led to a reduction in concentration difference between both wells of a duplicate. Five mixing cycles with a volume of 2 µl and a speed of 5 had to be applied to rinse the tip and completely submerge the plasma dilution in the PrimerMasterMix.

By testing five different pipetting protocols for the last pipetting step of plasma dilution transfer, we found single-dispense mode to be much more accurate than multi-dispense mode. As depicted in *Figure 10*, multi-dispense mode (methods 1, 3 and 5) showed considerably higher standard deviation than single-dispense mode (methods 4 and 6). The experiments also proved that a pre-wetting of the pipette tip (methods 5 and 6) increased the standard deviation compared to no pre-wetting (methods 3 and 4). In conclusion, method 4 with no pre-wetting and single-dispense mode proved to be the most accurate pipetting protocol.

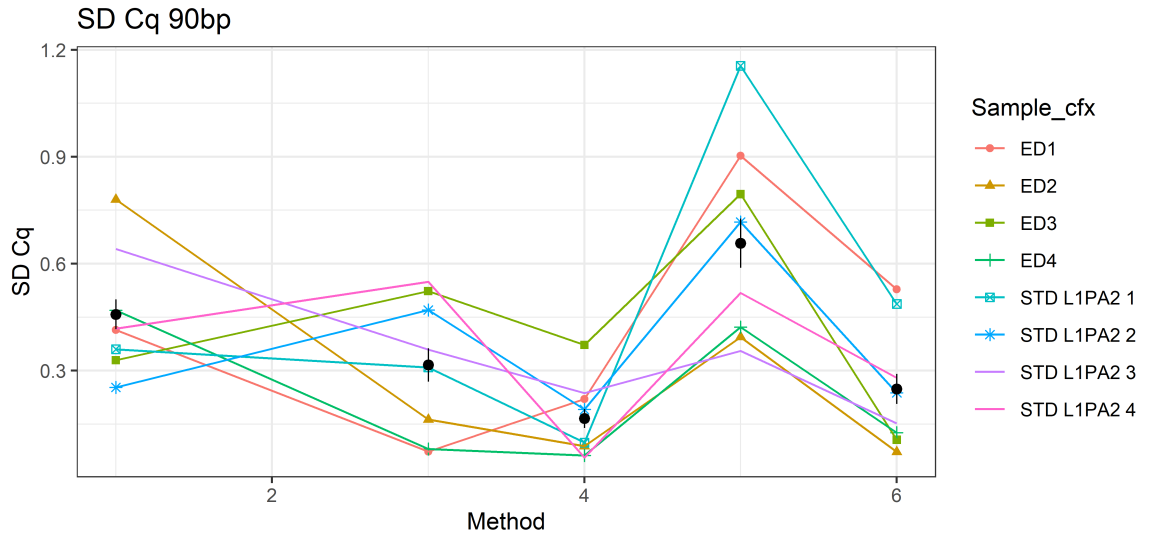

Figure 10 – Standard deviation (SD) of Cq values in duplicates for the 90 bp assay

Testing of five different pipetting protocols for the last pipetting step of plasma dilution transfer. Methods are numbered 1, 3, 4, 5 and 6. Eight samples were tested, four plasma sample dilutions (ED 1-4) and four standard fragment dilutions (STD L1PA2 1-4).

In the 222 bp assay, we added an extra step of creating a reaction sub-mix, which led to a lower standard deviation in cfDNA concentration between both wells of a duplicate. Therefore, the PMM was first distributed onto an empty 96 well plate in the third step. Afterwards, the dilution was added, and everything was mixed thoroughly five times with a high volume and speed (8 µl, speed 8). Each well then contained the volume later needed to pipette one PCR duplicate.

In the fourth step of the 222 bp protocol, the previously prepared reaction sub-mix was pipetted onto the qPCR plate. To ensure equal pipetting conditions for each well of a duplicate, the reaction mix was dispensed in multi-dispense mode (two steps of 5 µl with 0,5 µl post-dispense volume left in the tip). The total volume of 12 µl of reaction sub-mix proved sufficient to aspirate

the needed 10,5 µl. A slow pipetting speed of 3, an aspiration delay of 1 sec and a slow exit out of the liquid successfully ensured bubble-free aspiration of the reaction sub-mix.

4.2 Quantification of cfDNA in the MyoVasc study samples

4.2.1 Measurements with the 90bp assay

All MyoVasc study samples were first measured with our 90 bp qPCR assay. In total, a number 3109 samples were quantified for cfDNA concentration. All samples were sorted and pseudonymized in an Excel data table (*Table 8*). 381 of these samples had to be remeasured due to a difference in Cq values (Diff_Cq) > 0,5 cycles in the pipetted duplicates. This equals an outlier rate of 12.25 %. The samples were remeasured up to four times with newly prepared plasma dilutions each time. Only four samples needed to be measured four times.

Table 8 - Excerpt of the data table for the 90 bp assay measurements

A	B	C	D	E	F	G	H	I	J	K	L	M	N	O
Index	Sample_num_EN	Rack	Position	TubeID	IDkorrDLR	Note_Spomed	Rack_Spomed_90bp	Plate_position_row_90bp_Spomed	Plate_position_col_90bp_Spomed	Date_measurement_90bp	cfDNA_90bp	Cq_mean_90bp	Diff_Cq_90bp	Note_90bp
1	1	3000254011	A01	LEER										
2	2	3000254011	A02	4027760860	ad_cellfreedna_2933		3000254011	A	2	02.01.23	8,296827747	24,7	0,19	Erste Messung
3	3	3000254011	A03	4027760668	ad_cellfreedna_2931		3000254011	A	3	02.01.23	11,87527602	24,13	0,11	Erste Messung
4	4	3000254011	A04	4027760674	ad_cellfreedna_2932		3000254011	A	4	02.01.23	25,61461722	22,91	0,22	Erste Messung
5	5	3000254011	A05	4027820752	ad_cellfreedna_3073		3000254011	A	5	02.01.23	20,48959388	23,26	0,04	Erste Messung
6	6	3000254011	A06	4027804637	ad_cellfreedna_3024		3000254011	A	6	02.01.23	12,68729917	24,02	0,27	Erste Messung
7	7	3000254011	A07	4029375606	ad_cellfreedna_3144		3000254011	A	7	02.01.23	21,4561565	23,19	0,2	Erste Messung
8	8	3000254011	A08	4027820358	ad_cellfreedna_3071		3000254011	A	8	02.01.23	11,25622985	24,21	0,12	Erste Messung
9	9	3000254011	A09	4027804397	ad_cellfreedna_3022		3000254011	A	9	02.01.23	8,85850608	24,59	0,29	Erste Messung
10	10	3000254011	A10	4027804554	ad_cellfreedna_3023		3000254011	A	10	02.01.23	5,258389757	25,42	0,26	Erste Messung
11	11	3000254011	A11	4027804289	ad_cellfreedna_3021		3000254011	A	11	02.01.23	16,25051384	23,65	0,54	Erste Messung
12	12	3000254011	A12	4027816805	ad_cellfreedna_3053		3000099192	A	1	10.01.23	7,394273962	24,88	0,07	Erste Messung
13	13	3000254011	B01	4027803760	ad_cellfreedna_3020		3000254011	B	1	02.01.23	20,77923648	23,25	0,47	Erste Messung
14	14	3000254011	B02	4027818102	ad_cellfreedna_3061		3000254011	B	2	02.01.23	17,42172802	23,52	0,2	Erste Messung
15	15	3000254011	B03	4027820237	ad_cellfreedna_3070		3000254011	B	3	02.01.23	20,62138526	23,25	0,06	Erste Messung
16	16	3000254011	B04	LEER										
17	17	3000254011	B05	4027817490	ad_cellfreedna_3059		3000254011	B	5	02.01.23	15,77830642	23,68	0,28	Erste Messung
18	18	3000254011	B06	4029362010	ad_cellfreedna_3127		104	B	8	31.01.23	14,93867388	23,77	0,43	Zweite Messung
19	19	3000254011	B07	4027817219	ad_cellfreedna_3056		3000254011	B	7	02.01.23	17,75950328	23,49	0,33	Erste Messung
20	20	3000254011	B08	4027819499	ad_cellfreedna_3068		3000254011	B	8	02.01.23	16,35004231	23,62	0,31	Erste Messung
21	21	3000254011	B09	4027819517	ad_cellfreedna_3069		104	B	9	31.01.23	6,078739033	25,19	0,01	Zweite Messung
22	22	3000254011	B10	4029362201	ad_cellfreedna_3129		3000254011	B	10	02.01.23	6,815833103	25,01	0,13	Erste Messung
23	23	3000254011	B11	4029361841	ad_cellfreedna_3126		3000254011	B	11	02.01.23	34,94185078	22,43	0,37	Erste Messung
24	24	3000254011	B12	4027821911	ad_cellfreedna_3074		3000099192	B	1	10.01.23	16,80207202	23,59	0,37	Erste Messung

4.2.2 Measurements with the 222bp assay

The frozen plasma dilutions used for the 90 bp assay measurements were also used for the 222 bp assay measurements. These samples also were sorted and pseudonymized in an Excel data table (*Table 9*). 416 of the 3109 samples had to be remeasured due to a difference in Cq values (Diff_Cq) > 0,5 cycles in the pipetted duplicates. This equals an outlier rate of 13.38 %. The samples were remeasured up to three times with newly prepared plasma dilutions each time.

Table 9 - Excerpt of the data table for the 222 bp assay measurements

Index	Sample_num_EN	Rack	Position	TubeID	IDkorrDLR	Note_Spomed	Rack_Spomed_222bp	Plate_position_row_222bp_Spomed	Plate_position_col_222bp_Spomed	Date_measurement_222bp	cfDNA_222bp	Cq_mean_222bp	Diff_Cq_222bp	Note_222bp		Integrity (222bp/90bp)
1	1	3000254011	A01	LEER												
2	2	3000254011	A02	4027760860	ad_cellfreedna_2933		3000254011	A	2	13.03.23	3,301099527	25,76	0,38	erste Messung		0,397874902
3	3	3000254011	A03	4027760668	ad_cellfreedna_2931		3000254011	A	3	13.03.23	8,64785162	24,2	0	erste Messung		0,728223209
4	4	3000254011	A04	4027760674	ad_cellfreedna_2932		3000254011	A	4	13.03.23	10,2748976	23,93	0,17	erste Messung		0,401134146
5	5	3000254011	A05	4027820752	ad_cellfreedna_3073		3000254011	A	5	13.03.23	7,325454157	24,47	0,2	erste Messung		0,35752071
6	6	3000254011	A06	4027804637	ad_cellfreedna_3024		113	B	1	29.03.23	9,290008658	24,08	0,05	zweite Messung		0,732229022
7	7	3000254011	A07	4029375606	ad_cellfreedna_3144		3000254011	A	7	13.03.23	10,72868705	23,86	0,15	erste Messung		0,500028374
8	8	3000254011	A08	4027820358	ad_cellfreedna_3071		3000254011	A	8	13.03.23	3,851289446	25,5	0,23	erste Messung		0,342147371
9	9	3000254011	A09	4027804397	ad_cellfreedna_3022		3000254011	A	9	13.03.23	3,872170835	25,5	0,19	erste Messung		0,437113301
10	10	3000254011	A10	4027804554	ad_cellfreedna_3023		3000254011	A	10	13.03.23	2,895068883	25,96	0,04	erste Messung		0,550561867
11	11	3000254011	A11	4027804289	ad_cellfreedna_3021		3000254011	A	11	13.03.23	8,890497197	24,16	0,35	erste Messung		0,54709022
12	12	3000254011	A12	4027816805	ad_cellfreedna_3053		3000099192	A	1	28.03.23	2,000788648	26,55	0,11	erste Messung		0,270586221
13	13	3000254011	B01	4027803760	ad_cellfreedna_3020		113	B	2	29.03.23	8,924598754	24,15	0,27	zweite Messung		0,429495991
14	14	3000254011	B02	4027818102	ad_cellfreedna_3061		3000254011	B	2	13.03.23	8,949107205	24,15	0,03	erste Messung		0,513675061
15	15	3000254011	B03	4027820237	ad_cellfreedna_3070		3000254011	B	3	13.03.23	7,185073414	24,5	0,16	erste Messung		0,348428261
16	16	3000254011	B04	LEER												
17	17	3000254011	B05	4027817490	ad_cellfreedna_3059		3000254011	B	5	13.03.23	5,459450436	24,94	0,06	erste Messung		0,346009913
18	18	3000254011	B06	4029362010	ad_cellfreedna_3127		3000254011	B	6	13.03.23	7,154227589	24,51	0,03	erste Messung		0,478906471
19	19	3000254011	B07	4027817219	ad_cellfreedna_3056		3000254011	B	7	13.03.23	7,109880162	24,51	0,03	erste Messung		0,400342287
20	20	3000254011	B08	4027819499	ad_cellfreedna_3068		3000254011	B	8	13.03.23	9,408807492	24,06	0,09	erste Messung		0,575460743
21	21	3000254011	B09	4027819517	ad_cellfreedna_3069		113	B	3	29.03.23	2,524925321	26,18	0,04	zweite Messung		0,415369916
22	22	3000254011	B10	4029362201	ad_cellfreedna_3129		3000254011	B	10	13.03.23	3,080622092	25,86	0,02	erste Messung		0,451980271
23	23	3000254011	B11	4029361841	ad_cellfreedna_3126		3000254011	B	11	13.03.23	6,221821994	24,73	0,08	erste Messung		0,178062176
24	24	3000254011	B12	4027821911	ad_cellfreedna_3074		3000099192	B	1	28.03.23	5,3585528	24,97	0,06	erste Messung		0,318922142

4.2.3 Incurred sample reanalysis

296 of the 3109 samples were randomly selected for incurred sample reanalysis (ISR). Fresh plasma dilutions were prepared, and the samples were reanalysed with both the 90 bp and the 222 bp assay. Outliers were remeasured once to keep a high sample count for reanalysis.

In the 90bp assay (*Figure 11*, A), 33.76% of the reanalysed samples deviated >30% (dotted line) from the first measurement. 14.93% of the samples deviated >45% (dashed line) from the first measurement.

In the 222bp assay (*Figure 11*, B), 52.96% of the reanalysed samples deviated >30% (dotted line) from the first measurement. 34.21% of the samples deviated >45% (dashed line) from the first measurement.

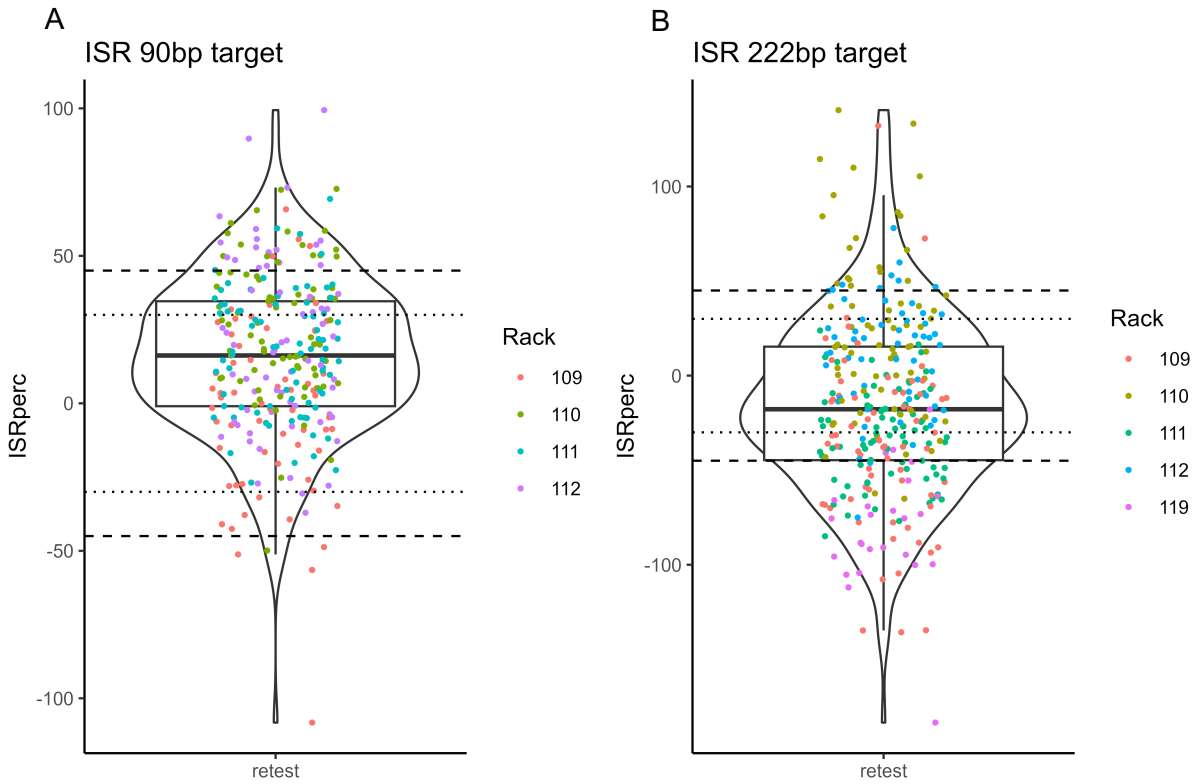

Figure 11 - Incurred sample reanalysis presented as violine plots

(A) *90bp assay, (B) 222bp assay*

4.2.4 Interplate quality control

In each qPCR run, a set of four quality control samples with known cfDNA concentrations was measured and checked for variances. *Figure 12* displays the results from all runs performed with the 90bp qPCR assay, for the Interplate samples 1 and 2 in graph A and B, respectively. The dashed line indicates ± 30% deviation from the mean cfDNA concentration in ng/ml. In *Figure 13*, the cfDNA levels of the reference samples are shown as a line plot over the time of measurements with the 90bp assay.

Figures 14 and 15 present the results for all measurements with the 222bp qPCR assay, respectively.

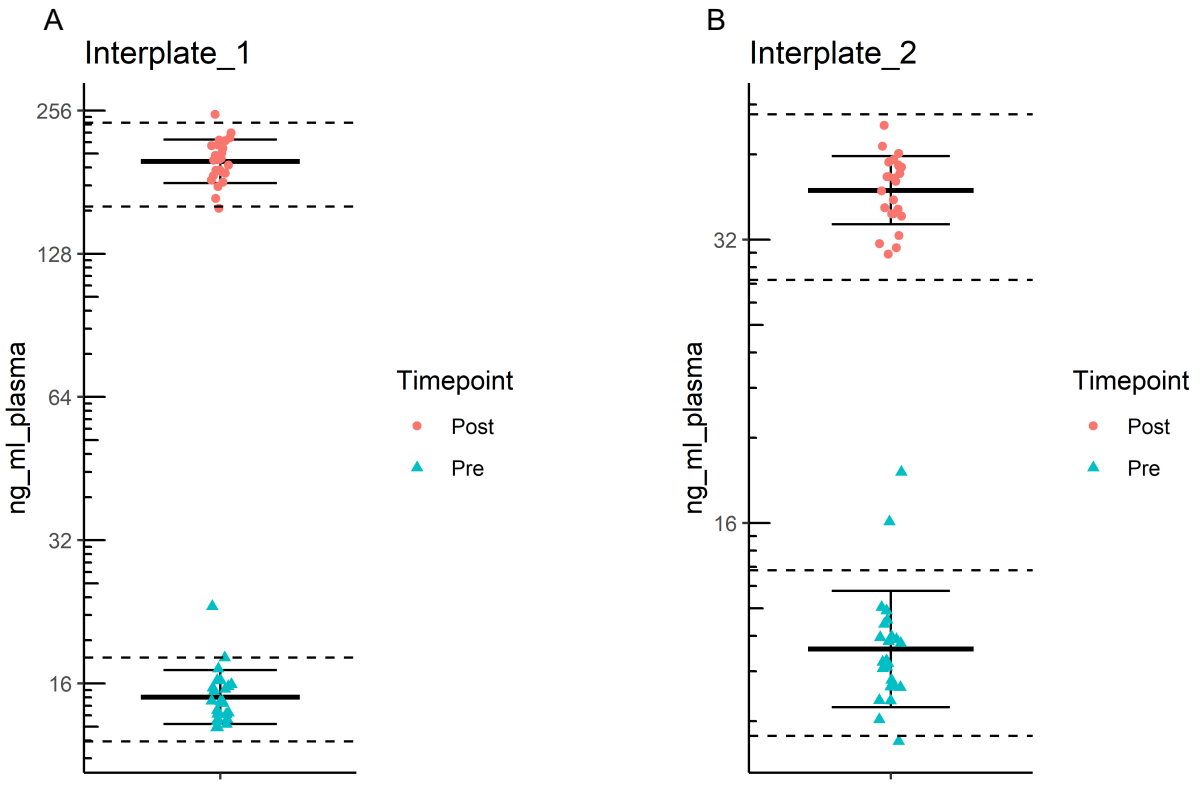

Figure 12 - Interplate sample 1 (A) and 2 (B) measured with the 90bp assay

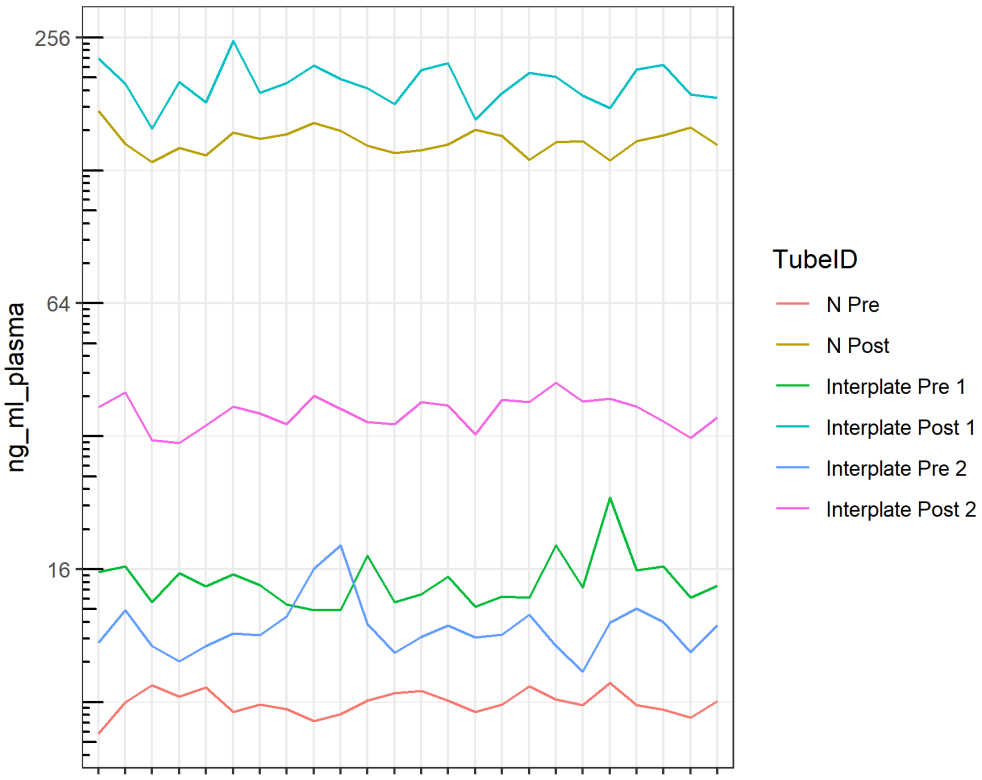

Figure 13 - Line plot for reference samples across all measurements with 90bp assay

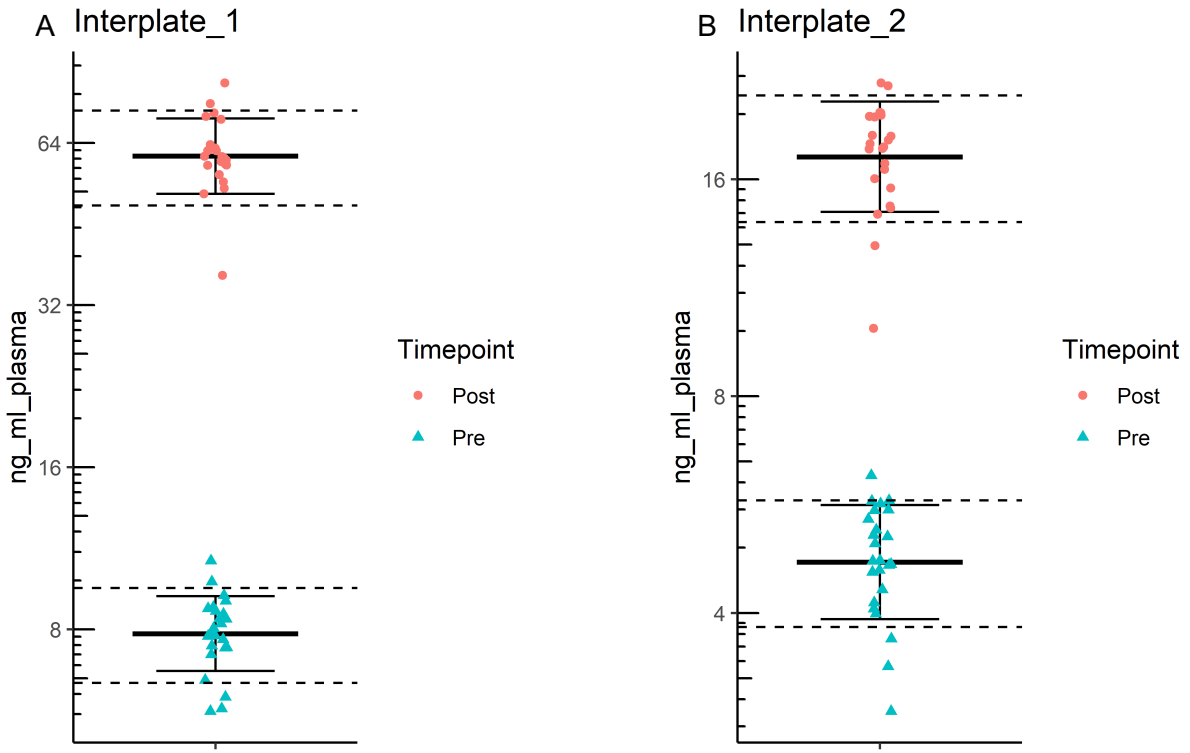

Figure 14 - Interplate sample 1 (A) and 2 (B) measured with the 222bp assay

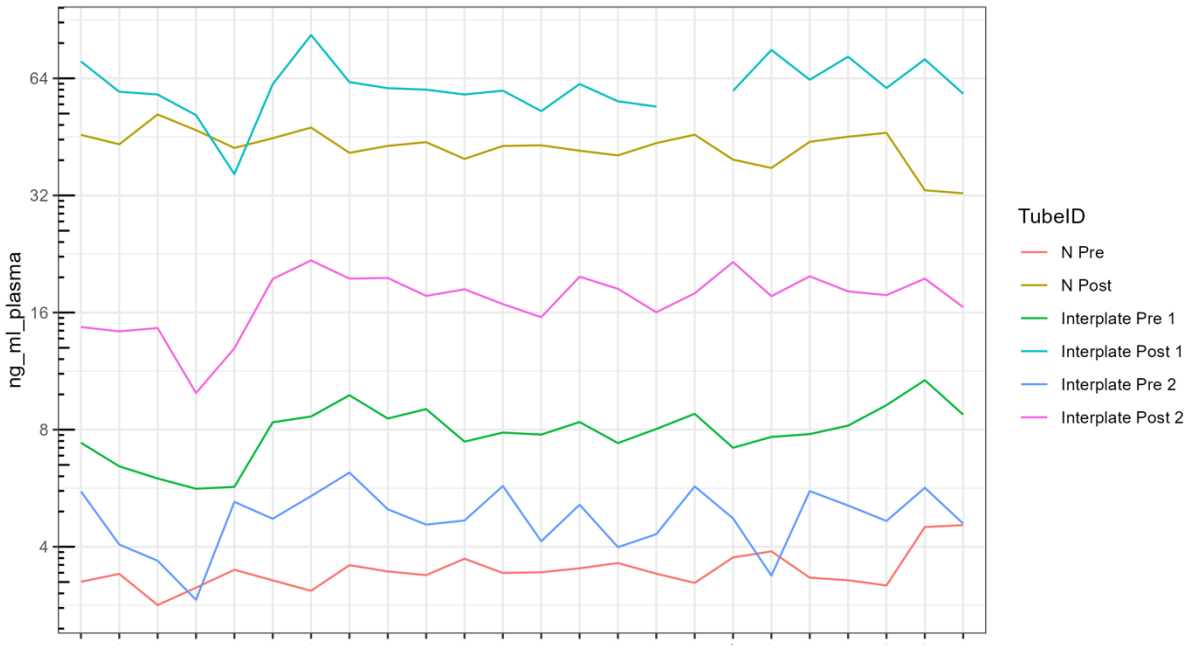

Figure 15 - Line plot for reference samples across all measurements with 222bp assay

4.3 Statistical analysis of cfDNA concentration in the MyoVasc study

4.3.1 Clinical baseline characteristics of study participants

Of 3289 subjects, n =180 needed to be excluded from the analysis with missing cfDNA values as no plasma samples were provided. All following analyses refer to a cohort of n = 3109 individuals. Clinical baseline characteristics of the study sample are reported according to quartiles of cfDNA concentrations (90bp assay in *Table 10*; 222bp assay in *Table 11*) and HF stages (*Table 12*) including a breakdown to HF phenotypes (*Table 13*). Increasing cfDNA quartiles were going along with increasing frequencies of individuals with male sex, higher age, hypertension, diabetes mellitus, obesity, dyslipidaemia, cancer, chronic kidney disease (CKD), chronic obstructive pulmonary disorder (COPD), coronary artery disease (CAD), peripheral artery disease (PAD), venous thromboembolism (VTE) and history of myocardial infarction (MI), stroke, or transient ischaemic attack (TIA). In addition, comorbidities like cardiovascular diseases (CVDs), chronic heart failure (CHF), atrial fibrillation (AF), chronic liver disease (CLD), non-alcoholic fatty liver disease (NAFLD), acute infection, rheumatoid arthritis, atopic dermatitis, pollinosis, endocarditis, palpitations, plaques, higher stiffness indices, and therapies like coronary revascularization (C. revasc.), pacemaker, dialysis, and implantable cardioverter-defibrillators (ICDs) were more prevalent in the highest cfDNA quartile. The opposite was found for smoking, as the highest quartile of cfDNA levels had the lowest proportion of smokers. Percentages of subjects with HFpEF, HFmrEF and HFrEF increased along with increasing cfDNA quartiles. While the proportions of individuals with NYHA class I decreased with increasing cfDNA quartiles, proportions of individuals with NYHA classes II, III and IV increased. Increasing cfDNA quartiles also showed increasing NT-proBNP values and decreasing ejection fractions (EF). With increasing cfDNA level quartiles, the left ventricular ejection fraction reduced and the E/E` ratio increased. Systolic blood pressure rose with increased cfDNA levels. While laboratory values like NT-proBNP, Troponin I, CRP and triglycerides increased with rising cfDNA levels, cholesterol concentrations decreased. The same associations were observed for the 90bp and 222bp cfDNA assays, except for rheumatoid arthritis, endocarditis, and dialysis, where no significant associations were found for cfDNA 222bp. cfDNA levels (90bp and 222bp) significantly increased with higher HF stages (stage 0/A vs stage B vs stage C/D) and HF phenotypes. The integrity index was associated with HF stages, HF phenotypes, and NT-proBNP concentrations (*Table 12, 13 and 15*).

Overall, the analysis sample was 64.6 ± 11.1 years old, ranging from 34 to 85 years, and included 1109 (35.7%) females (*Table 14*).

Table 10 - Characteristics of the study sample according to quartiles of cfDNA 90bp

	Quartiles of cfDNA concentrations			
	≤ 25%	**> 25%-50%**	**> 50%-75%**	**> 75%**
cfDNA 90bp	≤ 11 ng/ml	> 11ng/ml – 14.7 ng/ml	> 14.7 ng/ml – 20.1 ng/ml	> 20.1 ng/ml
Number	777	778	777	777
Age (years)	59.3 ± 11.5	64.0 ± 10.8	66.3 ± 10.1	69.3 ± 9.0
Sex (female)	42.2% (328/777)	33.5% (261/778)	32.9% (256/777)	34.0% (264/777)
CVRFs				
Hypertension	57.5% (447/777)	69.7% (542/778)	78.0% (606/777)	84.3% (655/777)
Diabetes mellitus	16.2% (126/777)	18.1% (141/778)	24.8% (193/777)	31.5% (245/777)
Smoking	19.2% (149/776)	14.4% (112/778)	12.2% (95/776)	7.7% (60/777)
Obesity	15.1% (117/777)	29.0% (226/778)	36.8% (286/777)	44.3% (344/777)
Dyslipidaemia	55.1% (428/777)	67.4% (524/778)	76.1% (591/777)	77.6% (603/777)
Cancer	10.3% (80/777)	16.5% (128/778)	16.3% (127/777)	20.7% (161/777)
Chronic kidney disease	16.3% (127/777)	21.2% (165/778)	27.8% (216/777)	40.2% (312/777)
COPD	19.8% (154/777)	19.5% (152/778)	23.4% (182/777)	24.2% (188/777)
Coronary artery disease	27.8% (216/777)	37.0% (288/778)	43.0% (334/777)	44.9% (349/777)
History of MI	17.8% (138/777)	24.3% (189/778)	26.1% (203/777)	28.4% (221/777)
History of stroke	4.2% (33/777)	8.2% (64/778)	9.9% (77/777)	12.2% (95/777)
History of TIA	3.6% (28/777)	5.9% (46/778)	6.7% (52/777)	8.4% (65/777)
Peripheral artery disease	11.6% (90/777)	14.0% (109/778)	16.6% (129/777)	17.0% (132/777)
VTE	4.5% (35/776)	8.0% (62/778)	9.4% (73/776)	12.1% (94/777)
Comorbidities				
Cardiovascular disease	48.8% (379/777)	68.3% (531/778)	80.4% (625/777)	89.2% (693/777)
Chronic heart failure	31.1% (242/777)	49.4% (384/778)	60.9% (473/777)	76.6% (595/777)
Atrial fibrillation	10.2% (79/777)	15.0% (117/778)	26.4% (205/777)	41.7% (324/777)
Chronic liver disease	6.3% (49/776)	9.4% (73/778)	8.1% (63/776)	10.8% (84/777)
NAFLD	18.8% (146/775)	33.2% (256/771)	41.6% (318/765)	49.5% (380/767)
Acute Infection	13.5% (103/763)	15.5% (120/773)	17.5% (134/767)	17.4% (134/771)
Rheumatoid arthritis	4.5% (34/754)	5.6% (42/751)	5.3% (40/749)	7.8% (58/740)
Atopic dermatitis	3.1% (24/773)	3.2% (25/775)	5.1% (40/777)	4.6% (36/777)
Pollinosis	16.5% (128/774)	14.3% (111/777)	11.9% (92/776)	9.5% (74/776)
Endocarditis	0.6% (5/774)	1.3% (10/777)	2.1% (16/777)	1.7% (13/777)

Palpitations	17.4% (135/777)	15.7% (122/778)	19.8% (154/777)	25.4% (197/777)
Plaques	45.8% (324/708)	59.4% (416/700)	64.3% (448/697)	75.3% (500/664)
Stiffness Index	9.02 (7.11/11.18)	9.17 (7.60/11.12)	9.46 (7.98/11.47)	9.76 (7.85/12.01)
Therapies				
C. revasc.	24.8% (193/777)	34.6% (269/778)	39.0% (303/777)	40.2% (312/777)
Pacemaker	2.8% (22/776)	6.3% (49/776)	8.3% (64/775)	13.0% (101/776)
Dialysis	0.5% (4/777)	0.4% (3/778)	1.0% (8/777)	2.3% (18/777)
ICD	3.7% (29/776)	8.2% (64/776)	9.4% (73/774)	14.5% (112/775)
HF phenotypes and NYHA classes				
HFpEF	10.6% (82/777)	18.0% (140/778)	27.7% (215/777)	31.7% (246/777)
HFmrEF	8.0% (62/777)	11.4% (89/778)	12.1% (94/777)	17.8% (138/777)
HFrEF	4.1% (32/777)	8.5% (66/778)	12.4% (96/777)	17.4% (135/777)
NYHA class I	82.6% (641/776)	74.3% (577/777)	61.5% (477/775)	48.7% (378/776)
NYHA class II	12.4% (96/776)	18.4% (143/777)	26.3% (204/775)	30.7% (238/776)
NYHA class III	3.4% (26/776)	5.8% (45/777)	8.9% (69/775)	16.9% (131/776)
NYHA class IV	1.7% (13/776)	1.5% (12/777)	3.2% (25/775)	3.7% (29/776)
Heart function				
LEVF (%)	57.8 ± 9.1	55.6 ± 10.4	53.7 ± 11.0	51.1 ± 12.4
E/E`	7.29 [5.79/9.35]	8.16 [6.41/10.61]	8.64 [6.52/11.78]	9.71 [7.51/13.19]
SBP (mmHG)	129.6 ± 16.2	132.0 ± 17.7	132.5 ± 18.4	133.7 ± 20.3
Laboratory				
Cholesterol (mmol/L)	202.0 [173.0/234.0]	200.0 [174.0/231.0]	196.0 [164.0/229.0]	193.0 [160.0/225.6]
Triglycerides (mg/dl)	96.0 [71.0/135.0]	109.0 [78.4/152.0]	117.0 [86.0/171.0]	122.5 [88.0/168.6]
eGFR (ml/min)	86.36 ± 16.74	80.91 ± 17.68	75.85 ± 18.47	68.55 ± 20.78
NT-proBNP (pg/ml)	88.00 [49.00/185.08]	132.50 [61.00/311.00]	197.00 [88.00/513.50]	424.50 [155.42/1276.25]
Troponin I (pg/ml)	2.20 [1.40/4.70]	3.50 [1.90/6.93]	4.40 [2.40/8.20]	6.10 [3.50/13.53]
CRP (mg/L)	1.20 [0.63/2.20]	1.60 [0.82/3.10]	1.90 [1.00/4.08]	2.90 [1.50/6.10]

N = 3109; CVRFs: Cardiovascular risk factors; COPD: Chronic obstructive pulmonary disorder; MI: Myocardial infarction; TIA: Transient ischaemic attack; VTE: Venous thromboembolism; NAFLD: Non-alcoholic fatty liver disease; C. revasc.: Coronary revascularization; ICD: Implantable cardioverter-defibrillator; HFpEF: Heart failure with preserved ejection fraction ≥ 50% LVEF; HFmrEF: Heart failure with mildly-reduced ejection fraction (LVEF 40-49%); HFrEF: Heart failure with reduced ejection fraction (LVEF ≤ 40%); NYHA: New York Heart Association; LVEF: Left ventricular ejection fraction; E/E`: diastolic function parameter; SBP: Systolic blood pressure; eGFR: estimated glomerular filtration rate; NT-proBNP: N-terminal natriuretic peptide type B; CRP: C-reactive protein

Table 11 - Characteristics of the study sample according to quartiles of cfDNA 222bp

	Quartiles of cfDNA concentrations			
	≤ 25%	**> 25%-50%**	**> 50%-75%**	**> 75%**
cfDNA 222bp	≤ 4.69 ng/ml	> 4.69 ng/ml – 6.46 ng/ml	> 6.46 ng/ml – 8.70 ng/ml	> 8.70 ng/ml
Number	777	778	777	777
Age (years)	61.6 ± 11.8	64.1 ± 11.2	66.6 ± 10.2	66.5 ± 10.1
Sex (female)	43.8% (340/777)	35.7% (278/778)	32.0% (249/777)	31.1% (242/777)
CVRFs				
Hypertension	60.4% (469/777)	68.9% (536/778)	79.2% (615/777)	81.1% (630/777)
Diabetes mellitus	16.1% (125/777)	19.5% (152/778)	24.2% (188/777)	30.9% (240/777)
Smoking	18.4% (143/776)	14.5% (113/778)	10.1% (78/776)	10.6% (82/777)
Obesity	17.9% (139/777)	25.7% (200/778)	36.7% (285/777)	44.9% (349/777)
Dyslipidaemia	56.6% (440/777)	68.3% (531/778)	73.2% (569/777)	78.0% (606/777)
Cancer	13.4% (104/777)	14.4% (112/778)	15.8% (123/777)	20.2% (157/777)
Chronic kidney disease	19.0% (148/777)	23.5% (183/778)	28.6% (222/777)	34.4% (267/777)
COPD	18.8% (146/777)	21.6% (168/778)	20.6% (160/777)	26.0% (202/777)
Coronary artery disease	31.0% (241/777)	36.6% (285/778)	42.2% (328/777)	42.9% (333/777)
History of MI	20.1% (156/777)	23.0% (179/778)	25.2% (196/777)	28.3% (220/777)
History of stroke	6.2% (48/777)	8.5% (66/778)	9.0% (70/777)	10.9% (85/777)
History of TIA	4.5% (35/777)	6.7% (52/778)	5.8% (45/777)	7.6% (59/777)
Peripheral artery disease	12.7% (99/777)	14.0% (109/778)	15.8% (123/777)	16.6% (129/777)
VTE	6.4% (50/776)	7.7% (60/778)	9.7% (75/777)	10.2% (79/776)
Comorbidities				
Cardiovascular disease	56.0% (435/777)	67.9% (528/778)	79.3% (616/777)	83.5% (649/777)
Chronic heart failure	39.1% (304/777)	49.6% (386/778)	59.8% (465/777)	69.4% (539/777)
Atrial fibrillation	13.5% (105/777)	17.7% (138/778)	27.2% (211/777)	34.9% (271/777)
Chronic liver disease	7.3% (57/776)	7.8% (61/778)	9.8% (76/777)	9.7% (75/776)
NAFLD	19.7% (152/771)	33.1% (256/774)	40.2% (309/768)	50.1% (383/765)
Acute Infection	14.5% (111/765)	15.4% (118/768)	14.4% (111/771)	19.6% (151/770)
Atopic dermatitis	2.6% (20/775)	3.9% (30/778)	5.2% (40/773)	4.5% (35/776)
Pollinosis	15.6% (121/775)	13.0% (101/777)	13.0% (101/776)	10.6% (82/775)
Palpitations	17.2% (134/777)	17.9% (139/778)	20.5% (159/777)	22.7% (176/777)
Plaques	48.9% (347/709)	61.0% (430/705)	64.8% (443/684)	69.7% (468/671)

Stiffness Index	8.95 (7.24/11.07)	9.21 (7.60/11.36)	9.72 (8.03/12.07)	9.55 (7.80/11.51)
Therapies				
C. revasc.	27.3% (212/777)	34.1% (265/778)	38.5% (299/777)	38.7% (301/777)
Pacemaker	3.9% (30/775)	7.7% (60/777)	7.8% (60/774)	11.1% (86/777)
ICD	5.8% (45/775)	7.5% (58/776)	8.7% (67/774)	13.9% (108/776)
HF phenotypes and NYHA classes				
HFpEF	12.9% (100/777)	19.8% (154/778)	26.4% (205/777)	28.8% (224/777)
HFmrEF	10.4% (81/777)	10.3% (80/778)	13.4% (104/777)	15.2% (118/777)
HFrEF	6.8% (53/777)	9.1% (71/778)	9.5% (74/777)	16.9% (131/777)
NYHA class I	77.7% (602/775)	71.7% (557/777)	64.9% (503/775)	52.9% (411/777)
NYHA class II	15.9% (123/775)	19.9% (155/777)	23.5% (182/775)	28.4% (221/777)
NYHA class III	5.3% (41/775)	6.3% (49/777)	9.4% (73/775)	13.9% (108/777)
NYHA class IV	1.2% (9/775)	2.1% (16/777)	2.2% (17/775)	4.8% (37/777)
Heart function				
LEVF (%)	56.7 ± 10.0	55.8 ± 10.5	54.3 ± 10.8	51.4 ± 12.2
E/E`	7.49 [5.85/9.92]	8.21 [6.32/10.47]	8.83 [6.69/11.58]	9.09 [7.00/12.79]
SBP (mmHG)	130.0 ± 17.5	131.9 ± 17.1	134.2 ± 18.3	131.8 ± 19.8
Laboratory				
Cholesterol (mmol/L)	199.0 [170.4/229.0]	202.0 [173.0/233.0]	196.5 [167.0/226.0]	196.0 [160.0/230.0]
Triglycerides (mg/dl)	95.0 [71.0/129.0]	111.0 [79.0/152.0]	117.5 [82.0/171.0]	126.0 [93.4/175.6]
eGFR (ml/min)	83.02 ± 18.41	80.14 ± 18.12	75.68 ± 19.22	72.83 ± 20.97
NT-proBNP (pg/ml)	110.00 [58.00/256.33]	133.00 [62.00/339.33]	199.00 [84.00/525.67]	300.00 [102.00/938.50]
Troponin I (pg/ml)	2.60 [1.40/5.71]	3.60 [1.90/7.20]	4.30 [2.40/8.50]	5.20 [2.80/10.93]
CRP (mg/L)	1.30 [0.66/2.50]	1.60 [0.81/3.28]	1.90 [0.99/4.30]	2.60 [1.30/5.70]

N = 3109; CVRFs: Cardiovascular risk factors; COPD: Chronic obstructive pulmonary disorder; MI: Myocardial infarction; TIA: Transient ischaemic attack; VTE: Venous thromboembolism; NAFLD: Non-alcoholic fatty liver disease; C. revasc.: Coronary revascularization; ICD: Implantable cardioverter-defibrillator; HFpEF: Heart failure with preserved ejection fraction ≥ 50% LVEF; HFmrEF: Heart failure with mildly-reduced ejection fraction (LVEF 40-49%); HFrEF: Heart failure with reduced ejection fraction (LVEF ≤ 40%); NYHA: New York Heart Association; LVEF: Left ventricular ejection fraction; E/E`: diastolic function parameter; SBP: Systolic blood pressure; eGFR: estimated glomerular filtration rate; NT-proBNP: N-terminal natriuretic peptide type B; CRP: C-reactive protein

Table 12 - Characteristics of the study sample according to HF stages (N=3,109)

	HF Stage 0/A	HF Stage B	HF Stage C/D
Proportion	17.2% (534/3109)	29.7% (923/3109)	53.1% (1652/3109)
Age (years)	55.8 ± 10.6	64.4 ± 10.4	67.8 ± 9.9
Sex (female)	44.8% (239/534)	35.3% (326/923)	32.9% (544/1652)
cfDNA 90bp (ng/ml)	10.99 [8.70/13.93]	13.37 [10.35/18.11]	17.11 [12.56/22.80]
cfDNA 222bp (ng/ml)	5.04 [4.07/6.88]	6.03 [4.48/8.06]	7.21 [5.15/9.47]
Integrity Index	0.47 [0.39/0.56]	0.43 [0.36/0.55]	0.41 [0.32/0.52]

Table 13 - Characteristics of the study sample according to HF stages including HF phenotypes (N=2,852)

	HF Stage 0	HF Stage A	HF Stage B	HFpEF	HFmrEF	HFrEF
Proportion	6.5% (186/2852)	12.2% (348/2852)	32.4% (923/2852)	23.9% (683/2852)	13.4% (383/2852)	11.5% (329/2852)
Age (years)	49.1 ± 8.6	59.5 ± 9.8	64.4 ± 10.4	69.9 ± 8.7	66.6 ± 10.5	66.1 ± 10.5
Sex (female)	57.5% (107/186)	37.9% (132/348)	35.3% (326/923)	45.2% (309/683)	24.5% (94/383)	14.3% (47/329)
cfDNA 90bp (ng/ml)	9.53 [7.69/11.98]	11.92 [9.49/15.63]	13.37 [10.35/18.11]	17.53 [13.06/23.24]	16.72 [12.10/23.11]	18.26 [13.49/23.40]
cfDNA 222bp (ng/ml)	4.58 [3.82/5.42]	5.41 [4.33/7.42]	6.03 [4.48/8.06]	7.45 [5.41/9.53]	7.03 [4.92/9.38]	7.59 [5.29/10.29]
Integrity Index	0.48 [0.40/0.59]	0.45 [0.38/0.55]	0.43 [0.36/0.55]	0.41 [0.32/0.52]	0.41 [0.33/0.52]	0.40 [0.32/0.52]

Table 14 - Characteristics of the study sample according to sex (N=3,109)

	Men	Women
Number	64.3% (2000/3109)	35.7% (1109/3109)
cfDNA 90bp (ng/ml)	14.94 [11.25/20.27]	14.08 [10.34/19.67]
cfDNA 222bp (ng/ml)	6.73 [4.86/8.90]	5.83 [4.34/8.28]
Integrity Index	0.44 [0.35/0.55]	0.42 [0.33/0.52]

Table 15 - Characteristics of the study sample according to quartiles of the integrity index

	Quartiles of cfDNA integrity index			
	≤ 25%	**> 25%-50%**	**> 50%-75%**	**> 75%**
Integrity Index	≤ 0.344	> 0.344 – 0.428	> 0.428 – 0.536	> 0.536
Number	777	778	777	777
Age (years)	67.6 ± 10.2	66.2 ± 10.3	63.1 ± 11.3	62.0 ± 11.4
Sex (female)	39.9% (310/777)	36.1% (281/778)	35.1% (273/777)	31.5% (245/777)
cfDNA 90bp (ng/ml)	19.00 [13.94/26.33]	15.39 [11.62/20.31]	13.55 [10.63/17.97]	12.19 [9.19/16.12]
cfDNA 222bp (ng/ml)	5.23 [3.75/7.38]	5.84 [4.53/7.91]	6.58 [5.00/8.49]	8.21 [6.00/11.27]
NT-proBNP (pg/ml)	88.00 [49.00/185.08]	132.50 [61.00/311.00]	197.00 [88.00/513.50]	424.50 [155.42/1276.25]

4.3.2 Relation between cfDNA levels and cardiac function

As presented in *Table 16*, the multivariable linear regression analysis for cfDNA 90bp showed a negative association with left ventricular ejection fraction (LVEF) (beta estimate, β = -2.32, 95% of CI [-2.71; -1.93]) when adjusted for age and sex (model 1), which remained in the model when further adjusted for cardiovascular risk factors (CVRFs) (model 2) (β = -2.04 [-2.43; -1.64]) and medication (model 3) (β = -0.973 [-1.34; -0.609]). In analogy, the same analysis for cfDNA 222bp presented with a negative association (β_{model_1} = -1.54 [-1.91; -1.16] and β_{model_2} = -1.27 [-1.64; -0.889] and β_{model_3} = -0.519 [-0.858; -0.181]) with LVEF.

The analysis between cfDNA levels and the diastolic function parameter, expressed as E/E' ratio, presented with a positive association for cfDNA 90bp (β_{model_1} = 0.0772 [0.0619; 0.0925] and β_{model_2} = 0.0599 [0.0442; 0.0756] and β_{model_3} = 0.0409 [0.0251; 0.0567]) and cfDNA 222bp (β_{model_1} = 0.0772 [0.0619; 0.0925] and β_{model_2} = 0.0599 [0.0442; 0.0756] and β_{model_3} = 0.0409 [0.0251; 0.0567]).

cfDNA 90bp and 222bp levels were positively associated with NT-proBNP concentrations (90bp: β_{model_1} = 0.394 [0.350; 0.438] and β_{model_2} = 0.362 [0.318; 0.406] and β_{model_3} = 0.218 [0.178; 0.258]; 222bp: β_{model_1} = 0.226 [0.182; 0.270] and β_{model_2} = 0.196 [0.153; 0.239] and β_{model_3} = 0.101 [0.0630; 0.138]). All associations were statistically significant with $p < 0.05$.

Table 16 – Association of cfDNA levels and cardiac function

	Model 1	Model 2	Model 3
LVEF			
cfDNA 90bp	β = -2.32 [-2.71; -1.93]	β = -2.04 [-2.43; -1.64]	β = -0.973 [-1.34; -0.609]
cfDNA 222bp	β = -1.54 [-1.91; -1.16]	β = -1.27 [-1.64; -0.889]	β = -0.519 [-0.858; -0.181]
E/E'			
cfDNA 90bp	β = 0.0772 [0.0619; 0.0925]	β = 0.0599 [0.0442; 0.0756]	β = 0.0409 [0.0251; 0.0567]
cfDNA 222bp	β = 0.0772 [0.0619; 0.0925]	β = 0.0599 [0.0442; 0.0756]	β = 0.0409 [0.0251; 0.0567]
NT-proBNP			
cfDNA 90bp	β = 0.394 [0.350; 0.438]	β = 0.362 [0.318; 0.406]	β = 0.218 [0.178; 0.258]
cfDNA 222bp	β = 0.226 [0.182; 0.270]	β = 0.196 [0.153; 0.239]	β = 0.101 [0.0630; 0.138]

Model 1: adjusted for age and sex; Model 2: adjusted for age, sex, and CVRFs; Model 3: adjusted for age, sex, CVRFs, and medication

4.3.3 Relation of cfDNA levels and HF stages

Logistic regression analyses on cfDNA levels were performed to calculate the risk of having HF stage C/D versus having no HF (stage 0/A) (*Table 17*). Increased cfDNA 90bp levels went along with an OR = 2.38 ([2.06; 2.77]; $p < 0.0001$) for having HF stage C/D, adjusted for age and sex (model 1). When further adjusted for cardiovascular risk factors (model 2), the odds ratio decreased, but stayed significantly elevated (OR = 2.17 [1.86; 2.55]; $p < 0.0001$). Similar effects were observed for cfDNA 222bp levels (OR_{model_2} = 1.52 [1.33; 1.73]; $p < 0.0001$).

Table 17 – Association of cfDNA levels and HF stages

Stage C/D vs. 0/A	Model 1	Model 2
cfDNA 90bp	OR = 2.38 [2.06; 2.77]; $p < 0.0001$	OR = 2.17 [1.86; 2.55]; $p < 0.0001$
cfDNA 222bp	OR = 1.68 [1.48; 1.90]; $p < 0.0001$	OR = 1.52 [1.33; 1.73]; $p < 0.0001$
Integrity Index	OR = 0.80 [0.71; 0.89]; $p = 0.00013$	OR = 0.79 [0.70; 0.90]; $p = 0.00029$

Model 1: adjusted for age and sex; Model 2: adjusted for age, sex, and CVRFs

4.3.4 Relation between cfDNA levels and worsening of HF, cardiac death, or all-cause death

The effect of cfDNA 90bp levels on **worsening of HF** in four years of follow-up was significant in whole sample analysis (HR_{model_1} = 1.433 [1.305; 1.595]; $p < 0.0001$), adjusted for age and sex (*Table 18*, *Figure 16*). It remained significant after further adjustments for CVRFs (model 2) (HR_{model_2} = 1.325 [1.190; 1.476]; $p < 0.0001$), and CVRFs plus medication (model 3) (HR_{model_3} = 1.198 [1.071; 1.341]; $p = 0.0016$). After additional adjustment for NT-proBNP (model 4), the influence of cfDNA levels on worsening of HF was no longer significant (HR_{model_4} = 1.008 [0.898; 1.132]; $p = 0.89$). The same effect was seen for cfDNA 222bp levels, although it already lost significance in model 3, when additionally adjusted for medication (HR_{model_3} = 1.108 [0.995; 1.234]; $p = 0.063$). The Integrity Index had no relevant effect on worsening of HF.

Looking at different stages of HF separately, stage C/D patients showed the same significant effect of cfDNA levels on worsening of HF as the whole sample, while in stage B patients there was no significant effect.

To further evaluate the effect of cfDNA levels on worsening of HF when added to a multivariable predictive model - adjusted for age, sex, CVRFs, and medication - and to compare it with the current gold-standard biomarker NT-proBNP, we performed C-statistics as presented in *Table 19*. NT-proBNP showed a significantly higher C index than cfDNA 90bp and cfDNA 222bp levels when added to the model. Additional adding of cfDNA levels to a model with NT-proBNP did not lead to higher C indices in the predictive model than obtained with NT-proBNP alone.

Table 18 - Effect of cfDNA levels on worsening of HF

	Model 1	Model 2	Model 3	Model 4
Whole sample				
cfDNA 90bp	HR = 1.433 [1.305; 1.595]; **$p < 0.0001$**	HR = 1.325 [1.190; 1.476]; **$p < 0.0001$**	HR = 1.198 [1.071; 1.341]; **$p = 0.0016$**	HR = 1.008 [0.898; 1.132]; $p = 0.89$
cfDNA 222bp	HR = 1.280 [1.153; 1.421]; **$p < 0.0001$**	HR = 1.202 [1.080; 1.338]; **$p = 0.00076$**	HR = 1.108 [0.995; 1.234]; $p = 0.063$	
Stage C/D				
cfDNA 90bp	HR = 1.377 [1.230; 1.541]; **$p < 0.0001$**	HR = 1.292 [1.148; 1.454]; **$p < 0.0001$**	HR = 1.206 [1.068; 1.362]; **$p = 0.0026$**	HR = 1.018 [0.896; 1.157]; $p = 0.78$
cfDNA 222bp	HR = 1.244 [1.108; 1.398]; **$p = 0.00022$**	HR = 1.189 [1.059; 1.334]; **$p = 0.0034$**	HR = 1.111 [0.989; 1.248]; $p = 0.077$	

Stage B	
cfDNA 90bp	HR = 1.204 [0.932; 1.555]; $p = 0.15$
cfDNA 222bp	HR = 1.147 [0.861; 1.527]; $p = 0.35$

Model 1: adjusted for age and sex; Model 2: adjusted for age, sex, and CVRFs; Model 3: adjusted for age, sex, CVRFs, and medication; Model 4: adjusted for ages, sex, CVRFs, medication, and NT-proBNP

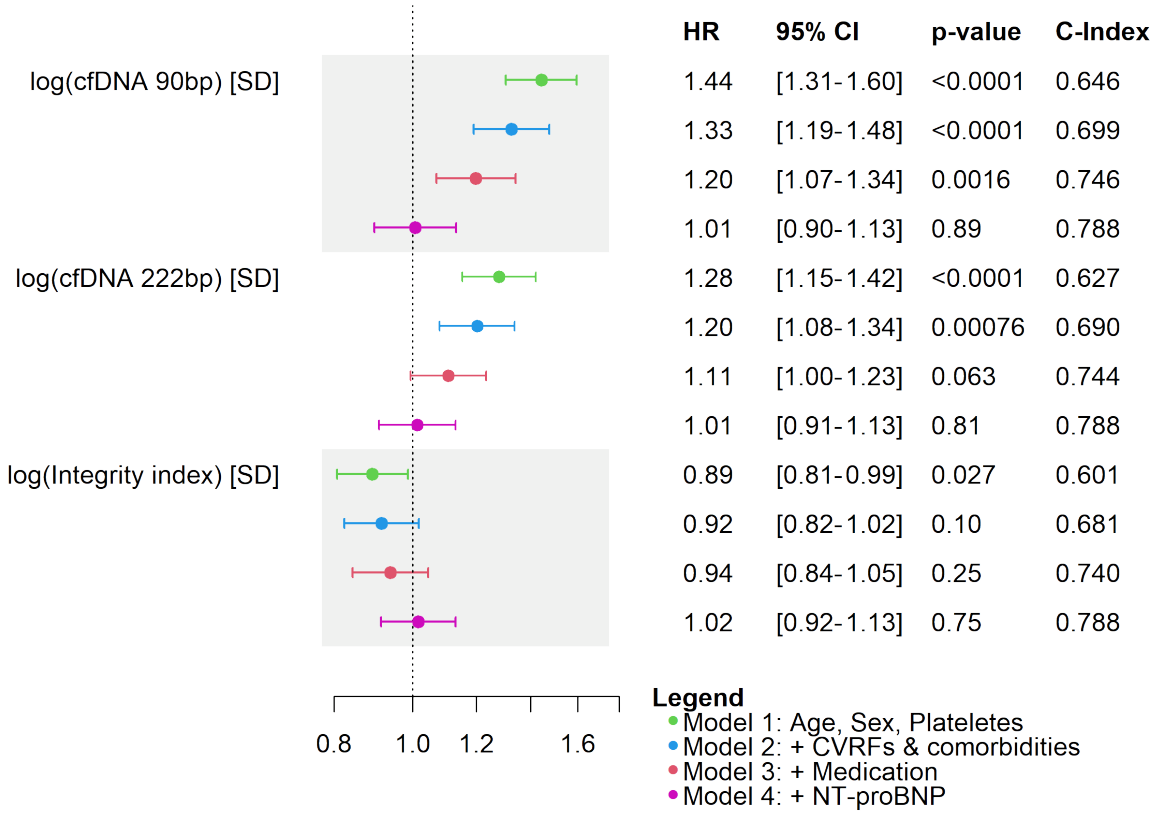

Figure 16 - Effect of cfDNA levels on worsening of HF in whole sample analysis

Table 19 – C-statistics for adding NT-proBNP, cfDNA or both to the multivariable predictive model (model 3) for worsening of HF

Worsening of HF at 4 years	**C index**	***p* Value for difference to NT-proBNP**
NT-proBNP	0.788	
cfDNA 90bp	0.746	***p* < 0.0001**
cfDNA 222bp	0.744	***p* < 0.0001**
NT-proBNP + cfDNA 90bp	0.788	$p = 0.20$
NT-proBNP + cfDNA 222bp	0.788	$p = 0.16$

The effect of cfDNA 90bp levels on **cardiac death** in six years of follow-up was significant in whole sample analysis (HR_{model_1} = 1.710 [1.484; 1.971]; $p < 0.0001$), adjusted for age and sex (*Table 20*, *Figure 17*). It remained significant after further adjustments for CVRFs (HR_{model_2} = 1.504 [1.291; 1.753]; $p < 0.0001$), and CVRFs plus medication (HR_{model_3} = 1.331 [1.131; 1.566]; $p = 0.00058$). After additional adjustment for NT-proBNP, the influence of cfDNA levels on cardiac death was no longer significant (HR_{model_4} = 1.071 [0.901; 1.274]; $p = 0.43$). The same effect was seen for cfDNA 222bp levels, although it already lost significance in model 3, when additionally adjusted for medication (HR_{model_3} = 1.149 [0.980; 1.346]; $p = 0.087$). The Integrity Index had no relevant effect on worsening of HF.

Looking at different stages of HF separately, stage C/D patients showed the same significant effect of cfDNA levels on cardiac death as the whole sample, while in stage B patients there was no significant effect.

In the C-statistics (*Table 21*) for cardiac death, adding of cfDNA levels to a model with NT-proBNP again did not increase C indices in the predictive model compared to the NT-proBNP-only model.

Table 20 - Effect of cfDNA levels on cardiac death

	Model 1	**Model 2**	**Model 3**	**Model 4**
Whole sample				
cfDNA 90bp	HR = 1.710 [1.484; 1.971]; ***p* < 0.0001**	HR = 1.504 [1.291; 1.753]; ***p* < 0.0001**	HR = 1.331 [1.131; 1.566]; ***p* = 0.00058**	HR = 1.071 [0.901; 1.274]; *p* = 0.43
cfDNA 222bp	HR = 1.404 [1.215; 1.622]; ***p* < 0.0001**	HR = 1.294 [1.109; 1.509]; ***p* = 0.0011**	HR = 1.149 [0.980; 1.346]; *p* = 0.087	
Stage C/D				
cfDNA 90bp	HR = 1.526 [1.304; 1.784]; ***p* < 0.0001**	HR = 1.388 [1.180; 1.634]; ***p* < 0.0001**	HR = 1.281 [1.079; 1.520]; ***p* = 0.0047**	HR = 1.062 [0.886; 1.273]; *p* = 0.51
cfDNA 222bp	HR = 1.340 [1.142; 1.573]; ***p* = 0.00034**	HR = 1.265 [1.074; 1.489]; ***p* = 0.0048**	HR = 1.152 [0.974; 1.363]; *p* = 0.098	
Stage B				
cfDNA 90bp	HR = 1.509 [0.862; 2.642]; *p* = 0.15			
cfDNA 222bp	HR = 1.282 [0.759; 2.167]; *p* = 0.35			

Model 1: adjusted for age and sex; Model 2: adjusted for age, sex, and CVRFs; Model 3: adjusted for age, sex, CVRFs, and medication; Model 4: adjusted for ages, sex, CVRFs, medication, and NT-proBNP

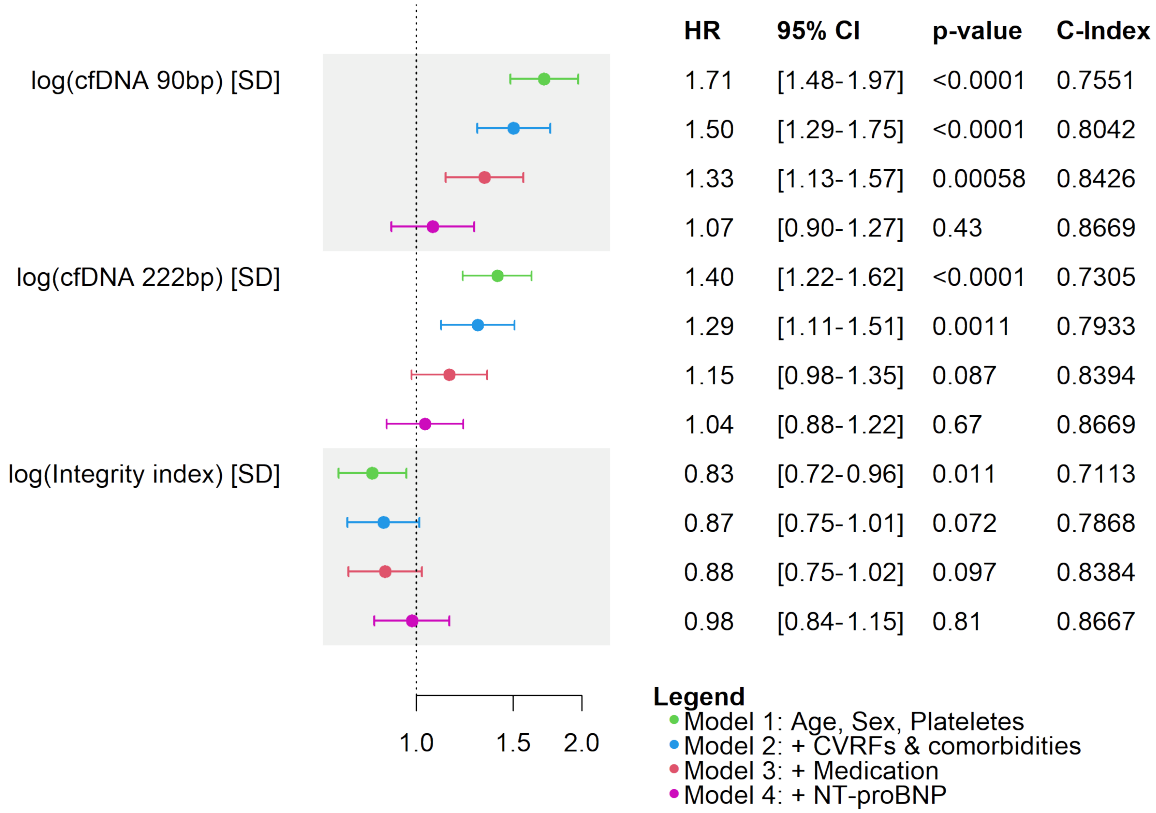

Figure 17 - Effect of cfDNA levels on cardiac death in whole sample analysis

Table 21 – C-statistics for adding NT-proBNP, cfDNA or both to the multivariable predictive model (model 3) for cardiac death

Cardiac death at 6 years	C index	*p* Value for difference to NT-proBNP
NT-proBNP	0.867	
cfDNA 90bp	0.843	***p* = 0.0034**
cfDNA 222bp	0.840	***p* = 0.0019**
NT-proBNP + cfDNA 90bp	0.867	*p* = 0.71
NT-proBNP + cfDNA 222bp	0.867	*p* = 0.55

Addressing the endpoint of **all-cause death** after nine years of follow-up (*Table 22*, *Figure 18*), cfDNA 90bp levels had a significant association with the outcome in whole sample analysis (HR_{model_1} = 1.510 [1.397; 1.633]; $p < 0.0001$). It remained significant even after adding NT-proBNP to the model (HR_{model_4} = 1.173 [1.073; 1.282]; $p = 0.00046$). In whole sample analysis, cfDNA 222bp levels only had a significant association with all-cause death without adjustment

for NT-proBNP (HR_{model_3} = 1.143 [1.054; 1.240]; p = 0.0013), while in stage C/D subjects the association remained significant with adjustment for NT-proBNP (HR_{model_4} = 1.121 [1.021; 1.231]; p = 0.017). There was no significant effect of cfDNA levels in subjects with HF stage B (90bp: HR_{model_1} = 1.216 [0.974; 1.519]; p = 0.084; 222bp: HR_{model_1} = 1.008 [0.823; 1.234]; p = 0.94). The Integrity Index only had a significant association with all-cause death in whole sample analysis and without adjustment for NT-proBNP.

In the case of all-cause death, the adding of cfDNA levels to a model with NT-proBNP lead to slightly, though not significantly higher C indices in the predictive model than with NT-proBNP alone (*Table 23*).

Table 22 - Effect of cfDNA levels on all-cause death

	Model 1	**Model 2**	**Model 3**	**Model 4**
Whole sample				
cfDNA 90bp	HR = 1.510 [1.397; 1.633]; ***p* < 0.0001**	HR = 1.426 [1.314; 1.546]; ***p* < 0.0001**	HR = 1.312 [1.205; 1.430]; ***p* < 0.0001**	HR = 1.173 [1.073; 1.282]; ***p* = 0.00046**
cfDNA 222bp	HR = 1.281 [1.186; 1.383]; ***p* < 0.0001**	HR = 1.235 [1.141; 1.337]; ***p* < 0.0001**	HR = 1.143 [1.054; 1.240]; ***p* = 0.0013**	HR = 1.085 [0.999; 1.180]; p = 0.054
Integrity Index	HR = 0.873 [0.811; 0.940]; ***p* = 0.00030**	HR = 0.891 [0.825; 0.961]; ***p* = 0.0029**	HR = 0.895 [0.828; 0.968]; ***p* = 0.0053**	HR = 0.947 [0.875; 1.025]; p = 0.18
Stage C/D				
cfDNA 90bp	HR = 1.436 [1.315; 1.569]; ***p* < 0.0001**	HR = 1.369 [1.252; 1.498]; ***p* < 0.0001**	HR = 1.302 [1.185; 1.430]; ***p* < 0.0001**	HR = 1.189 [1.079; 1.311]; ***p* = 0.00049**
cfDNA 222bp	HR = 1.286 [1.177; 1.405]; ***p* < 0.0001**	HR = 1.254 [1.145; 1.372]; ***p* < 0.0001**	HR = 1.180 [1.075; 1.295]; ***p* = 0.00048**	HR = 1.121 [1.021; 1.231]; ***p* = 0.017**
Integrity Index	HR = 0.922 [0.849; 1.000]; p = 0.050			
Stage B				
cfDNA 90bp	HR = 1.216 [0.974; 1.519]; p = 0.084			
cfDNA 222bp	HR = 1.008 [0.823; 1.234]; p = 0.94			
Integrity Index	HR = 0.827 [0.673; 1.017]; p = 0.071			

Model 1: adjusted for age and sex; Model 2: adjusted for age, sex, and CVRFs; Model 3: adjusted for age, sex, CVRFs, and medication; Model 4: adjusted for ages, sex, CVRFs, medication, and NT-proBNP

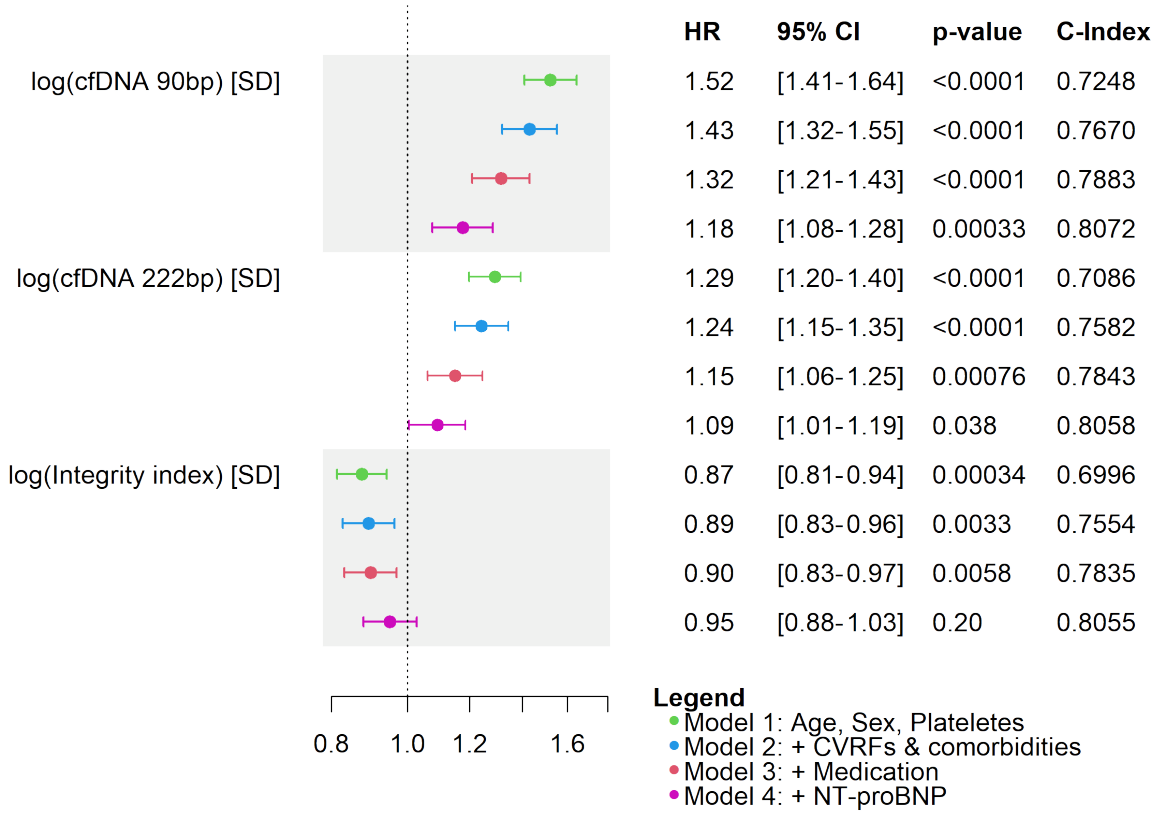

Figure 18 - Effect of cfDNA levels on all-cause death in whole sample analysis

Table 23 – C-statistics for adding NT-proBNP, cfDNA or both to the multivariable predictive model (model 3) for all-cause death

All-cause death at 9 years	C index	*p* Value for difference to NT-proBNP
NT-proBNP	0.805	
cfDNA 90bp	0.788	***p* < 0.0001**
cfDNA 222bp	0.784	***p* < 0.0001**
NT-proBNP + cfDNA 90bp	0.807	***p* = 0.050**
NT-proBNP + cfDNA 222bp	0.806	*p* = 0.42

Cumulative incidence (CI) plots (*Figures 19-21*) were created for worsening of HF, cardiac death, and all-cause death depending on quartiles of cfDNA levels (for the 90bp and the 222bp assay) and quartiles of the integrity index (A). Additional CI plots were created with dichotomised variables according to the median value (B) and to the 75th percentile (C). All

plots for cfDNA 90bp are found below. Plots for cfDNA 222bp and the integrity index are attached in the appendix (Figures A2-A7), as they essentially show the same tendencies.

Continuous (quartiles) and dichotomised cfDNA levels showed a significant trend for all three outcomes, i.e., worsening of HF, cardiac death, and all-cause death. The higher the cfDNA levels, the higher were the incidence rates in the categorized groups.

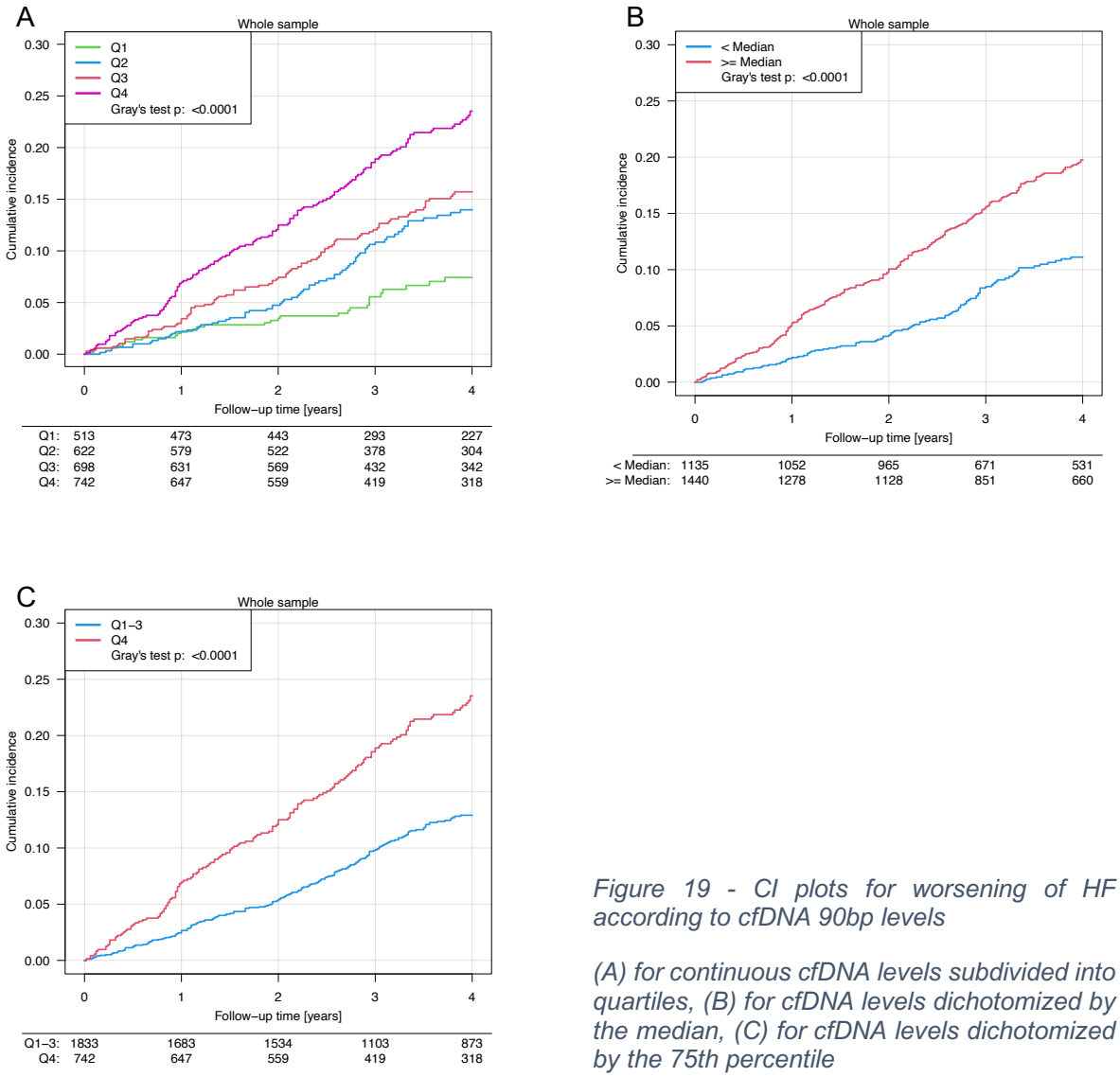

Figure 19 - CI plots for worsening of HF according to cfDNA 90bp levels

(A) for continuous cfDNA levels subdivided into quartiles, (B) for cfDNA levels dichotomized by the median, (C) for cfDNA levels dichotomized by the 75th percentile

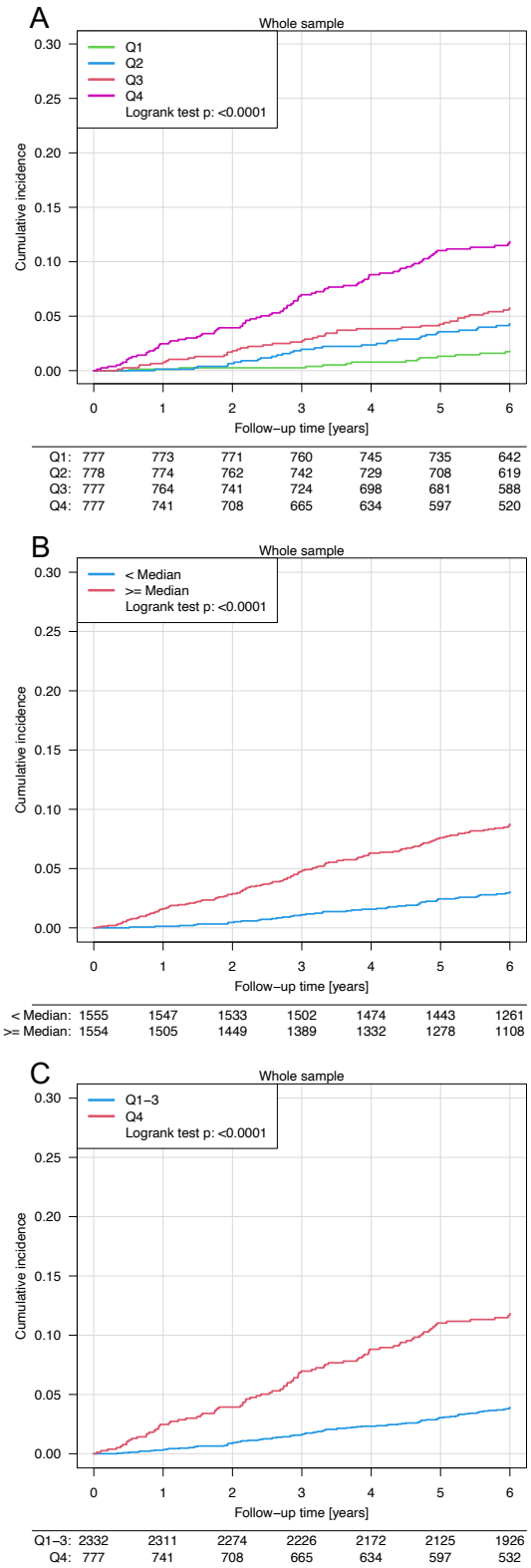

Figure 20 - CI plots for cardiac death according to cfDNA 90bp levels

(A) for continuous cfDNA levels subdivided into quartiles, (B) for cfDNA levels dichotomized by the median, (C) for cfDNA levels dichotomized by the 75th percentile

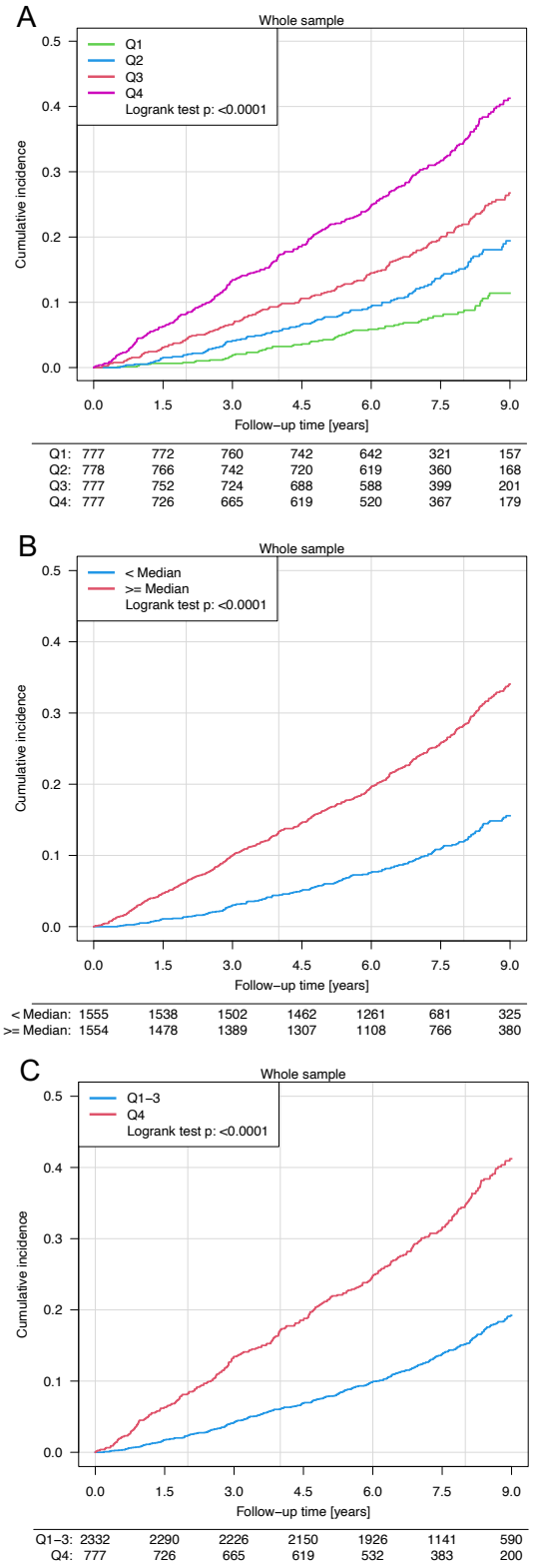

Figure 21 - CI plots for all-cause death according to cfDNA 90bp levels

(A) for continuous cfDNA levels subdivided into quartiles, (B) for cfDNA levels dichotomized by the median, (C) for cfDNA levels dichotomized by the 75th percentile

To compare the effect of cfDNA levels with NT-proBNP levels on outcome predicting models, patients were categorized according to median levels of cfDNA and NT-proBNP and displayed in CI plots. The graphs below (*Figure 22-24*) represent cfDNA 90bp levels, while additional CI plots for cfDNA 222bp and the integrity index are found in the appendix (Figures A8-A9), as they essentially show the same tendencies as cfDNA 90bp levels. Gray´s test was used to test the statistical significance between curves (a and b).

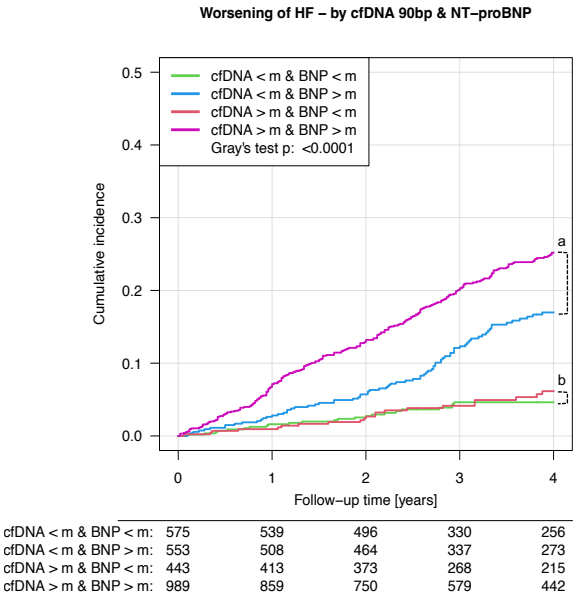

Figure 22 - CI plot for worsening of HF according to combinations of cfDNA and NT-proBNP levels

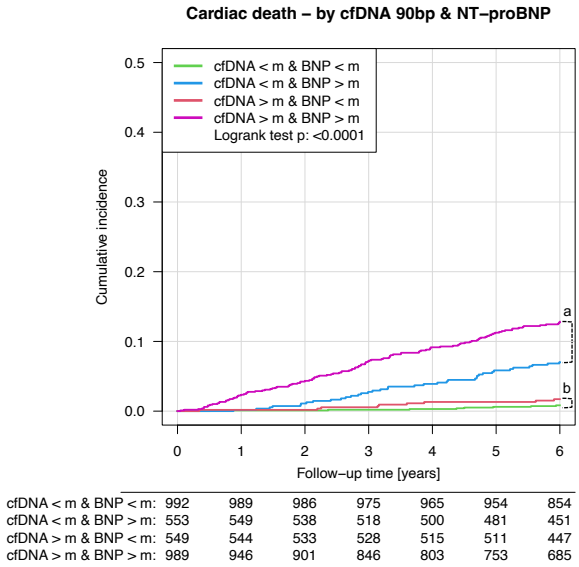

Figure 23 - CI plot for cardiac death according to combinations of cfDNA and NT-proBNP levels

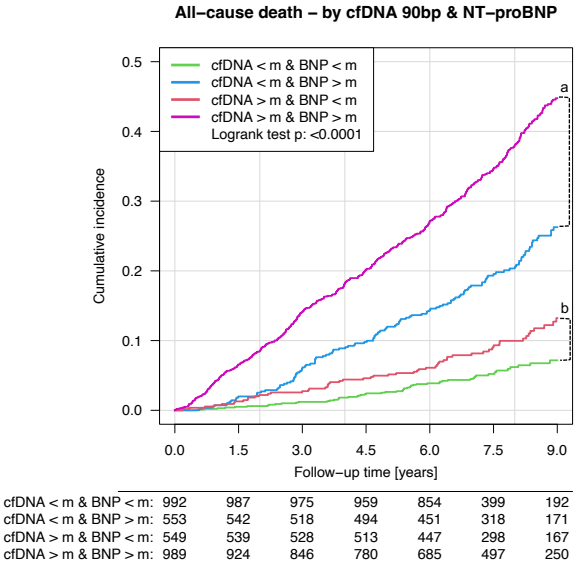

Figure 24 - CI plot for all-cause death according to combinations of cfDNA and NT-proBNP levels

When looking at **worsening of HF** (*Figure 22*), patients with elevations in both biomarkers (purple) showed the highest cumulative incidence, while those with low levels of both biomarkers (green) or elevated cfDNA levels only (red) showed the lowest incidence rate. There was no significant outcome difference in patients with elevated cfDNA levels compared to low cfDNA levels, if both groups had low NT-proBNP levels (b: *p=0.60*). Patients with low cfDNA levels, but high NT-proBNP levels (blue) showed the second highest incidence rate, significantly different to patients with both biomarkers elevated (a: *p<0.0001*). The same was observed when investigating the outcome of **cardiac death** (*Figure 23*) (a: *p<0.0001; b: p=0.16)*. When looking at the outcome of **all-cause death** (*Figure 24*), the cohort with elevated cfDNA levels and low NT-proBNP levels (red) had a significantly different cumulative incidence than the cohort with low levels of both biomarkers (green) (*b: p=0.0035)*. Patients with elevations in both biomarkers (purple) remain the highest incidence rate, significantly different to those with elevated NT-proBNP levels only (blue) (a: *p<0.0001)*.

4.3.5 Correlation between 90bp and 222bp assay measurements

The qPCR measurements with the 90bp and 222bp assays correlated well with a value of 0.62 (*Figure 25*). Both assays showed comparable accuracies with a mean Diff_Cq for duplicates of 0.19 (90bp) and 0.15 (222bp). Mean cfDNA 90bp levels were ~2.3-fold higher than 222bp levels, which leads to a mean integrity index (levels(222bp)/levels(90bp)) of 0.43.

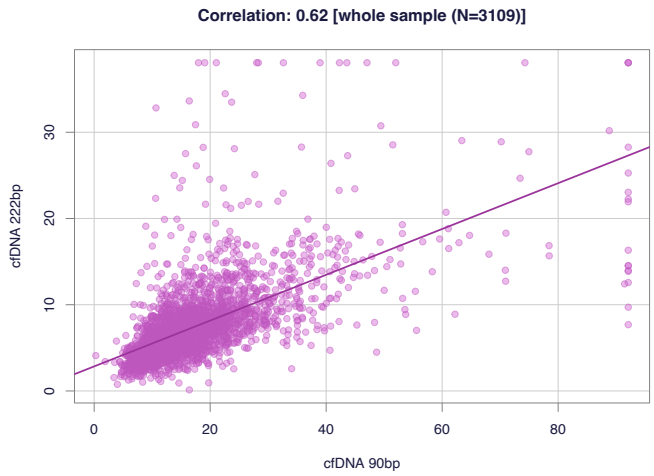

Figure 25 - Correlation between cfDNA 90bp and 222bp assay measurements

4.3.6 Correlation analyses for cfDNA with gold-standard biomarker NT-proBNP, HF stages and NYHA classes

cfDNA 90bp levels and NT-proBNP showed a moderate correlation with a value of 0.39 (*Figure 26*). The correlation of cfDNA 222bp and NT-proBNP levels was weaker with a value of 0.23. Further cfDNA levels correlated well with HF stages, HF phenotypes, and NYHA classes as exemplarily shown for cfDNA 90bp in the violine plots below (*Figure 27-29*).

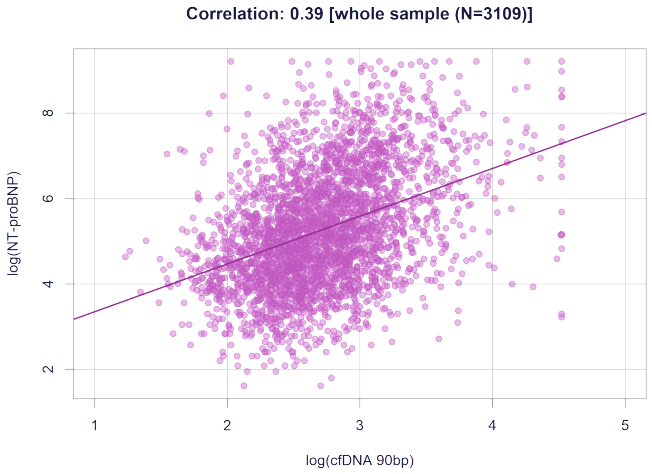

Figure 26 - Correlation between cfDNA 90bp levels and NT-proBNP

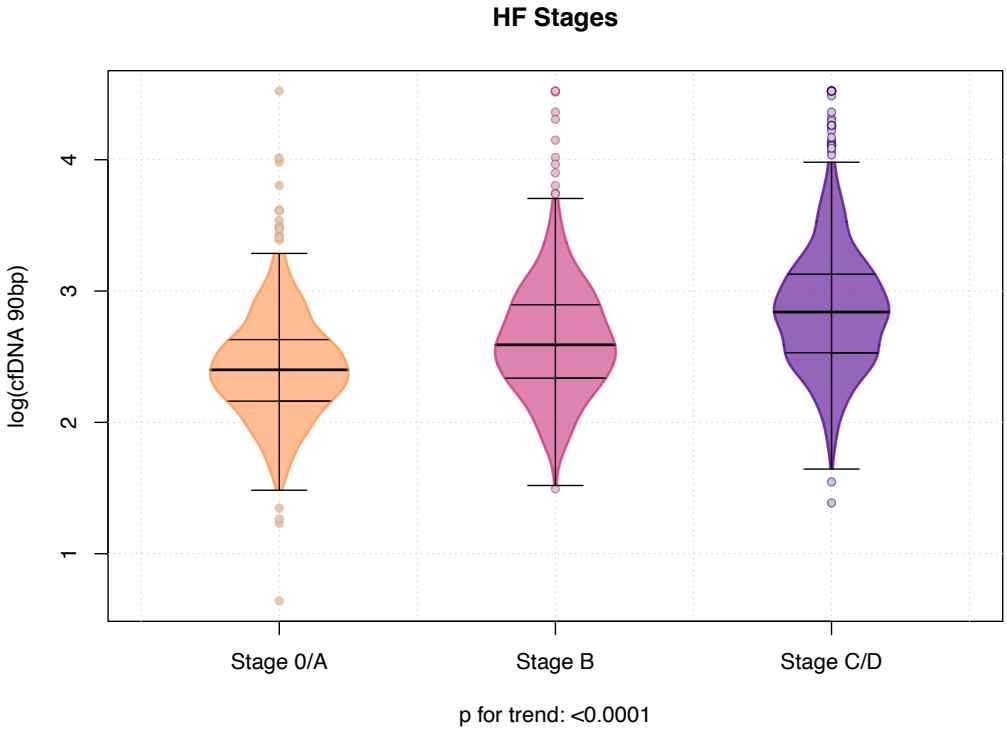

Figure 27 - Correlation between cfDNA 90bp levels and HF stages

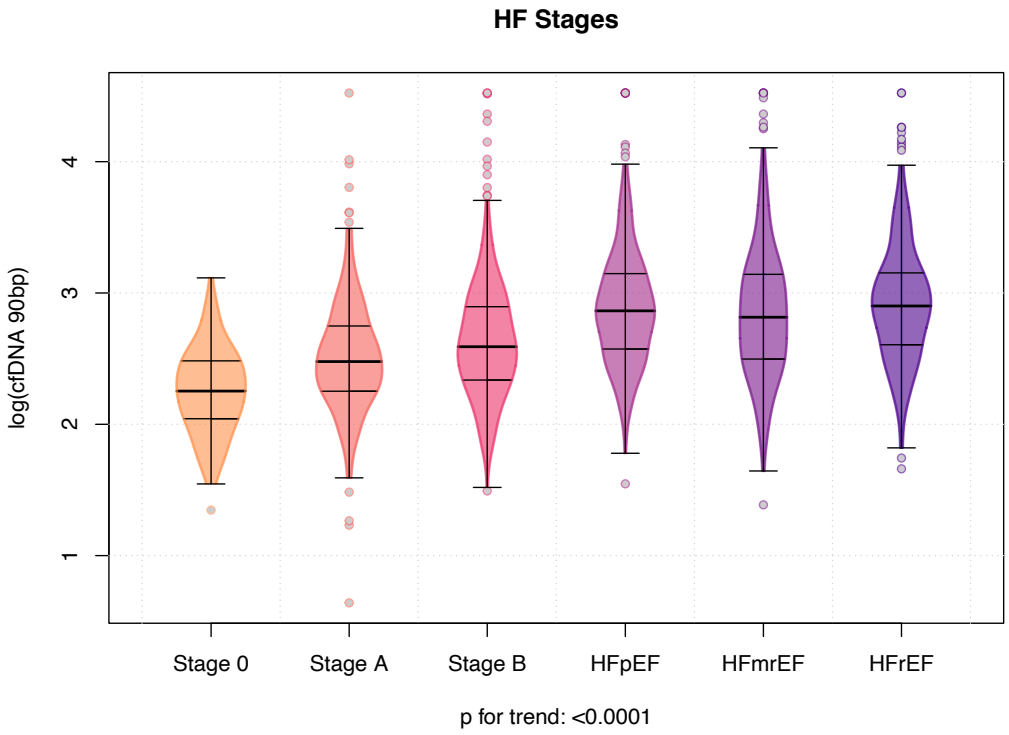

Figure 28 - Correlation between cfDNA 90bp levels and HF stages incl. HF phenotypes

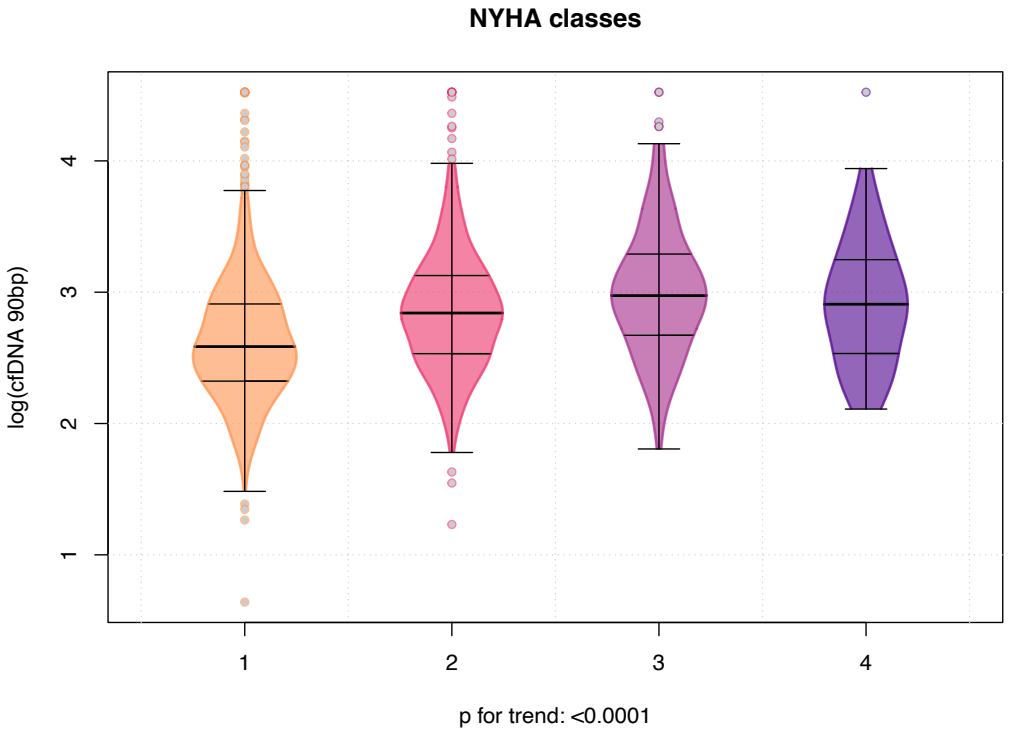

Figure 29 - Correlation between cfDNA 90bp levels and NYHA classes

5 Discussion

The present study is the first to analyze the relevance of cfDNA levels for cardiovascular disease prediction in a large study cohort with over 3100 probands, comparing HF patients and healthy individuals. Towards this goal, methods for a semi-automated, PCR-based quantification of total cfDNA directly from plasma had to be established and validated.

As a major result, the data revealed moderately elevated (+56%) *total* cfDNA concentrations in HF patients (stage C/D: 17.11 ng/ml) than in healthy subjects (stage 0/A: 10.99 ng/ml). In order to judge the potential benefit of cfDNA levels in disease outcome prediction relative to the established biomarker NT-proBNP, different statistical-analytical tests were performed. Cox proportional hazard regression analyses and C-statistics did not demonstrate significant additive value of cfDNA beyond NT-proBNP in predicting worsening of HF and cardiac death. However, cumulative incidence plots revealed that patients with elevations in both NT-proBNP *and* cfDNA exhibited higher incidence rates of adverse outcomes compared to those with elevated NT-proBNP alone. This observation suggests that cfDNA quantification may provide an additional prognostic value, particularly when used alongside established biomarkers. Moreover, in the prediction of all-cause death, cfDNA levels proved to be an independent risk factor in all three statistical approaches.

After first addressing technical considerations of cfDNA analytics, which facilitated measuring the large proband cohort with reasonable effort, the following discussion will focus on the implications of cfDNA quantification for predicting the outcome of HF. Strengths and limitations of the present work will be addressed, as well as directions for additional future experiments.

5.1 An automated pipetting system for high-throughput analysis of plasma cfDNA

Process automatization and technical improvements allowed us to quantify cfDNA in a large cohort of 3109 individuals. Until now, only few tumour-focused cfDNA studies have reached or exceeded this number of probands (122, 124), while the vast majority of studies has included less than 100 subjects (comp. references in the introduction). In the field of cardiovascular research, we substantially exceeded the number of participants of the Finnish “Health 2000 survey”, the largest study in this field so far (n ~ 1300 (7, 165)). It is to mention that the Finnish study measured cfDNA concentration with fluorometry based on a Qubit system, which is considered less accurate than our qPCR quantification method.

One key technical advancement that made our large-scale study feasible was the introduction of a direct cfDNA quantification method from unpurified plasma, as first described by Breitbach et al. (11). Not only does this prevent unwanted loss of cfDNA due to extraction, but it also speeds up the whole process significantly and saves substantial amounts of money by rendering commercially available cfDNA extraction kits redundant. This simplification enabled us to automate the complete process from plasma dilution to qPCR setup.

As the plasma samples arrived in the lab in 96-well format MICRONIC plates, we needed to ensure consistent measuring conditions over the whole plate. Key steps were the thawing and proper mixing of the samples to start with perfectly homogenised plasma. We achieved this via a 10 min water bath incubation at 30 °C, followed by conscientious manual vortexing of the MICRONIC plates. Later in the process, a dedicated plate shaker, the Eppendorf ThermoMixer® C, facilitated efficient mixing of the plasma dilutions and reaction mixes to ensure equal quantification conditions for each sample.

The workflow was optimised to reduce standing times of the mixed solutions, which could have led to demixing. During the pipetting process, where covering of the samples was not possible, the reduced standing time also prevented contamination. As the automated pipetting process required some manual preparations for each step, we could work in parallel and prepare the next step in advance. This led to a total preparation time of 60-90 min for one full 384-well qPCR plate. With a cycler running time of ~90 min, the next qPCR run could already be prepared after starting the cycler. This way it was possible to comfortably do four runs per day, equalling ~700 measured samples with one primer pair (target). Including remeasurements, it took about two working weeks for each target to quantify cfDNA in 3109 samples.

The MICRONIC storage system with its 96-well format racks works perfectly for automated processes. To further improve the workflow, one could replace the manual decapper tool by an automatic push cap decapper. This would speed up the decapping process and, more importantly, further reduce the risk of cross-contaminations between adjacent sample tubes.

Calculating experimental costs is mandatory if the method of semi-automated cfDNA quantification is to be applied in routine clinical diagnostics. The most important cost saving step in the presented method certainly was the omittance of kit-based DNA purification prior to qPCR measurements, as previously established by Breitbach et al. (11) and Neuberger et al. (183). Pure costs of chemicals and disposables in the present work were calculated to be less than 2 EUR per sample. Although instrumental and labour costs must of course be added,

these reaction costs can be considered competitive with conventional biomarker assays to measure NT-proBNP/BNP, e.g., an Enzyme-linked Immunosorbent Assay (ELISA).

5.2 General determinants of cfDNA levels in the cohort

This work confirmed several previous studies by showing positive associations between plasma cfDNA levels and phenotypic characteristics like male sex (169), older age (168), and a higher body mass index (BMI) (170). Hypothetically, higher muscle mass and red blood cell count in males (169), increased cell death accompanied by reduced clearance at older age (189), and augmented inflammatory processes in obese individuals with a continuous turnover of adipocytes may account for these correlations (190). In notable contrast to several other studies (169, 170, 191), we detected a negative association between cfDNA levels and smoking. This unexpected observation, however, requires further analyses and adjustments for additional variables for confirmation. In literature, it has well been established that smoking increases body inflammation and thereby leads to elevated cfDNA levels (169).

Among possible comorbidities, the autoimmune condition rheumatoid arthritis was associated with increased cfDNA levels in our analysis, as expected (191). Autoimmunity triggers inflammation, which leads to cfDNA release via NETosis and apoptosis of immune cells (192). Chronic kidney disease (CKD), a reduced estimated glomerular filtration rate (eGFR) and dialysis also showed elevated cfDNA levels in our study. This was also partly expectable according to published literature, as cfDNA increases during haemodialysis due to cell damage (193). In contrast, other small-scale studies previously reported no difference in plasma cfDNA levels between healthy subjects and patients with CKD (194, 195) and therefore assumed a low impact of renal clearance on plasma cfDNA levels. Our results indicate the contrary, pointing at the importance of renal clearance for cfDNA levels. An additional positive correlation of cfDNA amounts was observed in our data for patients with cancer. This confirms previous studies which addressed hepatocellular carcinoma as well as colorectal cancer entities (196, 197).

5.3 The predictive power of cfDNA as a biomarker of heart failure progression

The present large-scale study revealed moderately higher *total* cfDNA concentrations in HF patients than in healthy subjects. Furthermore, the data showed noticeable associations of *total* cfDNA levels with relevant established biomarkers like the often-used gold standard in HF diagnostics, NT-proBNP. In the following, these findings will be discussed with respect to important published studies on cfDNA and HF, which comprised at least medium-sized proband numbers and which applied comparable experimental strategies in cfDNA measurements and subsequent statistical analyses.

Yokokawa et al. (162) were the first to assess *cardiac-specific* cfDNA in HF patients, but could not discriminate between diseased and healthy subjects using *total* cfDNA levels. In their study analysing 28 healthy and 32 diseased individuals, *cardiac-specific* cfDNA was significantly increased in HF patients and correlated with high-sensitivity troponin I, but neither with BNP, nor eGFR. Most likely, these differences to the results of the present work are related to the low study size of only 60 individuals. Yokokawa et al. (162) assumed that cfDNA originating from other tissues substantially contributed to the amount of *total* cfDNA. This would consequently reduce the proportion of *total* cfDNA originating from damaged heart tissue. It can therefore be hypothesized that only a larger-scale study like the present one can generate enough statistical power to discover the moderate increases in *total* cfDNA levels in HF patients. An additional explanation for the relatively low *total* cfDNA concentrations as measured by Yokokawa et al. (2.63 ng/ml in control vs 3.03 ng/ml in diseased subjects) could be their applied protocol, in which the extraction of cfDNA from plasma preceded the qPCR measurements. As Breitbach et al. (11) previously reported, protocols without prior cfDNA extraction yielded on average 2.79-fold higher cfDNA levels than protocols applying cfDNA extraction. These authors thus confirmed substantial loss of cfDNA during extraction.

Particular attention must be paid to the question whether cfDNA levels possess informative value in disease prediction, which is comparable to or even better than the performance of already established biomarkers in cardiology. N-terminal pro B-type natriuretic peptide (NT-proBNP) and brain natriuretic peptide (BNP) are widely applied in clinical diagnostics as gold-standard biomarkers for monitoring right ventricular load, and levels of both proteins in blood correlate strongly with patient symptoms and disease progression in HF (198, 199). The two peptides originate from the same precursor protein, but they exert different physiological roles. NT-proBNP is an inactive fragment of 76 amino acids, while BNP (32 amino acids long) is the

biologically active hormone which promotes vasodilation, natriuresis, and diuresis to reduce cardiac stress. Volume overload during myocardial stress leads to a ventricular release of the peptides. Due to a longer half-life, NT-proBNP values are considered more stable than those of BNP. Yokokawa et al. (162) could not find a correlation between *cardiac-specific* cfDNA and BNP, and they thus assumed cfDNA would not be a suitable biomarker to monitor HF, but rather predominately indicate cardiomyocyte death in general. In contrast, this present study revealed a strong, statistically sound association of *total* cfDNA with NT-proBNP and with progressive HF stages. In fact, cumulative incidence plots for worsening of HF, cardiac death, and all-cause death (Figures 19-21) showed significant differences for all four quartiles of cfDNA concentration. For example, the incidence of cardiac death in the highest cfDNA quartile (>20.1 ng/ml) was 6-fold higher (~ 12% vs. ~ 2%) than in the lowest quartile (<11 ng/ml) (Figure 20 A). Hypothetically, Yokokawa et al. (162) did not find this association because of their considerably smaller study size or their cfDNA quantification protocol, as mentioned above.

Another mid-sized study, performed by Salzano et al. (163), investigated *total* cfDNA levels in HF patients, targeting the single-copy GAPDH gene by qPCR. The authors included 71 HF patients, but only with a reduced ejection fraction (EF) <50%, and 64 healthy subjects. In contrast to the max. 2-fold increase in cfDNA levels measured in the present study, Salzano et al. determined ~ 6-fold higher cfDNA levels in HF patients (19.4 ng/ml) than in healthy subjects (3.4 ng/ml). While our study measured approximately the same concentrations for patients with reduced ejection fraction (HFrEF: 18.26 ng/ml), we obtained three times higher cfDNA levels in healthy subjects (stage 0: 9.53 ng/ml). The much lower concentration in healthy subjects reported by Salzano et al. (163) can hypothetically be explained by a loss of material, due to the extraction of cfDNA prior to qPCR quantification. Note however that comparisons of absolute cfDNA concentrations between studies are notoriously difficult, especially when different qPCR targets are used.

While in the present work the entire study cohort including healthy controls was analysed, Salzano et al. (163) only calculated with the HF population, which was dichotomised into HF patients with low or high cfDNA levels according to the median. This limits the informative value of their study by only allowing conclusions to be drawn about the HF population, while not distinguishing between HF patients and healthy controls.

In fact, there is yet another difference concerning the statistical methodology between the present study and the work by Salzano et al.: In the survival analyses of the present work, three different endpoints (worsening of HF vs. cardiac death vs. all-cause death) were

analysed separately. Salzano et al. (163), in contrast, defined a combined endpoint of all-cause mortality and/or HF hospitalisation instead. This procedure increased their study power, but also reduced the information value. Analysing cfDNA levels as a continuous variable, Salzano et al. stated that they could not show a significant association with the outcome. The present study, however, could detect an increased Hazard Ratio (HR) = 1.18 for all-cause death in patients with elevated cfDNA levels even after adjustment for NT-proBNP (model 4; Table 22, Figure 18). The HR further increased when cfDNA was analysed as a dichotomous variable stratified by the median value (HR = 1.37). In contrast, for worsening of HF and cardiac death, no significant prediction capabilities could be found for cfDNA levels after adjustments for NT-proBNP. This would indicate no benefits from additionally measuring cfDNA concentrations to predict these outcomes better than by applying NT-proBNP measurements alone. Salzano et al. (163) calculated a slightly higher HR = 2.12 in patients with elevated cfDNA levels (dichotomised by the median) for their combined endpoint. Our results therefore indicate that the dominant component in Salzano et al.'s outcome prediction model is all-cause death rather than HF hospitalisation. In fact, the CI plots of the present study and the Kaplan-Meier curves reported by Salzano et al. (163) show comparable results with significantly higher incidence rates in patients with elevated cfDNA levels (Figures 20-22).

In an additional analytical approach to compare the relative benefits of cfDNA and NT-proBNP as biomarkers, patients were categorized according to median levels of cfDNA and NT-proBNP and displayed in CI plots (Figures 22-24). These results indicated that NT-proBNP is the weighing factor of choice to predict worsening of HF and cardiac death, whereas elevated cfDNA levels alone did not go along with significantly higher incidence rates for these outcomes. In combination with elevated NT-proBNP levels, however, cumulative incidences were significantly higher than in patients who only had elevated NT-proBNP levels. One can therefore conclude that cfDNA does indeed possess *additional* information value to predict worsening of HF and cardiac death. This hypothesis is also strengthened by the fact that cfDNA 90bp and NT-proBNP levels only correlated with a value of 0.39. Similar results were seen when looking at the outcome of all-cause death. Here, even patients who only had elevated cfDNA levels (but low NT-proBNP) showed significantly higher incidence rates compared to the cohort with low levels of both biomarkers. Although NT-proBNP remains the weighing factor here, too, cfDNA appears to have a stronger influence on all-cause death than on the other outcomes.

In a third approach to compare cfDNA and BNP levels as biomarkers, outcome prediction accuracies were assessed by ROC curve analysis with C-statistics, as also done by Salzano et al. (163). For worsening of HF and cardiac death, NT-proBNP showed a significantly higher C index than cfDNA 90bp and cfDNA 222bp levels when added to the model. Additional adding of cfDNA levels to a model with NT-proBNP did not lead to higher C indices in the predictive model than obtained with NT-proBNP alone. The application of C statistics thus confirms the results of the regression analysis above (Figures 22-24): cfDNA levels alone are not better in predicting worsening of HF and cardiac death than NT-proBNP. However, when predicting all-cause death, cfDNA levels displayed slightly higher C indices when added to the model with NT-proBNP (Table 23). In conclusion, cfDNA levels can have an *additional* use over NT-proBNP for predicting all-cause death.

The cfDNA integrity index can potentially be used as an additional criterion to infer disease outcome. In the present study, the integrity index significantly decreased with progressing stages of HF, which accounts for a higher fragmentation and a larger proportion of shorter cfDNA fragments in these patients. This is an expectable result, as current research in other chronic diseases like cancer (200) and systemic lupus erythematosus (SLE) (201) also showed a higher fragmentation of cfDNA fragments with most of the fragments being shorter than <145bp (cancer) or <115bp (SLE), whereas the average molecule of cfDNA is ~166 bp long (20). As the present study apparently is the first to investigate the integrity index in HF patients, the observed trend needs to be confirmed in future studies.

Table 24 - Overview on the predictive capabilities of cfDNA 90bp levels depending on the statistical analyses.

O: no statistically significant added value for outcome prediction over NT-proBNP. +: statistically significant added value for outcome prediction additionally to NT-proBNP.

		Predicted outcome of disease		
		worsening of HF	cardiac death	all-cause death
cfDNA90bp	regression models	O	O	+
	C statistics	O	O	+
	survival analysis (CI)	+	+	+

5.4 Strengths and limitations of the study

To the best of our knowledge, this represents the **most comprehensive study** to date investigating cfDNA levels in patients with heart failure (HF), with over 3,000 enrolled subjects and a follow-up period spanning six years. As a limitation, we only assessed **baseline cfDNA levels** in the current analysis. However, the bio-banked plasma samples collected at three additional timepoints (at 2, 4, and 6 years) will provide the opportunity for future longitudinal measurements. This is especially important since inter- and intra-individual variances of cfDNA levels were reported in several studies (202-204). Future follow-up analyses could yield further insights into the dynamic changes in cfDNA levels over time and their association with clinical outcomes.

The **semi-automated, high throughput cfDNA quantification method** employed in this study demonstrated robust and consistent measurement results across the experimental series. Nevertheless, it is important to note that this method's reliability critically depends on the use of standardized reagents, such as polymerase and PCR primers, which should ideally originate from the same batch of production. Variability introduced by different batches of reagents could potentially increase inter-plate variance, affecting the comparability of results across different qPCR plates. However, we mitigated this issue by calibrating our assay with samples of known cfDNA concentrations, which helped normalize inter-plate differences and maintain measurement accuracy. It will nevertheless always be a challenge to transfer the developed measurement protocol to another lab setting.

When considering the potential implementation of cfDNA quantification in routine clinical diagnostics, it is important to recognize that the present study was conducted under **optimized experimental conditions**, particularly with regard to sample collection and processing. Based on current knowledge, small delays in sample processing after blood withdrawal, as well as the transport through pneumatic tube systems, are unlikely to strongly impact cfDNA concentrations when blood is appropriately collected in EDTA tubes. It clearly has to be tested to which extent the entire workflow is functioning under less controlled, real-world clinical conditions.

Our findings support the potential use of cfDNA as a prognostic biomarker in heart failure management. Specifically, *total* cfDNA levels were shown to be an independent risk factor for predicting all-cause mortality in patients with HF. As a clear limitation, however, the ability of cfDNA to predict other outcomes, such as worsening of HF and cardiac death, varied

depending on the **statistical methods** which were employed. Regarding the use of statistical tests in the context of this exploratory study, the p-value should be seen as a continuous measure of the strength of evidence for an association. The smaller the p-value, the more likely a relevant association is.

5.5 Future work

Based upon the findings and limitations outlined in the present study, several directions for future research emerge. This future work aims to address existing gaps of knowledge, refine methodologies, and move towards a clinical applicability of cfDNA quantification in heart failure (HF).

One key future experiment series involves the **longitudinal analysis of cfDNA levels** using the bio-banked plasma samples collected at 2, 4, and 6 years. While the present study only assessed baseline cfDNA levels, analyzing these additional timepoints would allow for an improved understanding of cfDNA fluctuations over time. Such longitudinal measurements could provide valuable insights into the temporal relationship between cfDNA levels and disease progression, therapeutic response, and clinical outcomes. These analyses could also help establish whether data of cfDNA dynamics, rather than single timepoint measurements, hold greater prognostic value.

Further research is also needed to validate the **robustness of cfDNA quantification under routine clinical conditions**. While our study was conducted under controlled settings with optimized sample collection and processing protocols, the implementation of cfDNA as a diagnostic or prognostic biomarker in real-world clinical environments may encounter additional challenges. Investigating the impact of variations in sample handling –such as delays in processing or alternative transport methods– on cfDNA stability and measurement accuracy is critical. Small-scale confirmatory studies could help assess the feasibility and reliability of cfDNA quantification in less controlled settings, thereby bridging the gap between research and clinical practice.

The potential of cfDNA for more targeted analyses, such as methylation profiling, represents another promising direction for future work. ***Cardiac-specific* cfDNA methylation** enables differentiation between cfDNA originating from cardiac cells and other sources. Knowledge of DNA methylation patterns could significantly improve prognostic precision for outcomes like worsening HF or cardiac death. Technically, this approach will likely require implementation of

next-generation sequencing (NGS) methods and their bioinformatics. Long-read single-molecule NGS technologies like Oxford Nanopore (ONT) or Pacific Biosciences SMRT sequencing, which readily detect DNA methylation patterns without prior chemical modification steps (205), might soon emerge as the method of choice. Future efforts must focus on optimizing these technologies at acceptable costs and turnaround times to make them suitable for routine clinical use. Additionally, large studies are needed to validate a hypothetical advantage of *cardiac-specific* cfDNA over *total* cfDNA levels in diverse HF patient cohorts.

Another line of future experiments might explore the **combined utility of cfDNA and established biomarkers**, such as NT-proBNP. While our study observed that patients with elevations in both biomarkers had worse outcomes compared to those with elevated NT-proBNP alone, further research is necessary to clarify how cfDNA complements existing biomarkers. For instance, one could investigate whether cfDNA adds incremental prognostic value in specific patient subgroups, such as those with preserved ejection fraction or those undergoing novel HF therapies. Such analyses could help define the contexts which allow for a better integration of cfDNA measurements into standard clinical workflows.

Finally, while cfDNA may serve as a biomarker, it is necessary to further explore the **basic biological mechanisms underlying cfDNA release in HF**. For fully understanding the role of cfDNA in HF and for harvesting its full diagnostic potential, one needs to clarify its cellular origin, its regulation, and its eventual involvement in pathophysiological processes. For example, one might investigate the involvement of cfDNA in inflammatory processes, apoptosis, or oxidative stress associated with HF. This could provide valuable insights into disease mechanisms and -possibly- pinpoint novel therapeutic strategies.

In conclusion, several additional efforts will be essential for realizing the full potential of cfDNA as a biomarker in HF and in translating these findings into clinical practice.

6 Summary

Heart failure (HF) represents a major cause of mortality with a prevalence of 1-2% in the adult population in developed countries. As populations age, the role of HF is expected to grow. This comes with a steep increase in healthcare costs, placing a substantial burden on society. Identifying HF risk patients earlier, possibly even before symptoms manifest, becomes crucial to initiate interventions promptly, such as lifestyle adjustments or medication. In preventive medicine, the identification of suitable biomarkers plays a key role, as they allow an objective and early disease detection.

Cell-free DNA (cfDNA) is a widely used diagnostic biomarker in clinical fields like oncology or transplantation medicine. In clinical cardiology, however, cfDNA analytics does not yet play a major role. Only a handful of rather small-scale studies have so far investigated the potential of cfDNA diagnostics in HF patients, indicating that cfDNA could be an independent risk factor for cardiovascular disease and overall mortality. The aim of the present study was therefore to evaluate the potential of cfDNA in HF diagnostics in a large cohort of subjects and to compare its predictive power to the currently most often used biomarker, NT-proBNP.

To achieve this, a reliable, reproduceable, and quick high throughput cfDNA quantification method needed to be implemented. The existing manual, time- and labour-consuming qPCR assay was automated by testing and establishing an INTEGRA pipetting robot and tuning its workflow to the special needs of high-viscosity plasma samples. The assay was adjusted to reliably produce the same test results as with the already published qPCR assay established by Neuberger et al. (183). This way a consistent measuring of the study samples was ensured. cfDNA levels were then quantified in 3109 EDTA plasma samples from the prospective MyoVasc study (NCT04064450). Two qPCR assays of different amplicon lengths (cfDNA90 bp/ cfDNA222 bp), both targeting a repetitive LINE1 element, were used for cfDNA quantification and to calculate the cfDNA integrity index, which indicates the fragmentation level of the cfDNA. Competing risk models were applied to investigate the associations of cfDNA with worsening of HF, and Cox proportional hazard regression analyses were used to assess the endpoints of cardiac death and all-cause death. C-statistics were calculated and compared for each model. The participants were classified as 0 (healthy) or HF stages A (at risk for HF) to D (advanced HF) according to the current Universal Definition of Heart Failure. Analyses were adjusted for age, sex, cardiovascular risk factors (CVRFs) and medication (models 1-3) and additionally for NT-proBNP (model 4). Outcome data were presented as cumulative incidence plots for cfDNA90bp and 222bp levels and for the integrity index.

The cohort included 3109 study participants with an age between 34 to 85 years and 35.7% females. cfDNA concentration was lowest in stage 0/A subjects (n=534) with 10.99 (8.70/13.93) ng/ml (median (Q1/Q3)). Stage B (pre-HF) (n=923) or stage C/D subjects (n=1652) showed elevated cfDNA90bp concentrations with 13.37 (10.35/18.11) or 17.11 (12.56/22.80) ng/ml, respectively. Cox proportional hazard regression analyses indicated that the concentration of cfDNA90bp is a relevant prognostic marker for **all-cause death**, adjusted for age, sex, CVRFs and medication (HR = 1.312 [1.205-1.430], $p < 0.0001$). After additional adjustment for NT-proBNP, the effect estimates were lower, but still statistically significant (HR = 1.173 [1.073-1.282], $p = 0.00046$). Regarding the endpoints **worsening of HF** and **cardiac death**, the effect estimates were no longer significant after adjustment for NT-proBNP. A C-index comparison showed the same tendency, with a significant added value of testing cfDNA additionally to NT-proBNP only when looking at **all-cause death** (C = 0.807 vs. C = 0.805; $p = 0.050$). However, cumulative incidence plots for dichotomised values of NT-proBNP and cfDNA showed the highest incidence rates for all three outcomes in patients with elevations in both biomarkers, significantly higher than in patients with elevations of NT-pro BNP alone.

The present results indicate that cfDNA is a risk factor, which independently of NT-proBNP contributes to the prediction of overall mortality (all-cause death) in the study cohort. cfDNA also appears to possess additional information value to NT-proBNP for predicting worsening of HF and cardiac death.

7 Bibliography

1. Groenewegen A, Rutten FH, Mosterd A, Hoes AW. Epidemiology of heart failure. Eur J Heart Fail. 2020;22(8):1342-56.
2. Heidenreich PA, Trogdon JG, Khavjou OA, Butler J, Dracup K, Ezekowitz MD, et al. Forecasting the future of cardiovascular disease in the United States: a policy statement from the American Heart Association. Circulation. 2011;123(8):933-44.
3. Hummel EM, Hessas E, Muller S, Beiter T, Fisch M, Eibl A, et al. Cell-free DNA release under psychosocial and physical stress conditions. Transl Psychiatry. 2018;8(1):236.
4. Bronkhorst AJ, Ungerer V, Oberhofer A, Gabriel S, Polatoglou E, Randeu H, et al. New Perspectives on the Importance of Cell-Free DNA Biology. Diagnostics (Basel). 2022;12(9).
5. Thierry AR, El Messaoudi S, Gahan PB, Anker P, Stroun M. Origins, structures, and functions of circulating DNA in oncology. Cancer Metastasis Rev. 2016;35(3):347-76.
6. Zemmour H, Planer D, Magenheim J, Moss J, Neiman D, Gilon D, et al. Non-invasive detection of human cardiomyocyte death using methylation patterns of circulating DNA. Nat Commun. 2018;9(1):1443.
7. Jylhävä J, Lehtimäki T, Jula A, Moilanen L, Kesäniemi YA, Nieminen MS, et al. Circulating cell-free DNA is associated with cardiometabolic risk factors: the Health 2000 Survey. Atherosclerosis. 2014;233(1):268-71.
8. Devaux Y. Cardiomyocyte-Specific Cell-Free DNA as a Heart Failure Biomarker? Can J Cardiol. 2020;36(6):807-8.
9. Meddeb R, Pisareva E, Thierry AR. Guidelines for the Preanalytical Conditions for Analyzing Circulating Cell-Free DNA. Clin Chem. 2019;65(5):623-33.
10. Bronkhorst AJ, Aucamp J, Pretorius PJ. Cell-free DNA: Preanalytical variables. Clin Chim Acta. 2015;450:243-53.
11. Breitbach S, Tug S, Helmig S, Zahn D, Kubiak T, Michal M, et al. Direct quantification of cell-free, circulating DNA from unpurified plasma. PLoS One. 2014;9(3):e87838.
12. Goessl C, Krause H, Muller M, Heicappell R, Schrader M, Sachsinger J, et al. Fluorescent methylation-specific polymerase chain reaction for DNA-based detection of prostate cancer in bodily fluids. Cancer Res. 2000;60(21):5941-5.
13. Wang Y, Springer S, Mulvey CL, Silliman N, Schaefer J, Sausen M, et al. Detection of somatic mutations and HPV in the saliva and plasma of patients with head and neck squamous cell carcinomas. Sci Transl Med. 2015;7(293):293ra104.
14. Schmidt B, Carstensen T, Engel E, Jandrig B, Witt C, Fleischhacker M. Detection of cell-free nucleic acids in bronchial lavage fluid supernatants from patients with lung cancer. Eur J Cancer. 2004;40(3):452-60.
15. Wong LJ, Lueth M, Li XN, Lau CC, Vogel H. Detection of mitochondrial DNA mutations in the tumor and cerebrospinal fluid of medulloblastoma patients. Cancer Res. 2003;63(14):3866-71.
16. Lapaire O, Bianchi DW, Peter I, O'Brien B, Stroh H, Cowan JM, et al. Cell-free fetal DNA in amniotic fluid: unique fragmentation signatures in euploid and aneuploid fetuses. Clin Chem. 2007;53(3):405-11.
17. Li HG, Huang SY, Zhou H, Liao AH, Xiong CL. Quick recovery and characterization of cell-free DNA in seminal plasma of normozoospermia and azoospermia: implications for non-invasive genetic utilities. Asian J Androl. 2009;11(6):703-9.
18. Zhang J, Yang S, Xie Y, Chen X, Zhao Y, He D, et al. Detection of methylated tissue factor pathway inhibitor 2 and human long DNA in fecal samples of patients with colorectal cancer in China. Cancer Epidemiol. 2012;36(1):73-7.
19. Lo YM, Rainer TH, Chan LY, Hjelm NM, Cocks RA. Plasma DNA as a prognostic marker in trauma patients. Clin Chem. 2000;46(3):319-23.

20. Snyder MW, Kircher M, Hill AJ, Daza RM, Shendure J. Cell-free DNA Comprises an In Vivo Nucleosome Footprint that Informs Its Tissues-Of-Origin. Cell. 2016;164(1-2):57-68.
21. Zhong S, Ng MC, Lo YM, Chan JC, Johnson PJ. Presence of mitochondrial tRNA(Leu(UUR)) A to G 3243 mutation in DNA extracted from serum and plasma of patients with type 2 diabetes mellitus. J Clin Pathol. 2000;53(6):466-9.
22. Bronkhorst AJ, Ungerer V, Diehl F, Anker P, Dor Y, Fleischhacker M, et al. Towards systematic nomenclature for cell-free DNA. Hum Genet. 2021;140(4):565-78.
23. Mandel P, Metais P. Nuclear Acids In Human Blood Plasma. C R Seances Soc Biol Fil. 1948;142(3-4):241-3.
24. Tan EM, Schur PH, Carr RI, Kunkel HG. Deoxybonucleic acid (DNA) and antibodies to DNA in the serum of patients with systemic lupus erythematosus. J Clin Invest. 1966;45(11):1732-40.
25. Leon SA, Shapiro B, Sklaroff DM, Yaros MJ. Free DNA in the serum of cancer patients and the effect of therapy. Cancer Res. 1977;37(3):646-50.
26. Stroun M, Anker P, Maurice P, Lyautey J, Lederrey C, Beljanski M. Neoplastic characteristics of the DNA found in the plasma of cancer patients. Oncology. 1989;46(5):318-22.
27. Vasioukhin V, Anker P, Maurice P, Lyautey J, Lederrey C, Stroun M. Point mutations of the N-ras gene in the blood plasma DNA of patients with myelodysplastic syndrome or acute myelogenous leukaemia. Br J Haematol. 1994;86(4):774-9.
28. Lo YM, Corbetta N, Chamberlain PF, Rai V, Sargent IL, Redman CW, et al. Presence of fetal DNA in maternal plasma and serum. Lancet. 1997;350(9076):485-7.
29. Esteller M, Sanchez-Cespedes M, Rosell R, Sidransky D, Baylin SB, Herman JG. Detection of aberrant promoter hypermethylation of tumor suppressor genes in serum DNA from non-small cell lung cancer patients. Cancer Res. 1999;59(1):67-70.
30. Wong IH, Lo YM, Zhang J, Liew CT, Ng MH, Wong N, et al. Detection of aberrant p16 methylation in the plasma and serum of liver cancer patients. Cancer Res. 1999;59(1):71-3.
31. Lo YM, Tein MS, Pang CC, Yeung CK, Tong KL, Hjelm NM. Presence of donor-specific DNA in plasma of kidney and liver-transplant recipients. Lancet. 1998;351(9112):1329-30.
32. Rhodes A, Wort SJ, Thomas H, Collinson P, Bennett ED. Plasma DNA concentration as a predictor of mortality and sepsis in critically ill patients. Crit Care. 2006;10(2):R60.
33. Rainer TH, Wong LK, Lam W, Yuen E, Lam NY, Metreweli C, et al. Prognostic use of circulating plasma nucleic acid concentrations in patients with acute stroke. Clin Chem. 2003;49(4):562-9.
34. McCarthy CG, Wenceslau CF, Goulopoulou S, Ogbi S, Baban B, Sullivan JC, et al. Circulating mitochondrial DNA and Toll-like receptor 9 are associated with vascular dysfunction in spontaneously hypertensive rats. Cardiovasc Res. 2015;107(1):119-30.
35. Quinones I, Daniel B. Cell free DNA as a component of forensic evidence recovered from touched surfaces. Forensic Sci Int Genet. 2012;6(1):26-30.
36. Bronkhorst AJ, Ungerer V, Oberhofer A, Holdenrieder S. The rising tide of cell-free DNA profiling: from snapshot to temporal genome analysis. Journal of Laboratory Medicine. 2022;46(4):207-24.
37. Zocco D, Bernardi S, Novelli M, Astrua C, Fava P, Zarovni N, et al. Isolation of extracellular vesicles improves the detection of mutant DNA from plasma of metastatic melanoma patients. Sci Rep. 2020;10(1):15745.
38. Rykova EY, Pautova LV, Yakubov LA, Karamyshev VN, Vlassov VV. Serum immunoglobulins interact with oligonucleotides. FEBS Lett. 1994;344(1):96-8.
39. Chelobanov BP, Laktionov PP, Vlasov VV. Proteins involved in binding and cellular uptake of nucleic acids. Biochemistry (Mosc). 2006;71(6):583-96.
40. Gahan PB, Stroun M. The virtosome-a novel cytosolic informative entity and intercellular messenger. Cell Biochem Funct. 2010;28(7):529-38.

41. Rykova EY, Morozkin ES, Ponomaryova AA, Loseva EM, Zaporozhchenko IA, Cherdyntseva NV, et al. Cell-free and cell-bound circulating nucleic acid complexes: mechanisms of generation, concentration and content. Expert Opin Biol Ther. 2012;12 Suppl 1:S141-53.
42. Tamkovich S, Laktionov P. Cell-surface-bound circulating DNA in the blood: Biology and clinical application. IUBMB Life. 2019;71(9):1201-10.
43. Breitbach S, Tug S, Simon P. Circulating cell-free DNA: an up-coming molecular marker in exercise physiology. Sports Med. 2012;42(7):565-86.
44. Jiang P, Chan CW, Chan KC, Cheng SH, Wong J, Wong VW, et al. Lengthening and shortening of plasma DNA in hepatocellular carcinoma patients. Proc Natl Acad Sci U S A. 2015;112(11):E1317-25.
45. Gao YJ, He YJ, Yang ZL, Shao HY, Zuo Y, Bai Y, et al. Increased integrity of circulating cell-free DNA in plasma of patients with acute leukemia. Clin Chem Lab Med. 2010;48(11):1651-6.
46. Umetani N, Kim J, Hiramatsu S, Reber HA, Hines OJ, Bilchik AJ, et al. Increased integrity of free circulating DNA in sera of patients with colorectal or periampullary cancer: direct quantitative PCR for ALU repeats. Clin Chem. 2006;52(6):1062-9.
47. Wang BG, Huang HY, Chen YC, Bristow RE, Kassauei K, Cheng CC, et al. Increased plasma DNA integrity in cancer patients. Cancer Res. 2003;63(14):3966-8.
48. Diehl F, Li M, Dressman D, He Y, Shen D, Szabo S, et al. Detection and quantification of mutations in the plasma of patients with colorectal tumors. Proc Natl Acad Sci U S A. 2005;102(45):16368-73.
49. Mouliere F, Robert B, Arnau Peyrotte E, Del Rio M, Ychou M, Molina F, et al. High fragmentation characterizes tumour-derived circulating DNA. PLoS One. 2011;6(9):e23418.
50. Jahr S, Hentze H, Englisch S, Hardt D, Fackelmayer FO, Hesch RD, et al. DNA fragments in the blood plasma of cancer patients: quantitations and evidence for their origin from apoptotic and necrotic cells. Cancer Res. 2001;61(4):1659-65.
51. Vizza E, Corrado G, De Angeli M, Carosi M, Mancini E, Baiocco E, et al. Serum DNA integrity index as a potential molecular biomarker in endometrial cancer. J Exp Clin Cancer Res. 2018;37(1):16.
52. de Miranda FS, Barauna VG, Dos Santos L, Costa G, Vassallo PF, Campos LCG. Properties and Application of Cell-Free DNA as a Clinical Biomarker. Int J Mol Sci. 2021;22(17).
53. Nagata S, Nagase H, Kawane K, Mukae N, Fukuyama H. Degradation of chromosomal DNA during apoptosis. Cell Death Differ. 2003;10(1):108-16.
54. Golstein P, Kroemer G. Cell death by necrosis: towards a molecular definition. Trends Biochem Sci. 2007;32(1):37-43.
55. van der Vaart M, Pretorius PJ. The origin of circulating free DNA. Clin Chem. 2007;53(12):2215.
56. Viorritto IC, Nikolov NP, Siegel RM. Autoimmunity versus tolerance: can dying cells tip the balance? Clin Immunol. 2007;122(2):125-34.
57. Suzuki N, Kamataki A, Yamaki J, Homma Y. Characterization of circulating DNA in healthy human plasma. Clin Chim Acta. 2008;387(1-2):55-8.
58. Nagata S. DNA degradation in development and programmed cell death. Annu Rev Immunol. 2005;23:853-75.
59. Holdenrieder S, Stieber P. Apoptotic markers in cancer. Clin Biochem. 2004;37(7):605-17.
60. Jiang WW, Zahurak M, Goldenberg D, Milman Y, Park HL, Westra WH, et al. Increased plasma DNA integrity index in head and neck cancer patients. Int J Cancer. 2006;119(11):2673-6.

61. Delgado PO, Alves BC, Gehrke Fde S, Kuniyoshi RK, Wroclavski ML, Del Giglio A, et al. Characterization of cell-free circulating DNA in plasma in patients with prostate cancer. Tumour Biol. 2013;34(2):983-6.
62. Deligezer U, Eralp Y, Akisik EE, Akisik EZ, Saip P, Topuz E, et al. Size distribution of circulating cell-free DNA in sera of breast cancer patients in the course of adjuvant chemotherapy. Clin Chem Lab Med. 2008;46(3):311-7.
63. Stroun M, Maurice P, Vasioukhin V, Lyautey J, Lederrey C, Lefort F, et al. The origin and mechanism of circulating DNA. Ann N Y Acad Sci. 2000;906:161-8.
64. Stroun M, Anker P. Nucleic acids spontaneously released by living frog auricles. Biochem J. 1972;128(3):100P-1P.
65. Rogers JC, Boldt D, Kornfeld S, Skinner A, Valeri CR. Excretion of deoxyribonucleic acid by lymphocytes stimulated with phytohemagglutinin or antigen. Proc Natl Acad Sci U S A. 1972;69(7):1685-9.
66. Bronkhorst AJ, Wentzel JF, Aucamp J, van Dyk E, du Plessis L, Pretorius PJ. Characterization of the cell-free DNA released by cultured cancer cells. Biochim Biophys Acta. 2016;1863(1):157-65.
67. Wang W, Kong P, Ma G, Li L, Zhu J, Xia T, et al. Characterization of the release and biological significance of cell-free DNA from breast cancer cell lines. Oncotarget. 2017;8(26):43180-91.
68. Aucamp J, Bronkhorst AJ, Peters DL, Van Dyk HC, Van der Westhuizen FH, Pretorius PJ. Kinetic analysis, size profiling, and bioenergetic association of DNA released by selected cell lines in vitro. Cell Mol Life Sci. 2017;74(14):2689-707.
69. Lui YY, Chik KW, Chiu RW, Ho CY, Lam CW, Lo YM. Predominant hematopoietic origin of cell-free DNA in plasma and serum after sex-mismatched bone marrow transplantation. Clin Chem. 2002;48(3):421-7.
70. Tug S, Helmig S, Deichmann ER, Schmeier-Jurchott A, Wagner E, Zimmermann T, et al. Exercise-induced increases in cell free DNA in human plasma originate predominantly from cells of the haematopoietic lineage. Exerc Immunol Rev. 2015;21:164-73.
71. Moss J, Magenheim J, Neiman D, Zemmour H, Loyfer N, Korach A, et al. Comprehensive human cell-type methylation atlas reveals origins of circulating cell-free DNA in health and disease. Nat Commun. 2018;9(1):5068.
72. Thiam HR, Wong SL, Wagner DD, Waterman CM. Cellular Mechanisms of NETosis. Annu Rev Cell Dev Biol. 2020;36:191-218.
73. Brinkmann V, Reichard U, Goosmann C, Fauler B, Uhlemann Y, Weiss DS, et al. Neutrophil extracellular traps kill bacteria. Science. 2004;303(5663):1532-5.
74. Papayannopoulos V, Metzler KD, Hakkim A, Zychlinsky A. Neutrophil elastase and myeloperoxidase regulate the formation of neutrophil extracellular traps. J Cell Biol. 2010;191(3):677-91.
75. Branzk N, Papayannopoulos V. Molecular mechanisms regulating NETosis in infection and disease. Semin Immunopathol. 2013;35(4):513-30.
76. Villanueva E, Yalavarthi S, Berthier CC, Hodgin JB, Khandpur R, Lin AM, et al. Netting neutrophils induce endothelial damage, infiltrate tissues, and expose immunostimulatory molecules in systemic lupus erythematosus. J Immunol. 2011;187(1):538-52.
77. Rangé H, Labreuche J, Louedec L, Rondeau P, Planesse C, Sebbag U, et al. Periodontal bacteria in human carotid atherothrombosis as a potential trigger for neutrophil activation. Atherosclerosis. 2014;236(2):448-55.
78. Warnatsch A, Ioannou M, Wang Q, Papayannopoulos V. Inflammation. Neutrophil extracellular traps license macrophages for cytokine production in atherosclerosis. Science. 2015;349(6245):316-20.

79. Saffarzadeh M, Juenemann C, Queisser MA, Lochnit G, Barreto G, Galuska SP, et al. Neutrophil extracellular traps directly induce epithelial and endothelial cell death: a predominant role of histones. PLoS One. 2012;7(2):e32366.
80. Kessenbrock K, Krumbholz M, Schonermarck U, Back W, Gross WL, Werb Z, et al. Netting neutrophils in autoimmune small-vessel vasculitis. Nat Med. 2009;15(6):623-5.
81. Relja B, Land WG. Damage-associated molecular patterns in trauma. Eur J Trauma Emerg Surg. 2020;46(4):751-75.
82. Fuchs TA, Brill A, Duerschmied D, Schatzberg D, Monestier M, Myers DD, Jr., et al. Extracellular DNA traps promote thrombosis. Proc Natl Acad Sci U S A. 2010;107(36):15880-5.
83. Cools-Lartigue J, Spicer J, McDonald B, Gowing S, Chow S, Giannias B, et al. Neutrophil extracellular traps sequester circulating tumor cells and promote metastasis. J Clin Invest. 2013;123(8):3446-58.
84. Xu J, Zhang X, Pelayo R, Monestier M, Ammollo CT, Semeraro F, et al. Extracellular histones are major mediators of death in sepsis. Nat Med. 2009;15(11):1318-21.
85. Luo L, Zhang S, Wang Y, Rahman M, Syk I, Zhang E, et al. Proinflammatory role of neutrophil extracellular traps in abdominal sepsis. Am J Physiol Lung Cell Mol Physiol. 2014;307(7):L586-96.
86. Demers M, Wong SL, Martinod K, Gallant M, Cabral JE, Wang Y, et al. Priming of neutrophils toward NETosis promotes tumor growth. Oncoimmunology. 2016;5(5):e1134073.
87. Pinegin B, Vorobjeva N, Pinegin V. Neutrophil extracellular traps and their role in the development of chronic inflammation and autoimmunity. Autoimmun Rev. 2015;14(7):633-40.
88. Beiter T, Fragasso A, Hartl D, Niess AM. Neutrophil extracellular traps: a walk on the wild side of exercise immunology. Sports Med. 2015;45(5):625-40.
89. Yipp BG, Kubes P. NETosis: how vital is it? Blood. 2013;122(16):2784-94.
90. Yipp BG, Petri B, Salina D, Jenne CN, Scott BN, Zbytnuik LD, et al. Infection-induced NETosis is a dynamic process involving neutrophil multitasking in vivo. Nat Med. 2012;18(9):1386-93.
91. Pilsczek FH, Salina D, Poon KK, Fahey C, Yipp BG, Sibley CD, et al. A novel mechanism of rapid nuclear neutrophil extracellular trap formation in response to Staphylococcus aureus. J Immunol. 2010;185(12):7413-25.
92. Théry C, Witwer KW, Aikawa E, Alcaraz MJ, Anderson JD, Andriantsitohaina R, et al. Minimal information for studies of extracellular vesicles 2018 (MISEV2018): a position statement of the International Society for Extracellular Vesicles and update of the MISEV2014 guidelines. J Extracell Vesicles. 2018;7(1):1535750.
93. Torralba D, Baixauli F, Villarroya-Beltri C, Fernandez-Delgado I, Latorre-Pellicer A, Acin-Perez R, et al. Priming of dendritic cells by DNA-containing extracellular vesicles from activated T cells through antigen-driven contacts. Nat Commun. 2018;9(1):2658.
94. Raposo G, Stoorvogel W. Extracellular vesicles: exosomes, microvesicles, and friends. J Cell Biol. 2013;200(4):373-83.
95. Fernando MR, Jiang C, Krzyzanowski GD, Ryan WL. New evidence that a large proportion of human blood plasma cell-free DNA is localized in exosomes. PLoS One. 2017;12(8):e0183915.
96. Neuberger EWI, Hillen B, Mayr K, Simon P, Kramer-Albers EM, Brahmer A. Kinetics and Topology of DNA Associated with Circulating Extracellular Vesicles Released during Exercise. Genes (Basel). 2021;12(4).
97. Edgar JR. Q&A: What are exosomes, exactly? BMC Biol. 2016;14:46.
98. McGough IJ, Vincent JP. Exosomes in developmental signalling. Development. 2016;143(14):2482-93.

99. Takahashi A, Okada R, Nagao K, Kawamata Y, Hanyu A, Yoshimoto S, et al. Exosomes maintain cellular homeostasis by excreting harmful DNA from cells. Nat Commun. 2017;8:15287.
100. Aucamp J, Bronkhorst AJ, Badenhorst CPS, Pretorius PJ. The diverse origins of circulating cell-free DNA in the human body: a critical re-evaluation of the literature. Biol Rev Camb Philos Soc. 2018;93(3):1649-83.
101. Kowarsky M, Camunas-Soler J, Kertesz M, De Vlaminck I, Koh W, Pan W, et al. Numerous uncharacterized and highly divergent microbes which colonize humans are revealed by circulating cell-free DNA. Proc Natl Acad Sci U S A. 2017;114(36):9623-8.
102. Grumaz S, Stevens P, Grumaz C, Decker SO, Weigand MA, Hofer S, et al. Next-generation sequencing diagnostics of bacteremia in septic patients. Genome Med. 2016;8(1):73.
103. Ngan RK, Yip TT, Cheng WW, Chan JK, Cho WC, Ma VW, et al. Circulating Epstein-Barr virus DNA in serum of patients with lymphoepithelioma-like carcinoma of the lung: a potential surrogate marker for monitoring disease. Clin Cancer Res. 2002;8(4):986-94.
104. Wichmann D, Panning M, Quack T, Kramme S, Burchard GD, Grevelding C, et al. Diagnosing schistosomiasis by detection of cell-free parasite DNA in human plasma. PLoS Negl Trop Dis. 2009;3(4):e422.
105. Spisák S, Solymosi N, Ittzés P, Bodor A, Kondor D, Vattay G, et al. Complete genes may pass from food to human blood. PLoS One. 2013;8(7):e69805.
106. Lo YM, Tein MS, Lau TK, Haines CJ, Leung TN, Poon PM, et al. Quantitative analysis of fetal DNA in maternal plasma and serum: implications for noninvasive prenatal diagnosis. Am J Hum Genet. 1998;62(4):768-75.
107. Gielis EM, Ledeganck KJ, De Winter BY, Del Favero J, Bosmans JL, Claas FH, et al. Cell-Free DNA: An Upcoming Biomarker in Transplantation. Am J Transplant. 2015;15(10):2541-51.
108. Tamkovich SN, Cherepanova AV, Kolesnikova EV, Rykova EY, Pyshnyi DV, Vlassov VV, et al. Circulating DNA and DNase activity in human blood. Ann N Y Acad Sci. 2006;1075:191-6.
109. Cherepanova AV, Tamkovich SN, Bryzgunova OE, Vlassov VV, Laktionov PP. Deoxyribonuclease activity and circulating DNA concentration in blood plasma of patients with prostate tumors. Ann N Y Acad Sci. 2008;1137:218-21.
110. Gahan PB. Biology of circulating nucleic acids and possible roles in diagnosis and treatment in diabetes and cancer. Infect Disord Drug Targets. 2012;12(5):360-70.
111. Velders M, Treff G, Machus K, Bosnyak E, Steinacker J, Schumann U. Exercise is a potent stimulus for enhancing circulating DNase activity. Clin Biochem. 2014;47(6):471-4.
112. Hisazumi J, Kobayashi N, Nishikawa M, Takakura Y. Significant role of liver sinusoidal endothelial cells in hepatic uptake and degradation of naked plasmid DNA after intravenous injection. Pharm Res. 2004;21(7):1223-8.
113. Emlen W, Mannik M. Kinetics and mechanisms for removal of circulating single-stranded DNA in mice. J Exp Med. 1978;147(3):684-99.
114. Su YH, Wang M, Brenner DE, Ng A, Melkonyan H, Umansky S, et al. Human urine contains small, 150 to 250 nucleotide-sized, soluble DNA derived from the circulation and may be useful in the detection of colorectal cancer. J Mol Diagn. 2004;6(2):101-7.
115. Emlen W, Mannik M. Effect of DNA size and strandedness on the in vivo clearance and organ localization of DNA. Clin Exp Immunol. 1984;56(1):185-92.
116. Lo YM, Zhang J, Leung TN, Lau TK, Chang AM, Hjelm NM. Rapid clearance of fetal DNA from maternal plasma. Am J Hum Genet. 1999;64(1):218-24.
117. Diehl F, Schmidt K, Choti MA, Romans K, Goodman S, Li M, et al. Circulating mutant DNA to assess tumor dynamics. Nat Med. 2008;14(9):985-90.

118. Dang DK, Park BH. Circulating tumor DNA: current challenges for clinical utility. J Clin Invest. 2022;132(12).
119. Christenson ES, Dalton WB, Chu D, Waters I, Cravero K, Zabransky DJ, et al. Single-Nucleotide Polymorphism Leading to False Allelic Fraction by Droplet Digital PCR. Clin Chem. 2017;63(8):1370-6.
120. Parsons HA, Beaver JA, Cimino-Mathews A, Ali SM, Axilbund J, Chu D, et al. Individualized Molecular Analyses Guide Efforts (IMAGE): A Prospective Study of Molecular Profiling of Tissue and Blood in Metastatic Triple-Negative Breast Cancer. Clin Cancer Res. 2017;23(2):379-86.
121. Parikh AR, Van Seventer EE, Siravegna G, Hartwig AV, Jaimovich A, He Y, et al. Minimal Residual Disease Detection using a Plasma-only Circulating Tumor DNA Assay in Patients with Colorectal Cancer. Clin Cancer Res. 2021;27(20):5586-94.
122. Kasi PM, Sawyer S, Guilford J, Munro M, Ellers S, Wulff J, et al. BESPOKE study protocol: a multicentre, prospective observational study to evaluate the impact of circulating tumour DNA guided therapy on patients with colorectal cancer. BMJ Open. 2021;11(9):e047831.
123. Cohen JD, Li L, Wang Y, Thoburn C, Afsari B, Danilova L, et al. Detection and localization of surgically resectable cancers with a multi-analyte blood test. Science. 2018;359(6378):926-30.
124. Nadauld LD, McDonnell CH, 3rd, Beer TM, Liu MC, Klein EA, Hudnut A, et al. The PATHFINDER Study: Assessment of the Implementation of an Investigational Multi-Cancer Early Detection Test into Clinical Practice. Cancers (Basel). 2021;13(14).
125. Garcia-Pardo M, Makarem M, Li JJN, Kelly D, Leighl NB. Integrating circulating-free DNA (cfDNA) analysis into clinical practice: opportunities and challenges. Br J Cancer. 2022;127(4):592-602.
126. Cristiano S, Leal A, Phallen J, Fiksel J, Adleff V, Bruhm DC, et al. Genome-wide cell-free DNA fragmentation in patients with cancer. Nature. 2019;570(7761):385-9.
127. Oellerich M, Budde K, Osmanodja B, Bornemann-Kolatzki K, Beck J, Schutz E, et al. Donor-derived cell-free DNA as a diagnostic tool in transplantation. Front Genet. 2022;13:1031894.
128. De Vlaminck I, Valantine HA, Snyder TM, Strehl C, Cohen G, Luikart H, et al. Circulating cell-free DNA enables noninvasive diagnosis of heart transplant rejection. Sci Transl Med. 2014;6(241):241ra77.
129. Saukkonen K, Lakkisto P, Pettila V, Varpula M, Karlsson S, Ruokonen E, et al. Cell-free plasma DNA as a predictor of outcome in severe sepsis and septic shock. Clin Chem. 2008;54(6):1000-7.
130. Dwivedi DJ, Toltl LJ, Swystun LL, Pogue J, Liaw KL, Weitz JI, et al. Prognostic utility and characterization of cell-free DNA in patients with severe sepsis. Crit Care. 2012;16(4):R151.
131. Vajpeyee A, Wijatmiko T, Vajpeyee M, Taywade O. Cell free DNA: A Novel Predictor of Neurological Outcome after Intravenous Thrombolysis and/or Mechanical Thrombectomy in Acute Ischemic Stroke Patients. Neurointervention. 2018;13(1):13-9.
132. Shaked G, Douvdevani A, Yair S, Zlotnik A, Czeiger D. The role of cell-free DNA measured by a fluorescent test in the management of isolated traumatic head injuries. Scand J Trauma Resusc Emerg Med. 2014;22:21.
133. Koffler D, Agnello V, Winchester R, Kunkel HG. The occurrence of single-stranded DNA in the serum of patients with systemic lupus erythematosus and other diseases. J Clin Invest. 1973;52(1):198-204.
134. Tug S, Helmig S, Menke J, Zahn D, Kubiak T, Schwarting A, et al. Correlation between cell free DNA levels and medical evaluation of disease progression in systemic lupus erythematosus patients. Cell Immunol. 2014;292(1-2):32-9.

135. Hendy OM, Motalib TA, El Shafie MA, Khalaf FA, Kotb SE, Khalil A, et al. Circulating cell free DNA as a predictor of systemic lupus erythematosus severity and monitoring of therapy. Egyptian Journal of Medical Human Genetics. 2016;17(1):79-85.
136. Xu Y, Song Y, Chang J, Zhou X, Qi Q, Tian X, et al. High levels of circulating cell-free DNA are a biomarker of active SLE. Eur J Clin Invest. 2018;48(11):e13015.
137. Atamaniuk J, Hsiao YY, Mustak M, Bernhard D, Erlacher L, Fodinger M, et al. Analysing cell-free plasma DNA and SLE disease activity. Eur J Clin Invest. 2011;41(6):579-83.
138. Bartoloni E, Ludovini V, Alunno A, Pistola L, Bistoni O, Crino L, et al. Increased levels of circulating DNA in patients with systemic autoimmune diseases: A possible marker of disease activity in Sjogren's syndrome. Lupus. 2011;20(9):928-35.
139. Hajizadeh S, DeGroot J, TeKoppele JM, Tarkowski A, Collins LV. Extracellular mitochondrial DNA and oxidatively damaged DNA in synovial fluid of patients with rheumatoid arthritis. Arthritis Res Ther. 2003;5(5):R234-40.
140. Abdelal IT, Zakaria MA, Sharaf DM, Elakad GM. Levels of plasma cell-free DNA and its correlation with disease activity in rheumatoid arthritis and systemic lupus erythematosus patients. The Egyptian Rheumatologist. 2016;38(4):295-300.
141. Hashimoto T, Yoshida K, Hashimoto N, Nakai A, Kaneshiro K, Suzuki K, et al. Circulating cell free DNA: a marker to predict the therapeutic response for biological DMARDs in rheumatoid arthritis. Int J Rheum Dis. 2017;20(6):722-30.
142. Honda H, Miharu N, Ohashi Y, Ohama K. Successful diagnosis of fetal gender using conventional PCR analysis of maternal serum. Clin Chem. 2001;47(1):41-6.
143. Leung TN, Zhang J, Lau TK, Chan LY, Lo YM. Increased maternal plasma fetal DNA concentrations in women who eventually develop preeclampsia. Clin Chem. 2001;47(1):137-9.
144. Mackie FL, Hemming K, Allen S, Morris RK, Kilby MD. The accuracy of cell-free fetal DNA-based non-invasive prenatal testing in singleton pregnancies: a systematic review and bivariate meta-analysis. BJOG. 2017;124(1):32-46.
145. Porreco RP, Garite TJ, Maurel K, Marusiak B, Obstetrix Collaborative Research N, Ehrich M, et al. Noninvasive prenatal screening for fetal trisomies 21, 18, 13 and the common sex chromosome aneuploidies from maternal blood using massively parallel genomic sequencing of DNA. Am J Obstet Gynecol. 2014;211(4):365 e1-12.
146. Chitty LS, Finning K, Wade A, Soothill P, Martin B, Oxenford K, et al. Diagnostic accuracy of routine antenatal determination of fetal RHD status across gestation: population based cohort study. BMJ. 2014;349:g5243.
147. Saito H, Sekizawa A, Morimoto T, Suzuki M, Yanaihara T. Prenatal DNA diagnosis of a single-gene disorder from maternal plasma. Lancet. 2000;356(9236):1170.
148. Chiu RW, Lau TK, Leung TN, Chow KC, Chui DH, Lo YM. Prenatal exclusion of beta thalassaemia major by examination of maternal plasma. Lancet. 2002;360(9338):998-1000.
149. Neuberger EWI, Sontag S, Brahmer A, Philippi KFA, Radsak MP, Wagner W, et al. Physical activity specifically evokes release of cell-free DNA from granulocytes thereby affecting liquid biopsy. Clin Epigenetics. 2022;14(1):29.
150. Atamaniuk J, Vidotto C, Tschan H, Bachl N, Stuhlmeier KM, Muller MM. Increased concentrations of cell-free plasma DNA after exhaustive exercise. Clin Chem. 2004;50(9):1668-70.
151. Tug S, Mehdorn M, Helmig S, Breitbach S, Ehlert T, Simon P. Exploring the Potential of Cell-Free-DNA Measurements After an Exhaustive Cycle-Ergometer Test as a Marker for Performance-Related Parameters. Int J Sports Physiol Perform. 2017;12(5):597-604.
152. Breitbach S, Sterzing B, Magallanes C, Tug S, Simon P. Direct measurement of cell-free DNA from serially collected capillary plasma during incremental exercise. J Appl Physiol (1985). 2014;117(2):119-30.

153. Fatouros IG, Destouni A, Margonis K, Jamurtas AZ, Vrettou C, Kouretas D, et al. Cell-free plasma DNA as a novel marker of aseptic inflammation severity related to exercise overtraining. Clin Chem. 2006;52(9):1820-4.
154. Beiter T, Fragasso A, Hudemann J, Schild M, Steinacker J, Mooren FC, et al. Neutrophils release extracellular DNA traps in response to exercise. J Appl Physiol (1985). 2014;117(3):325-33.
155. Mooren FC, Bloming D, Lechtermann A, Lerch MM, Volker K. Lymphocyte apoptosis after exhaustive and moderate exercise. J Appl Physiol (1985). 2002;93(1):147-53.
156. Atamaniuk J, Stuhlmeier KM, Vidotto C, Tschan H, Dossenbach-Glaninger A, Mueller MM. Effects of ultra-marathon on circulating DNA and mRNA expression of pro- and anti-apoptotic genes in mononuclear cells. Eur J Appl Physiol. 2008;104(4):711-7.
157. Haller N, Helmig S, Taenny P, Petry J, Schmidt S, Simon P. Circulating, cell-free DNA as a marker for exercise load in intermittent sports. PLoS One. 2018;13(1):e0191915.
158. Andreatta MV, Curty VM, Coutinho JVS, Santos MAA, Vassallo PF, de Sousa NF, et al. Cell-Free DNA as an Earlier Predictor of Exercise-Induced Performance Decrement Related to Muscle Damage. Int J Sports Physiol Perform. 2018;13(7):953-6.
159. Haller N, Tug S, Breitbach S, Jorgensen A, Simon P. Increases in Circulating Cell-Free DNA During Aerobic Running Depend on Intensity and Duration. Int J Sports Physiol Perform. 2017;12(4):455-62.
160. Haller N, Ehlert T, Schmidt S, Ochmann D, Sterzing B, Grus F, et al. Circulating, Cell-Free DNA for Monitoring Player Load in Professional Football. Int J Sports Physiol Perform. 2019;14(6):718-26.
161. Chang CP, Chia RH, Wu TL, Tsao KC, Sun CF, Wu JT. Elevated cell-free serum DNA detected in patients with myocardial infarction. Clin Chim Acta. 2003;327(1-2):95-101.
162. Yokokawa T, Misaka T, Kimishima Y, Shimizu T, Kaneshiro T, Takeishi Y. Clinical Significance of Circulating Cardiomyocyte-Specific Cell-Free DNA in Patients With Heart Failure: A Proof-of-Concept Study. Can J Cardiol. 2020;36(6):931-5.
163. Salzano A, Israr MZ, Garcia DF, Middleton L, D'Assante R, Marra AM, et al. Circulating cell-free DNA levels are associated with adverse outcomes in heart failure: testing liquid biopsy in heart failure. Eur J Prev Cardiol. 2021;28(9):e28-e31.
164. Dutta A, Das M, Ghosh A, Rana S. Molecular and cellular pathophysiology of circulating cardiomyocyte-specific cell free DNA (cfDNA): Biomarkers of heart failure and potential therapeutic targets. Genes Dis. 2023;10(3):948-59.
165. Kananen L, Hurme M, Jylhä M, Härkänen T, Koskinen S, Stenholm S, et al. Circulating cell-free DNA level predicts all-cause mortality independent of other predictors in the Health 2000 survey. Sci Rep. 2020;10(1):13809.
166. Polina IA, Ilatovskaya DV, DeLeon-Pennell KY. Cell free DNA as a diagnostic and prognostic marker for cardiovascular diseases. Clin Chim Acta. 2020;503:145-50.
167. Zaravinos A, Tzoras S, Apostolakis S, Lazaridis K, Spandidos DA. Levosimendan reduces plasma cell-free DNA levels in patients with ischemic cardiomyopathy. J Thromb Thrombolysis. 2011;31(2):180-7.
168. Meddeb R, Dache ZAA, Thezenas S, Otandault A, Tanos R, Pastor B, et al. Quantifying circulating cell-free DNA in humans. Sci Rep. 2019;9(1):5220.
169. Kananen L, Hurme M, Burkle A, Moreno-Villanueva M, Bernhardt J, Debacq-Chainiaux F, et al. Circulating cell-free DNA in health and disease - the relationship to health behaviours, ageing phenotypes and metabolomics. Geroscience. 2023;45(1):85-103.
170. Caboux E, Lallemand C, Ferro G, Hemon B, Mendy M, Biessy C, et al. Sources of pre-analytical variations in yield of DNA extracted from blood samples: analysis of 50,000 DNA samples in EPIC. PLoS One. 2012;7(7):e39821.
171. Gaillard C, Strauss F. Avoiding adsorption of DNA to polypropylene tubes and denaturation of short DNA fragments. Technical Tips Online. 1998;3(1):63-5.

172. Lam NY, Rainer TH, Chiu RW, Lo YM. EDTA is a better anticoagulant than heparin or citrate for delayed blood processing for plasma DNA analysis. Clin Chem. 2004;50(1):256-7.
173. El Messaoudi S, Thierry, A.R. Pre-analytical Requirements for Analyzing Nucleic Acids from Blood. In: Gahan PB, editor. Circulating Nucleic Acids in Early Diagnosis, Prognosis and Treatment Monitoring: Advances in Predictive, Preventive and Personalised Medicine. Dordrecht: Springer Netherlands; 2015. p. 45-69.
174. Costa F, Barbisan F, Assmann CE, Araujo NKF, de Oliveira AR, Signori JP, et al. Seminal cell-free DNA levels measured by PicoGreen fluorochrome are associated with sperm fertility criteria. Zygote. 2017;25(2):111-9.
175. Scientific TF. PicoGreen® Assay for dsDNA 2008 [Available from: https://assets.thermofisher.com/TFS-Assets/CAD/manuals/PicoGreen-dsDNA-protocol.pdf.]
176. Chiminqgi M, Moutereau S, Pernet P, Conti M, Barbu V, Lemant J, et al. Specific real-time PCR vs. fluorescent dyes for serum free DNA quantification. Clin Chem Lab Med. 2007;45(8):993-5.
177. Bronkhorst AJ, Ungerer V, Holdenrieder S. Comparison of methods for the quantification of cell-free DNA isolated from cell culture supernatant. Tumour Biol. 2019;41(8):1010428319866369.
178. Oberhofer A, Bronkhorst AJ, Uhlig C, Ungerer V, Holdenrieder S. Tracing the Origin of Cell-Free DNA Molecules through Tissue-Specific Epigenetic Signatures. Diagnostics (Basel). 2022;12(8).
179. Fleischhacker M, Schmidt B, Weickmann S, Fersching DM, Leszinski GS, Siegele B, et al. Methods for isolation of cell-free plasma DNA strongly affect DNA yield. Clin Chim Acta. 2011;412(23-24):2085-8.
180. Manokhina I, Singh TK, Penaherrera MS, Robinson WP. Quantification of cell-free DNA in normal and complicated pregnancies: overcoming biological and technical issues. PLoS One. 2014;9(7):e101500.
181. Lyu N, Rajendran VK, Diefenbach RJ, Charles K, Clarke SJ, Engel A, et al. Multiplex detection of ctDNA mutations in plasma of colorectal cancer patients by PCR/SERS assay. Nanotheranostics. 2020;4(4):224-32.
182. BioRad. Digital PCR and Real-Time PCR (qPCR) Choices for Different Applications [Available from: https://www.bio-rad.com/de-de/life-science/learning-center/digital-pcr-and-real-time-pcr-qpcr-choices-for-different-applications#What_are_the_Strengths_of_dPCR_and_qPCR?]
183. Neuberger EWI, Brahmer A, Ehlert T, Kluge K, Philippi KFA, Boedecker SC, et al. Validating quantitative PCR assays for cfDNA detection without DNA extraction in exercising SLE patients. Sci Rep. 2021;11(1):13581.
184. Ovchinnikov I, Rubin A, Swergold GD. Tracing the LINEs of human evolution. Proc Natl Acad Sci U S A. 2002;99(16):10522-7.
185. Kent WJ, Sugnet CW, Furey TS, Roskin KM, Pringle TH, Zahler AM, et al. The human genome browser at UCSC. Genome Res. 2002;12(6):996-1006.
186. FDA US. Bioanalytical Method Validation: Guidance for Industry. 2018.
187. Nolan T, Hands RE, Bustin SA. Quantification of mRNA using real-time RT-PCR. Nat Protoc. 2006;1(3):1559-82.
188. Ma H, Bell KN, Loker RN. qPCR and qRT-PCR analysis: Regulatory points to consider when conducting biodistribution and vector shedding studies. Mol Ther Methods Clin Dev. 2021;20:152-68.
189. Jylhava J, Kotipelto T, Raitala A, Jylha M, Hervonen A, Hurme M. Aging is associated with quantitative and qualitative changes in circulating cell-free DNA: the Vitality 90+ study. Mech Ageing Dev. 2011;132(1-2):20-6.

190. Haghiac M, Vora NL, Basu S, Johnson KL, Presley L, Bianchi DW, et al. Increased death of adipose cells, a path to release cell-free DNA into systemic circulation of obese women. Obesity (Silver Spring). 2012;20(11):2213-9.
191. Thorsen SU, Moseholm KF, Clausen FB. Circulating cell-free DNA and its association with cardiovascular disease: what we know and future perspectives. Curr Opin Lipidol. 2023.
192. Duvvuri B, Lood C. Cell-Free DNA as a Biomarker in Autoimmune Rheumatic Diseases. Front Immunol. 2019;10:502.
193. Celec P, Vlkova B, Laukova L, Babickova J, Boor P. Cell-free DNA: the role in pathophysiology and as a biomarker in kidney diseases. Expert Rev Mol Med. 2018;20:e1.
194. Korabecna M, Opatrna S, Wirth J, Rulcova K, Eiselt J, Sefrna F, et al. Cell-free plasma DNA during peritoneal dialysis and hemodialysis and in patients with chronic kidney disease. Ann N Y Acad Sci. 2008;1137:296-301.
195. McGuire AL, Urosevic N, Chan DT, Dogra G, Inglis TJ, Chakera A. The impact of chronic kidney disease and short-term treatment with rosiglitazone on plasma cell-free DNA levels. PPAR Res. 2014;2014:643189.
196. Ma K, Liu J, Wang Y, Zhong Y, Wu Z, Fan R, et al. Relationship between plasma cell-free DNA (cfDNA) and prognosis of TACE for primary hepatocellular carcinoma. J Gastrointest Oncol. 2020;11(6):1350-63.
197. Wu Z, Yu L, Hou J, Cui L, Huang Y, Chen Q, et al. Plasma cfDNA for the Diagnosis and Prognosis of Colorectal Cancer. J Oncol. 2022;2022:9538384.
198. Panagopoulou V, Deftereos S, Kossyvakis C, Raisakis K, Giannopoulos G, Bouras G, et al. NTproBNP: an important biomarker in cardiac diseases. Curr Top Med Chem. 2013;13(2):82-94.
199. McKie PM, Burnett JC, Jr. NT-proBNP: The Gold Standard Biomarker in Heart Failure. J Am Coll Cardiol. 2016;68(22):2437-9.
200. Mouliere F, El Messaoudi S, Pang D, Dritschilo A, Thierry AR. Multi-marker analysis of circulating cell-free DNA toward personalized medicine for colorectal cancer. Mol Oncol. 2014;8(5):927-41.
201. Chan RW, Jiang P, Peng X, Tam LS, Liao GJ, Li EK, et al. Plasma DNA aberrations in systemic lupus erythematosus revealed by genomic and methylomic sequencing. Proc Natl Acad Sci U S A. 2014;111(49):E5302-11.
202. Brodbeck K, Kern S, Schick S, Steinbruck A, Schwerer M, Bayer B, et al. Quantitative analysis of individual cell-free DNA concentration before and after penetrating trauma. Int J Legal Med. 2019;133(2):385-93.
203. Keup C, Storbeck M, Hauch S, Hahn P, Sprenger-Haussels M, Tewes M, et al. Cell-Free DNA Variant Sequencing Using CTC-Depleted Blood for Comprehensive Liquid Biopsy Testing in Metastatic Breast Cancer. Cancers (Basel). 2019;11(2).
204. Orntoft MW, Jensen SO, Ogaard N, Henriksen TV, Ferm L, Christensen IJ, et al. Age-stratified reference intervals unlock the clinical potential of circulating cell-free DNA as a biomarker of poor outcome for healthy individuals and patients with colorectal cancer. Int J Cancer. 2021;148(7):1665-75.
205. Sigurpalsdottir BD, Stefansson OA, Holley G, Beyter D, Zink F, Hardarson M, et al. A comparison of methods for detecting DNA methylation from long-read sequencing of human genomes. Genome Biol. 2024;25(1):69.

8 Appendix

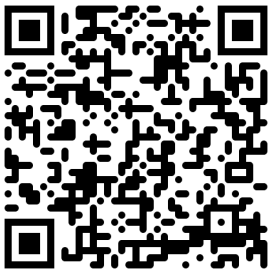

https://seafile.rlp.net/d/ef703fc2695b43d8a587/

Figure A1 - QR-Code/Link for the detailed VIALAB program reports

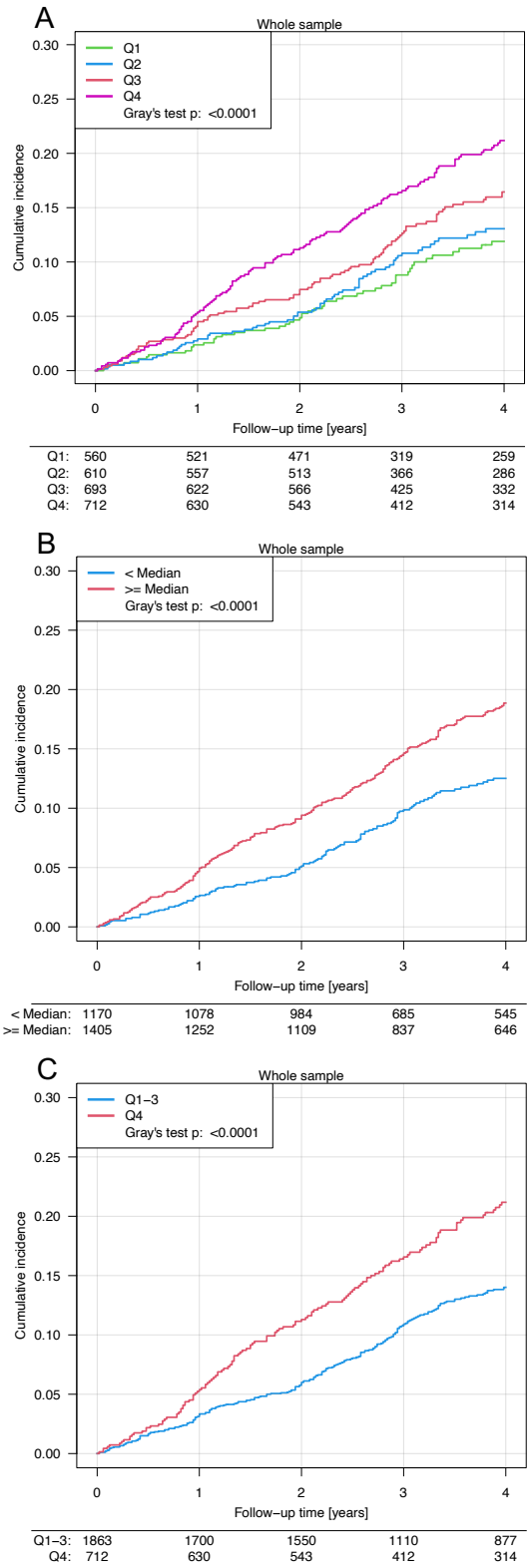

Figure A2 - CI plots for worsening of HF according to cfDNA 222bp levels

(A) for continuous cfDNA levels subdivided into quartiles, (B) for cfDNA levels dichotomized by the median, (C) for cfDNA levels dichotomized by the 75th percentile

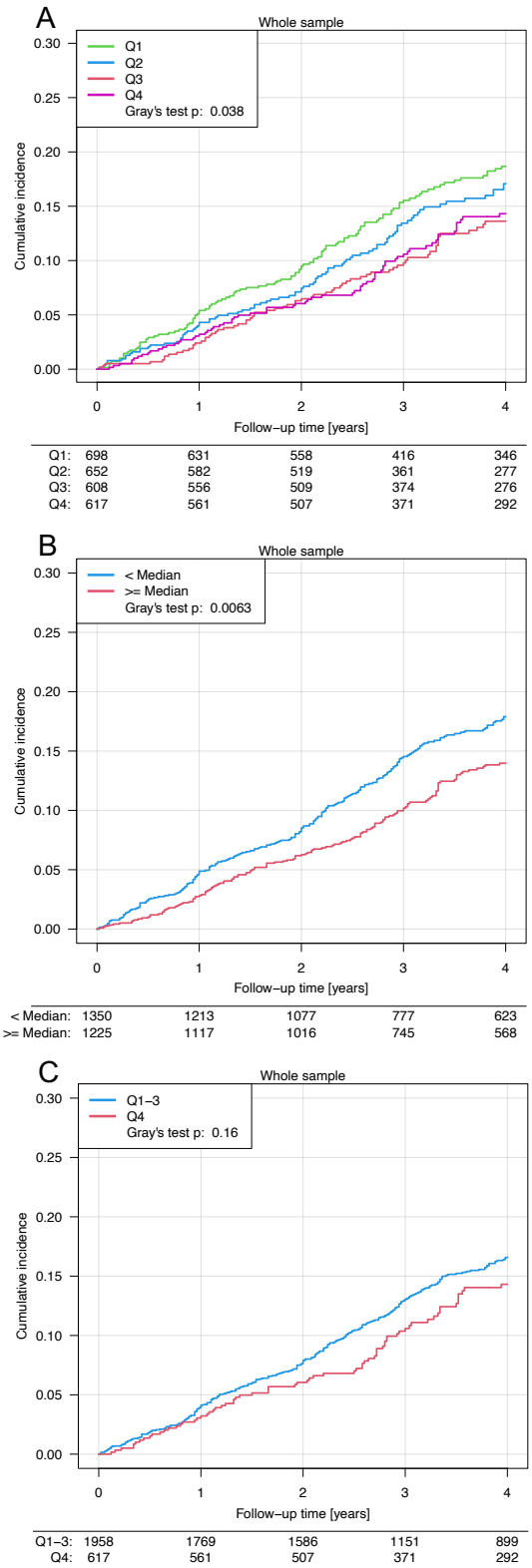

Figure A3 - CI plots for worsening of HF according to cfDNA Integrity Index

(A) for continuous cfDNA levels subdivided into quartiles, (B) for cfDNA levels dichotomized by the median, (C) for cfDNA levels dichotomized by the 75th percentile

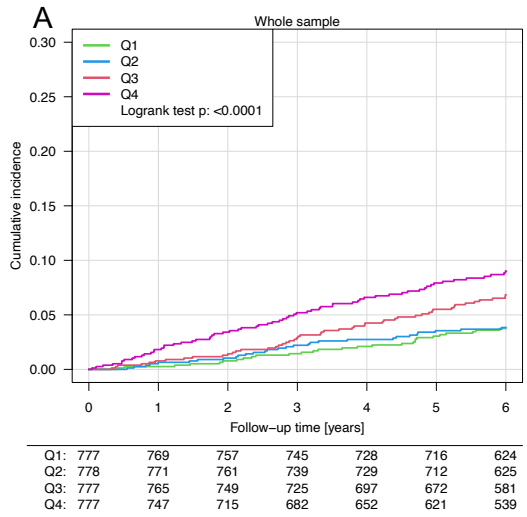

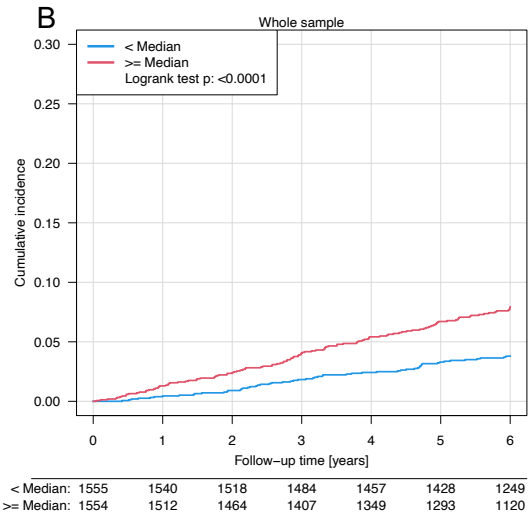

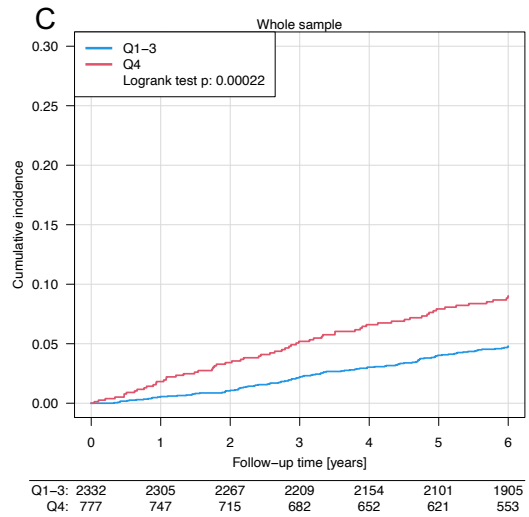

Figure A4 - CI plots for cardiac death according to cfDNA 222bp levels

(A) for continuous cfDNA levels subdivided into quartiles, (B) for cfDNA levels dichotomized by the median, (C) for cfDNA levels dichotomized by the 75th percentile

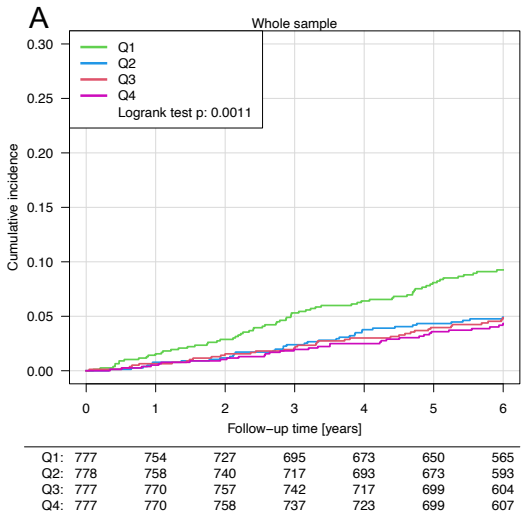

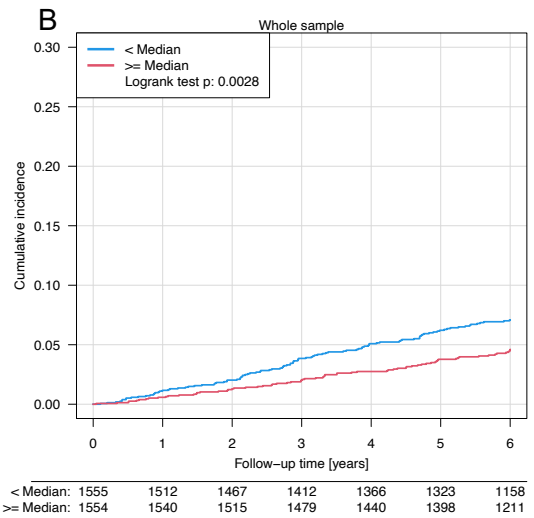

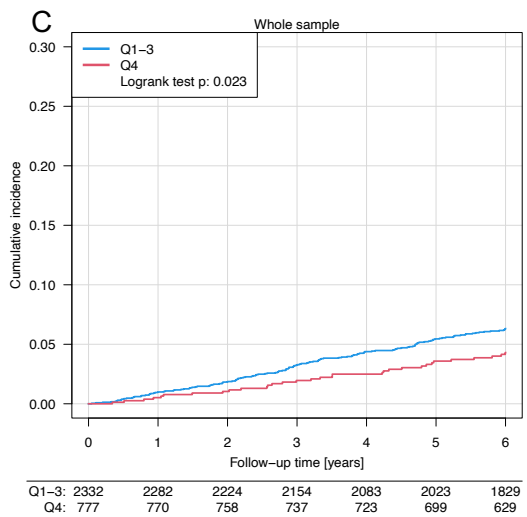

Figure A5 - CI plots for cardiac death according to cfDNA Integrity Index

(A) for continuous cfDNA levels subdivided into quartiles, (B) for cfDNA levels dichotomized by the median, (C) for cfDNA levels dichotomized by the 75th percentile

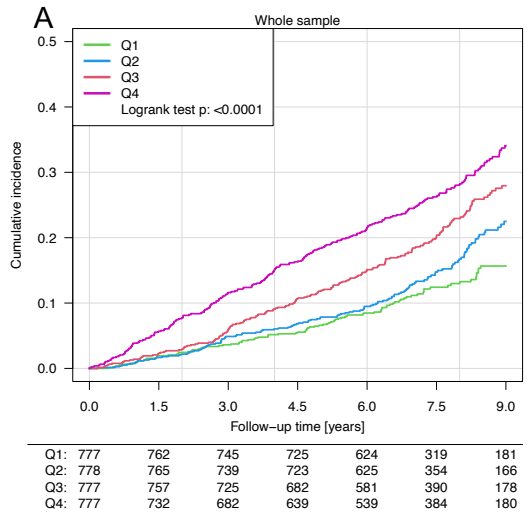

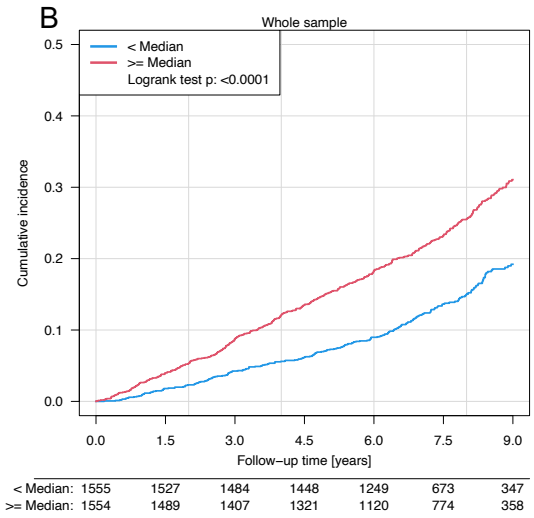

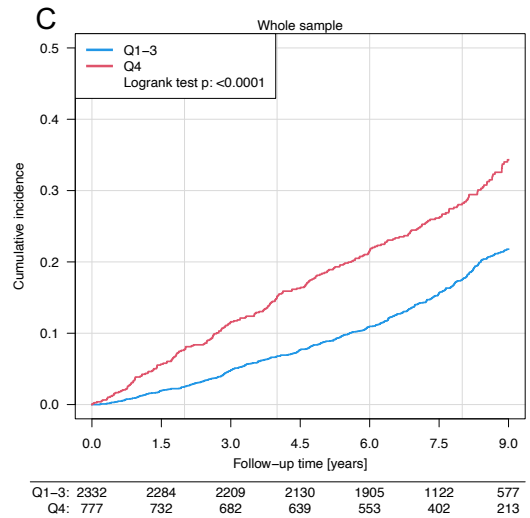

Figure A7 - CI plots for all-cause death according to cfDNA 222bp levels

(A) for continuous cfDNA levels subdivided into quartiles, (B) for cfDNA levels dichotomized by the median, (C) for cfDNA levels dichotomized by the 75th percentile

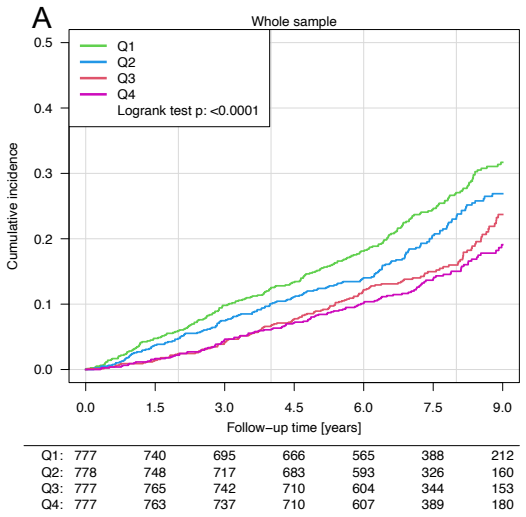

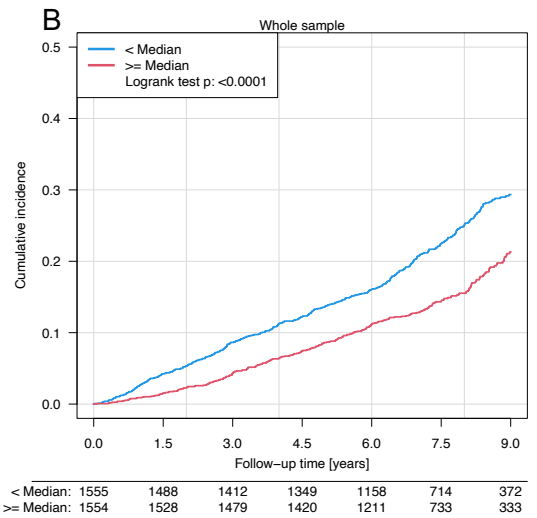

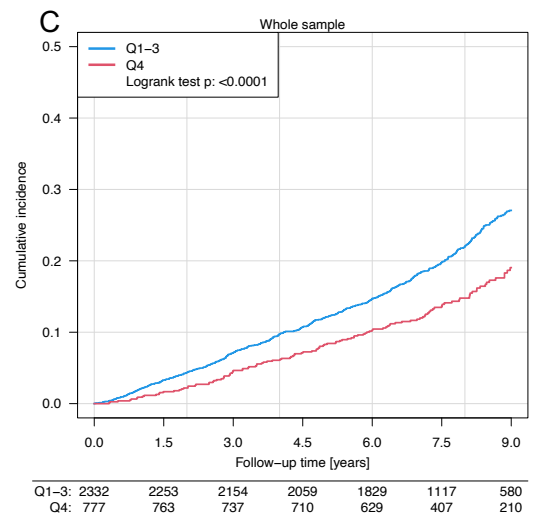

Figure A6 - CI plots for all-cause death according to cfDNA Integrity Index

(A) for continuous cfDNA levels subdivided into quartiles, (B) for cfDNA levels dichotomized by the median, (C) for cfDNA levels dichotomized by the 75th percentile

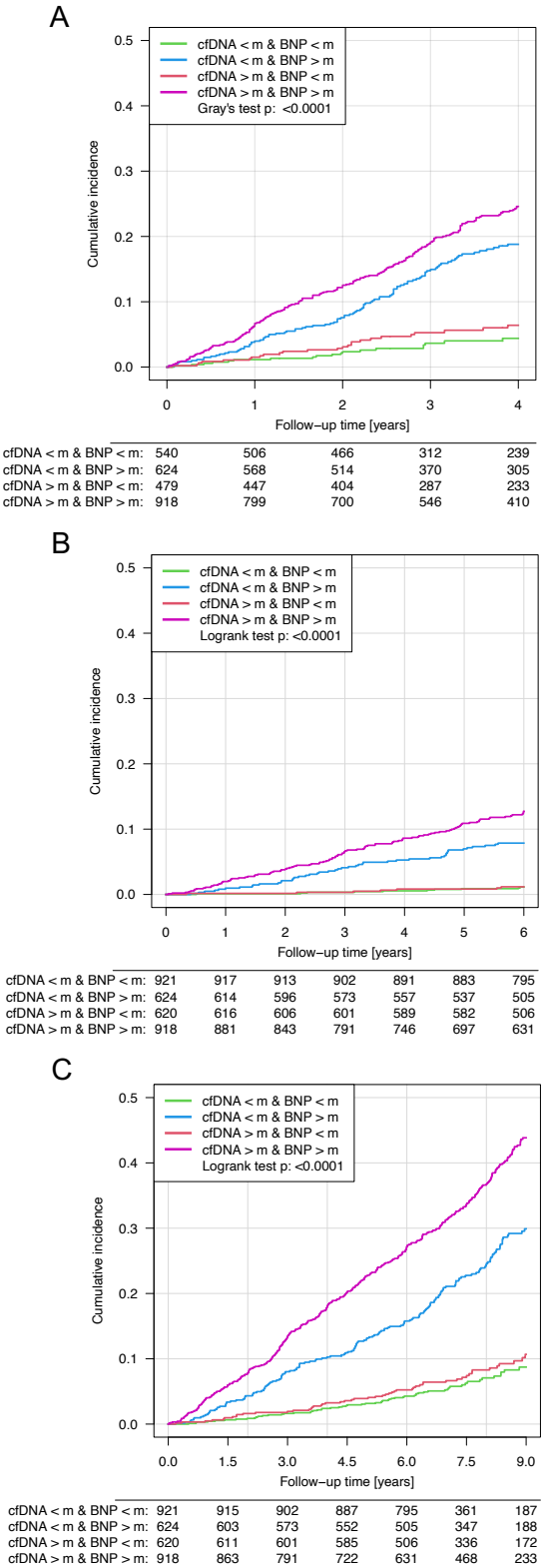

Figure A8 - CI plots for outcome prediction according to combinations of cfDNA 222bp and NT-proBNP levels

(A) for worsening of HF, (B) for cardiac death, (C) for all-cause death

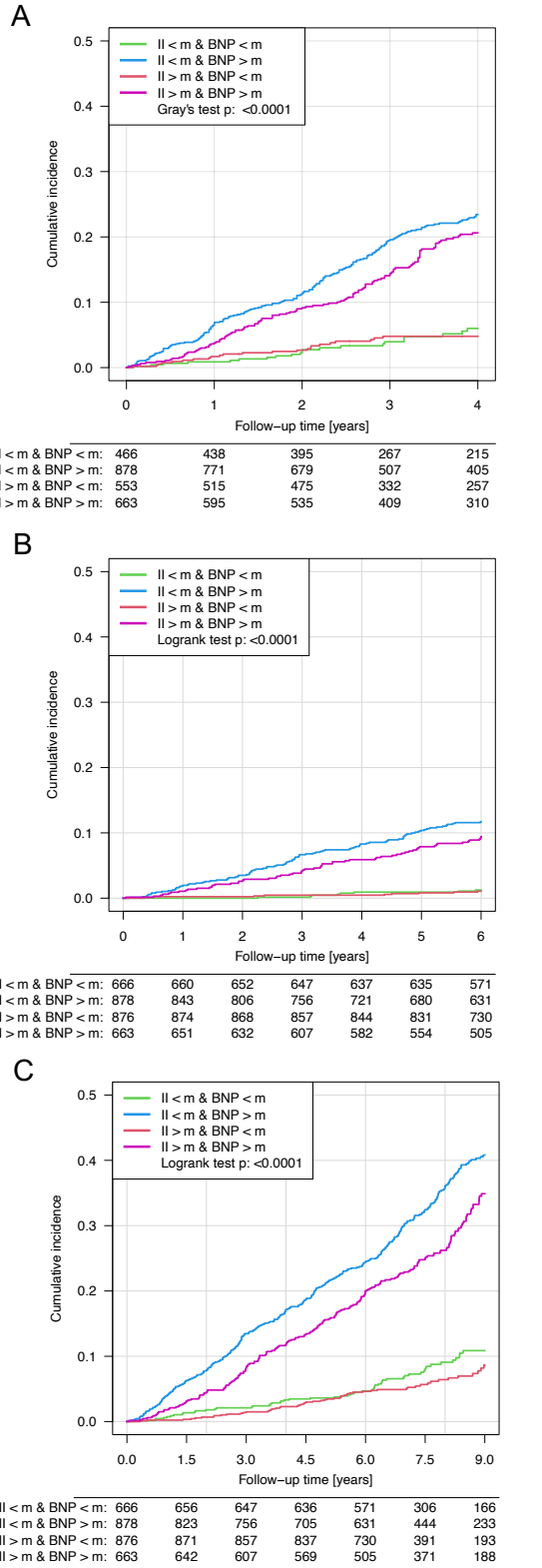

Figure A9 - CI plots for outcome prediction according to combinations of cfDNA Integrity Index and NT-proBNP levels

(A) for worsening of HF, (B) for cardiac death, (C) for all-cause death

9 Acknowledgements

I would like to express my profound gratitude to the many individuals and institutions whose support and contributions have made the completion of this medical doctoral thesis possible.

I am deeply indebted to my dedicated thesis supervisors, Prof. Dr P. Wild and Prof. Dr Dr P. Simon. Your guidance, expertise, and encouragement throughout this research journey have been invaluable. Your mentorship has enriched the quality of this thesis and significantly contributed to my personal and professional growth.

I extend my sincere appreciation to my lab supervisor Dr Elmo Neuberger, who was always available for me, tirelessly answered all my questions and helped me with every little problem encountered during this time. Special thanks for your assistance in the MyoVasc sample measurements and your experience in organizational aspects and data management.

I would like to thank all members of the Institute for Sports Medicine, Prevention and Rehabilitation for your warm welcome in the team and the great working atmosphere. I had an awesome time working with you. Aleks, Alfonso, Carina, Ema, Kira and Vincent, your collective wisdom and camaraderie have made this time even more rewarding, and your humour helped to overcome every research setback.

This research would not have been feasible without the great background work of the whole MyoVasc study team. To be emphasized is Mr. Alexander Gieswinkel, who performed the statistical analysis and never got tired of new instructions or changes of plan. I am deeply grateful to all the participants and patients who consented to be part of the MyoVasc study and willingly made their data available for research.

I gratefully acknowledge scientific and financial support by the MAInz-DOC doctoral scholarship in the framework of the TransMed programme from the University Medical Center of the Johannes Gutenberg-University Mainz.

The MyoVasc study was supported by funding from the German Center for Cardiovascular Research (DZHK; grant number 81Z0210101), the Center for Translational Vascular Biology (CTVB), and the Preventive Cardiology and Preventive Medicine, Center for Cardiology, University Medical Center of the Johannes Gutenberg University Mainz, Germany.

To my family, friends, and loved ones, thank you so much!

Tim Hankeln, February 2024

10 Curriculum vitae

Tim Jeremy Hankeln

Born: 03.09.1996 in Wiesbaden, Germany

Education

10/2023 – 12/2024 **Study of human medicine / practical year**

Technical University of Munich

- Klinikum rechts der Isar, Munich
- Berner Reha Zentrum Heiligenschwendi, Switzerland
- Klinikum rechts der Isar, Munich

10/2017 – 10/2023 **Study of human medicine**

Johannes Gutenberg University Mainz

- doctoral thesis at the Centre for Thrombosis and Haemostasis and the Institute for Sports Medicine, Prevention and Rehabilitation
- MAInz-DOC doctoral scholarship holder

05/2017 **Test for medical degree programmes (TMS)**

11/2016 – 03/2017 **Pre-semester medicine**

IFS Student Courses, Frankfurt a. M.

09/2007 – 03/2016 **General qualification for university entrance**

Rabanus-Maurus-Gymnasium, Mainz